# INTRACELLULAR BETAINE REGULATION IN DEVELOPING MOUSE OOCYTES AND PREIMPLANTATION EMBRYOS

**EMILY MCINTOSH**

Thesis submitted to the University of Ottawa in partial fulfillment of the requirements for the M.Sc. program in Cellular and Molecular Medicine

Department of Cellular and Molecular Medicine
Faculty of Medicine
University of Ottawa

**Abstract**

The organic osmolyte betaine (*N, N, N*-trimethylglycine) has two key roles in mouse oocytes and preimplantation embryos, as a cell volume regulator and a major methyl donor. However, several aspects of the mechanisms of intracellular betaine regulation have not been fully elucidated. The origin of endogenous betaine in immature oocytes and the amount accumulated over oogenesis is unknown. Betaine levels are maintained at nearly constant levels through preimplantation embryo development but decrease at the blastocyst stage. The maintenance of betaine levels is hypothesized to be regulated by limiting its efflux through the swelling-activated, volume-sensitive organic osmolyte and anion channels (VSOACs). Which isoforms of VSOAC that are expressed in preimplantation embryos has not been determined, and it is unknown if VSOAC induces betaine efflux. In the inner cell mass of the blastocyst, betaine supplies the methyl pool by serving as the substrate for the enzyme betaine homocysteine methyltransferase (BHMT). There may be a link between metabolism by BHMT and the decrease in betaine by the blastocyst stage. Here, I investigate the mechanisms of betaine accumulation, retention, and loss from oogenesis to the blastocyst stage.

Low levels of endogenous betaine were present in small growing oocytes from postnatal day 5 (P5) ovaries, and the amount remained nearly constant through the rest of oogenesis. Growing follicles contained a large reservoir of betaine and choline by the time they were fully grown. Saturable betaine transporter activity was observed in growing follicles (from P17 ovaries) and fully-grown antral follicles (P21). However, denuded oocytes did not exhibit any saturable betaine transport on any postnatal day. In preimplantation embryos, endogenous betaine levels were conserved from the two-cell stage to the morula stage both *in vivo* and *in vitro*. However, there was a swelling-induced loss of betaine when one-cell embryos were

transferred to hypotonic media, which indicated the presence of VSOACs. We therefore attempted to elucidate the subunits of the channel that were expressed. We determined by conventional PCR that transcripts for four of the five *Lrrc8* isoforms (*Lrrc8a, b, d,* and *e*) were variously expressed during oocyte and preimplantation embryo development. We confirmed by quantitative RT-qPCR that *Lrrc8a* mRNA is present at the highest levels from the GV oocyte to the two-cell embryo stage and then decreases. Since suitable primers for the other isoforms for RT-qPCR could not be found, we used an available RNAseq data set to determine the expression patterns for all five *Lrrc8* isoform transcripts. Finally, it was anticipated that *Bhmt*$^{-/-}$ blastocysts would have endogenous betaine levels comparable to morulae instead of exhibiting the normal decrease, because betaine would not be metabolized for its methyl group. However, blastocysts isolated from both *Bhmt*$^{-/-}$ and *Bhmt*$^{+/+}$ mice had nearly the same levels of endogenous betaine, indicating that the decrease in betaine must be through another mechanism. To conclude, I have built on previous work to provide further insight into the mechanisms by which betaine is accumulated and stored in the mouse oocyte and preimplantation embryo.

**Table of Contents**

**List of Figures**

**List of Tables**

**List of Abbreviations**

ANOVA = analysis of variance

APC/C = anaphase-promoting complex/cyclosome

ART = Assisted Reproductive Techniques

ATP = adenosine triphosphate

BADH = betaine aldehyde dehydrogenase

BGT1 = betaine transporter

BHMT = betaine homocysteine methyltransferase

BMP = bone morphogenic protein

bp = base pairs

CaM = calmodulin

cAMP = cyclic adenosine monophosphate

CEEF = cumulus expansion enabling factor

CDC25 = Cell division cycle 25

CDK1 = cyclin dependent kinase 1

cDNA = complementary deoxyribonucleic acid

cGMP = cyclic guanosine monophosphate

cGMP-PDE = cGMP-phosphodiesterase

CHDH = choline dehydrogenase

c-KIT = tyrosine kinase receptor

COC = cumulus oocyte complex

COX = cyclooxygenase

CPM = counts per minute

CSF = cytostatic factor

Cx = connexin

CZB = Chatot Ziomek Bavister embryo culture medium

dbcAMP = dibutyryl cyclic adenosine monophosphate

EGF = epidermal growth factor

EGFR = epidermal growth factor receptor

EMI = early mitotic inhibitor

ER = endoplasmic reticulum

Fmole = femtomole

FSH = follicle stimulating hormone

GABA = y-aminobutyric acid

GADD34 = growth arrest and DNA damage-inducible protein 34

GC = granulosa cells

GDF = growth differentiation factor

GLYT1 = glycine transporter 1

GPR = g-protein linked receptor

GMC = glucose-methanol-choline enzyme

GTP = guanylyl trisphosphate

GV = Germinal Vesicle

GVBD = Germinal Vesicle Breakdown

h = hour

HA = hyaluronic acid

HAS = hyaluronic synthase

hCG = human chorionic gonadotropin

HPLC = high performance liquid chromatography

ICM = inner cell mass

i.p. = intraperitoneally

$IP_3$ = inositol 1,4,5-triphosphate

IU = international units

ISR = integrated stress response

IVF = in vitro fertilization

IVM = in vitro maturation

JAK = Janus kinase

KL = kit ligand

KSOM = $K^+$ simplex optimized medium

LC-MS/MS = liquid chromatography with dual mass spectroscopy

LH = luteinizing hormone

LPC = lysophosphatidylcholine

MAPK = mitogen-activated protein kinase

MEK = MAPK kinase

MEM = minimum essential medium

MGCs = mural granulosa cells

MI = metaphase I

MII = metaphase II

MPF = Maturation Promoting Factor

MTX = methotrexate

MYTI = membrane-associated tyrosine/threonine-specific Cdc2-inibitory kinase

NCBI = National Center for Biotechnology Information

NHE = $Na^+/H^+$ antiporter

NPPC = natriuretic peptide precursor type C

NPR = guanylyl cyclase natriuretic peptide receptor

NTT = neurotransmitter transporter

OCM = one-carbon metabolism

P1-P21 = Postnatal day 1-21

PB = polar body

PC = phosphatidylcholine

PCR = polymerase chain reaction

PDE = phosphodiesterase

PGCs = primordial germ cells

$pH_i$ = intracellular pH

PI = preimplantation

PKA = protein kinase A

PLCζ = phospholipase C zeta

PMID# = PubMed identifiers

PMSG = pregnant mare's serum gonadotropin

Pmole = picomole

PN = pronuclei

PP1 = protein phosphatase 1

PROT = proline transporter

PVA = polyvinyl alcohol

PVS = perivitelline space

RNA = ribonucleic acid

ROS = reactive oxygen species

RVI = regulatory volume increase

RVD = regulatory volume decrease

RT-PCR = reverse-transcribed polymerase chain reaction

SAH = S-adenosyl homocysteine

SAM = S-adenosylmethionine

SAPK/JNK = stress-activated protein kinase/Jun-amino-terminal kinase

SEM = standard error of the mean

SIT1 = imino acid transporter 1

SMIT = $Na^+$/myo-inositol transporter

SNAT = $Na^+$-dependent neutral amino acid transporter

TAUT = taurine/β -amino acid transporter

TonEBP = Tonicity enhancer binding protein

TSG-6 = tumor necrosis factor stimulated gene-6

UV = Ultraviolet

VRAC = volume-regulated anion channels

VSOAC = volume-sensitive organic osmolyte and anion channels

Wee1 = Wee1 $G_2$ checkpoint kinase

ZGA = zygotic genome activation

ZP = zona pellucida

**Acknowledgements**

The research collected in this thesis was accomplished under the supervision of Dr. Jay Baltz (Department of Cellular and Molecular Medicine, University of Ottawa, Ottawa Hospital Research Institute, Chronic Disease Program, Obstetrics and Gynecology). I would like to express my gratitude and sincerely thank Dr. Baltz for his mentorship, patience, and overall support throughout my Masters degree. I feel so fortunate to have been mentored by someone so passionate and knowledgeable about his field of research and am grateful to have had the opportunity to work in his lab.

I would like to thank the members of my Thesis Advisory Committee, Dr. Barbara Vanderhyden (Department of Cellular and Molecular Medicine, University of Ottawa, Ottawa Hospital Research Institute, Cancer Therapeutics Program) and Dr. Johné Liu (Department of Biochemistry, Microbiology and Immunology, University of Ottawa, Ottawa Hospital Research Institute, Chronic Disease Program), for their insight and feedback throughout my degree. I truly appreciate having such reputable scientists on my team, challenging me to think of my project in different ways, and ultimately improving all aspects of my research.

I would like to extend my thanks to my colleagues in the Baltz lab who have provided me with incredible mentorship and support. I would like to first acknowledge Ms. Taylor McClatchie, for teaching me all the technical laboratory skills, and for her friendship especially in our last year at the lab. I would also like to thank Dr. Allison Tscherner for extending her guidance and amazing problem-solving skills. I would like to especially thank my roommate and sister Ms. Chyna Ortman, for being my rock throughout my Masters degree, and for helping me find my place in a new city. I could not have finished this degree without her boundless support, and tough love.

Finally, I would like to thank my new friends in Ottawa, who have shown me so much support and love throughout my mouse trauma, and my mom, for always being my biggest fan, and for supporting every single one of my dreams.

This graduate work was supported by Canadian Institutes of Health Research (CIHR) (Contact grant number: PJT169185) obtained by Dr. Baltz. I would also like to thank the University of Ottawa Graduate and Postdoctoral Studies for the financial support through the Admission Scholarship program.

## 1.0 Introduction

### 1.1 Mammalian folliculogenesis and oogenesis

The first signs of oogenesis are primordial germ cells (PGCs) that appear in the extraembryonic mesoderm of the posterior amniotic fold (Ginsburg *et al*., 1990). PGCs proliferate and migrate from the gut endoderm to the genital ridges and eventually colonize each primordial gonad as oogonia (Hogan *et al.,* 1994). Sexual differentiation of the ovary, oogenesis, and folliculogenesis are induced by PGCs in the gonad. As proliferation ceases, oogonia differentiate into primary oocytes enclosed by a single squamous layer of early granulosa cells (GCs) and are referred to as primordial follicles (Eppig, 2001). It is this pool of primordial follicles that serves as the source of oocytes and developing follicles over the span of a female's reproductive life. Primary oocytes within primordial follicles enter meiosis but are arrested at prophase I of the first meiotic division. The growth of the oocyte occurs synchronously with follicle growth, while remaining arrested in prophase I. During growth, the oocyte will synthesize and secrete glycoproteins to form a rigid extracellular layer surrounding the oocyte referred to as the zona pellucida (ZP).

A large proportion of primordial follicles that develop in the ovary degenerate at birth, however, at each reproductive cycle, primordial follicles selected for development enter the growth phase and progress into primary follicles, which are characterized by a layer of cuboidal GCs (Eppig, 2001). Secondary follicles consist of more than one layer of GCs and have differentiated theca cells that form a theca interna that separates the GCs by a basement membrane, and theca externa that forms the outer layers of the follicle (Fauser & Van Heusden, 1997). Follicle growth from the primordial to the secondary follicle stage occurs independently of follicle-stimulating hormone (FSH) regulation and is instead controlled by bidirectional

communication between the oocyte and follicle (Gershon & Dekel, 2020). Small, fluid-filled cavities begin to form within the secondary follicle and eventually coalesce to form a large antrum. The formation of the antrum further divides GCs into cumulus GCs that surround the oocyte, and mural GCs that line the inside of the follicle wall. Most follicles undergo atretic degeneration at the antral stage. However, the ones that are selected for maturation become stimulated by FSH that is released from the pituitary gland. The influence of FSH induces further GC proliferation and supports oocyte growth. The fully grown follicles that reach the preovulatory stage are termed Graafian follicles in humans (McGee & Hsueh, 2000). The oocyte will be ovulated from the mature Graafian follicle, leaving the remaining granulosa and theca cells to form the corpus luteum that will support pregnancy.

Oocyte growth is mutually interdependent with the differentiation and growth of the follicle (Hutt & Albertini, 2007). Over oogenesis, the oocyte increases from approximately 20 μM to 70-120 μM, depending on the species (Erdogan *et al*., 2005). Oocytes that have reached approximately 80% of their full size (~75-85 μM in mice), become meiotically competent and can progress past prophase I (Wasserman *et al*., 1979; Demeestere *et al*., 2012). Luteinizing hormone (LH) is secreted from the pituitary gland and binds to receptors in GCs. This induces fully mature oocytes to complete meiosis I and re-arrest at metaphase II (MII) of the second meiotic cycle until fertilization. In humans, a single follicle containing a meiotically competent oocyte will usually be ovulated in response to the LH surge, whereas 8-12 oocytes may be stimulated to undergo ovulation in mice (Martin-Coello *et al*., 2008).

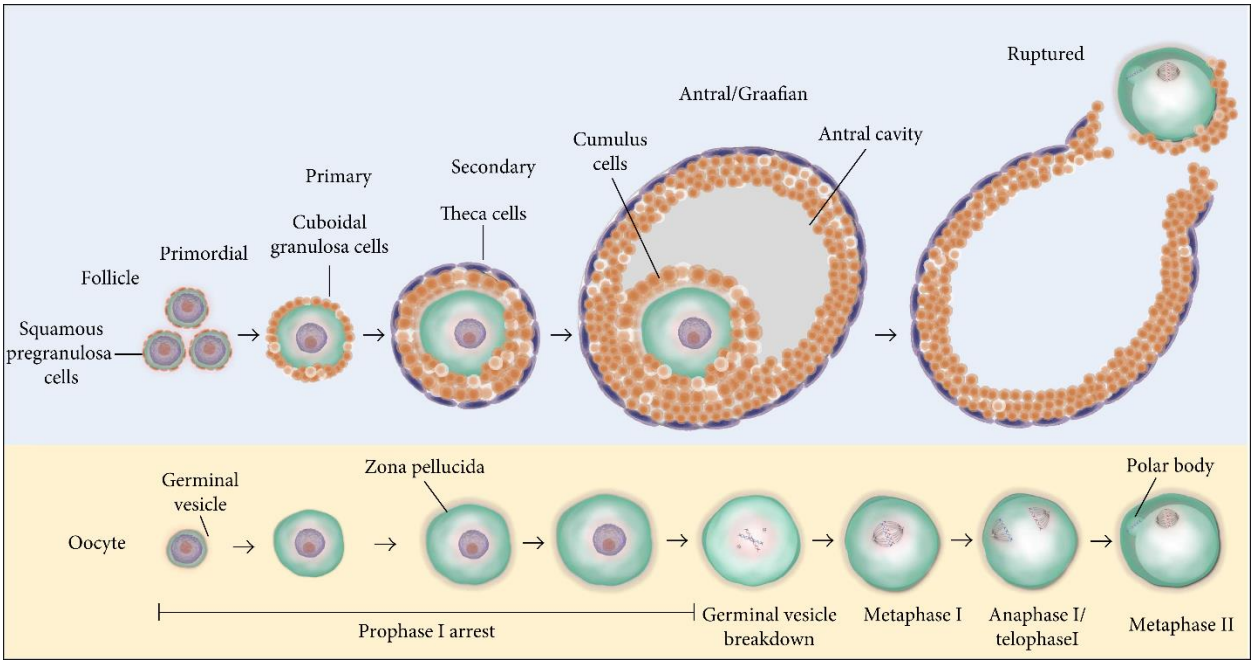


**Figure 1. Folliculogenesis and oocyte maturation.**

Schematic progression of follicle and oocyte growth, from the immature oocyte within the primordial follicle to the ruptured metaphase II (MII) oocyte from the antral follicle. Primordial follicles with pregranulosa cells surround an immature GV oocyte arrested at prophase I. As the pregranulosa cells change to cuboidal in shape, the primary follicle is formed. The secondary follicle is characterized by the proliferation of granulosa cells that form multiple layers, the theca layer, and a zona pellucida surrounding the oocyte. The antral/Graafian follicle forms with the development of the fluid-filled antrum. The oocyte achieves meiotic competence involving germinal vesicle breakdown and the completion of meiosis I in the last stage of folliculogenesis and a mature MII oocyte is released from the follicle. This image was obtained with permission from Mihalas, B.P., Redgrove, K.A., McLaughlin, E.A., & Nixon, B. (2017). Molecular Mechanisms Responsible for Increased Vulnerability of the Ageing Oocyte to Oxidative Damage. *Oxid Med Cell Longev.* doi: 10.1155/2017/4015874.

## 1.2 Cell communication within the ovarian follicle

There is an overall interdependence between compartments within the ovarian follicle and two distinct modes of intercellular communication: direct and secreted transfer signalling (Marchais *et al*., 2022). Follicle viability is supported through direct transfer signalling, such as the diffusion and exchange of peptides, hormones, and metabolites (Russell *et al.,* 2016). The oocyte is largely dependent on the enclosing cumulus cells to conduct communication via the transfer of various molecules (Macaulay *et al*., 2014; Turanthum *et al*., 2021). Cumulus cells provide a supportive role involving metabolism, cytoskeletal arrangements, and meiotic arrest and resumption (Coticchio *et al*., 2015). Cumulus cells form a pseudostratified epithelium and communicate with the oocyte via membrane extensions (Turathum *et al*., 2021). Paracrine signalling through the follicular fluid from the outer follicular cells towards the cumulus-oocyte complex increases as the follicle grows (Marchais *et al*., 2022). Several molecules are secreted by GCs that support folliculogenesis such a neurotrophins and neuronal growth factors (Streiter *et al.,* 2016; Chang *et al.,* 2019), and epidermal growth factor (EGF)-peptides for receptors expressed on cumulus cells (Richani & Gilchrist, 2018)

One mechanism of communication between the oocyte and follicular somatic cells is through gap junctions. Connexins are trans-membrane proteins that assemble to form gap junctions spanning two cell membranes. The small pore size of the intercellular cytoplasmic channel allows for the transfer of ions, metabolites, amino acids, and secondary messengers like cyclic adenosine monophosphate (cAMP) and cyclic guanosine monophosphate (cGMP) (Bruzzone *et al.*, 1996). The connexins particularly important for communication within the follicle are connexin 37 (Cx37) and connexin 43 (Cx43). Cx37 forms the gap junction between the oocyte and cumulus cells, whereas Cx43 is between the cumulus and granulosa cells

(Gershon *et al*., 2008). Both Cx37 and Cx43 are necessary for folliculogenesis, as mice lacking either connexin show arrested follicular development (Simon *et al.,* 1997; Ackert *et al*., 2001).

The oocyte also has a crucial part in supporting folliculogenesis. Oocyte-derived factors such as growth differentiation factor-9 (GDF9), and bone morphogenic protein-15 (BMP-15) regulate granulosa and cumulus cell proliferation and follicular growth rate (Gilchrist *et al*., 2008; Russell *et al*., 2016). Furthermore, oocyte growth and follicular growth support each other mutually. The growth factor kit ligand (KL) is secreted from GCs and binds to its tyrosine kinase receptor (c-KIT), expressed in oocytes (Parrott & Skinner, 1997; Thomas & Vanderhyden, 2006). This promotes oocyte growth. The KL/c-KIT interaction may also be important for primordial follicle activation, and subsequent follicular growth from the primordial to preovulatory stage (Yoshida *et al.,* 1997).

### 1.3 Meiotic Arrest at Prophase 1

Meiotically incompetent oocytes exist within the follicle from the primordial stage until ovulation is triggered from the mature Graafian follicle. Oocytes gradually acquire competence as they grow and accumulate sufficient levels of maturation- or M phase promoting factor (MPF). Cyclin dependent kinase 1 (CDK1) and cyclin B make up the enzymatic and regulatory subunits of the MPF complex, whose activity regulates the $G_2$ to M phase transition (Eppig *et al*., 2004). The meiotic arrest at prophase I is attributed to low MPF activity, due to the reversible inhibitory phosphorylation of CDK1 (Adhikari *et al*., 2012) and high levels of cAMP (Liu & Adhikari, 2014). Protein kinase A (PKA) is activated with elevated cAMP and will phosphorylate the substrate Wee1 $G_2$ checkpoint kinase (Wee1) and the membrane-associated tyrosine/threonine-specific Cdc2-inhibitory kinase (PKMYT1, or MYT1) (Liu & Adhikari,

2014). Both Wee1 and MYT1inhibit CDK1 through phosphorylation on threonine-14 and tyrosine-15 (Duckworth *et al*., 2002). Cell division cycle 25 (Cdc25) has a role in reversing negative regulation of CDK1 by the Wee1/MYT1 kinases (Kiyokawa & Ray, 2008). In mouse oocytes specifically, cell division cycle 25 b (Cdc25b) may be inactivated by PKA through phosphorylation on serine-321, which also contributes to meiotic arrest (Zhang *et al*., 2008).

The level of cAMP within the oocyte is the overarching mechanism of maintaining meiotic arrest. cAMP is synthesized from G-protein-linked receptor (GPR) 3 and GPR12 in mice (Liu *et al*., 2013) that stimulates $G_s$ protein which in turn activates the enzyme adenyl cyclase in the plasma membrane (Mehlmann, 2005). Elevated levels of cAMP are maintained when the enzyme phosphodiesterase (PDE) 3A is inhibited and incapable of hydrolyzing cAMP. The negative regulation of PDE3A is dependent on high levels of cGMP that is synthesized in cumulus and mural GCs and diffuses into the oocyte via gap junctions (Masciarelli *et al*., 2004; Norris *et al*., 2009). cGMP directly inhibits PDE3A by binding to the catalytic site and acting as a competitive inhibitor of cAMP hydrolysis (Norris *et al*., 2009). cGMP is synthesized from guanosine triphosphate (GTP) by guanylyl cyclase natriuretic peptide receptor 2 (NPR2), located on the membrane of cumulus GCs (Robinson et al., 2012). The ligand natriuretic peptide type C (NPPC) is secreted by mural GCs but binds to NPR2 and stimulates its activity in the cumulus GCs (Wigglesworth *et al*., 2013). This coordinated series of steps maintains sufficient levels of cGMP and cAMP required for meiotic arrest.

### 1.4 Meiotic Maturation

The immature oocyte arrested in prophase I is characterized by a large nucleus with a single nucleolus at its center, referred to as the germinal vesicle (GV). Meiotic maturation is

defined as the transition from GV oocyte to MII egg at the time of ovulation that is triggered by a surge in LH (Sorensen & Wassarman, 1976). Around the time of antrum formation and as the oocyte nears the completion of the growth phase, meiosis I resumes and the nuclear envelope of the oocyte breaks down. Germinal vesicle breakdown (GVBD), condensation of chromosomes, meiotic spindle formation and the extrusion of the first polar body mark the process of meiotic maturation (Sorensen & Wassarman, 1976). Mouse oocytes are required to be a certain diameter for GVBD to occur, as oocytes smaller than 60 μM in diameter remain indefinitely meiotically incompetent (Sorensen & Wassarman, 1976). This could be due to suboptimal levels of essential cell cycle components such as CDK1 or insufficient dimerization of cyclin B, mediated by Wee1 and Cdc25, that prevents the complex from localizing to the nucleus and regaining MPF activity (Mitra & Schultz, 1996; Kanatsu-Shinohara *et al*., 2000; Solc *et al*., 2010).

Following the surge in LH, meiosis can resume *in vivo* when LH binds to its receptors which are restricted to the mural GCs. In response, mural GCs produce and secrete EGFs that bind to EGF receptors (EGFRs) located on the cumulus cells directly surrounding the oocyte (Park *et al*., 2004). Once activated, EGFR undergoes autophosphorylation and stimulates the activation of several signalling pathways involved in meiotic resumption. One of these pathways involves mitogen-activated protein kinases (MAPKs), specifically MAPK3/1 (also known as ERK1/2) (Liang *et al*., 2007). MAPK activity reduces the permeability of gap junctions between cumulus cells and the oocyte by phosphorylating Cx43 (Norris *et al*., 2008). This contributes to a decrease in both cAMP and cGMP in the oocyte that induces both meiotic resumption and cumulus expansion prior to ovulation (Okudaira *et al.,* 2017; Turathum *et al*., 2017). Sufficiently low levels of cGMP releases PDE3A from its inactive state and allows for cAMP to be hydrolyzed, which also reactivates MPF (Norris *et al.,* 2009; He *et al*., 2021). When LH levels

increase, adenylate cyclase inactivates and causes a subsequent decrease in cAMP, that in turn downregulates PKA activity (Liang *et al*., 2007). Both MAPK activation in GCs and PKA inactivation in the oocyte allows the MPF complex to reactivate through the inhibition of MYT1 and phosphorylation of Cdc25. Once activated, Cdc25 catalyzes the dephosphorylation of CDK1 (Kiyokawa & Ray, 2008). This sequence of events activated by the surge in LH and subsequent decrease in cAMP are necessary for meiosis to resume.

One of the major underlying mechanisms of meiotic resumption after the LH surge is the decrease in cGMP in the surrounding cumulus cells, but the precise transfer of signalling and changes to cGMP dynamics have not been completely defined. The LH surge decreases the permeability of gap junctions between the GCs throughout the follicle, effectively reducing the diffusion and therefore concentration of cGMP (Norris *et al*., 2009). Within 20 minutes of LH signaling, NPR2 is inactivated in the mural GCs (Robinson *et al*., 2012), and a corresponding decrease in cGMP occurs in the oocyte, mural, and cumulus GCs (Shuhaibar *et al.,* 2015). NPR2 activity in the cumulus cells decreases after 2-3 hours, likely as a result of the location of LH receptors in the mural GCs (Robinson *et al*., 2012). There is a requirement for a continuous supply of NPPC from the mural GCs, and the removal of the GV oocyte or COC from the follicle induces meiotic resumption even in the absence of LH *in vivo* (Richard & Baltz, 2017). *Nppc* mRNA significantly decreases after LH receptor stimulation (Kawamura *et al*., 2011) and may consequently lower NPPC levels in the follicle at a time that corresponds to nuclear envelope breakdown in the oocyte (Robinson *et al*., 2012). However, it has been suggested that the decrease in NPPC is specifically induced by EGF-like factors derived from LH signalling (Pan & Li, 2019). EGF-like factors in the mural GCs may act as autocrine or paracrine factors and bind to EGFR to decrease NPPC, or contribute to NPR2 inactivity in cumulus GCs,

respectively (Pan & Li, 2019). The inactivation of NPR2 likely only contributes to a part of the cGMP decrease. cGMP-Phosphodiesterases (cGMP-PDEs), specifically cGMP-PDE5, are upregulated following the LH surge, and may play a vital role in the resumption of meiosis (Egbert *et al*., 2018). The reduced permeability of gap junctions, NPPC/NPR2 signalling, and the upregulation of cGMP-PDEs all contribute in part to decreased levels of cGMP in the follicle, however, some aspects of the complex signalling pathways are still not understood.

The reactivation of MPF allows the oocyte to progress past metaphase I (MI). In mammalian cells, completing meiosis I appears to be mediated by the degradation of cyclin B, by anaphase-promoting complex/cyclosome (APC/C) (Jones, 2005). MPF levels decrease with the first meiosis to allow the segregation of homologous chromosomes (Jones, 2005), but are re-established after the first polar body is extruded. The high level of MPF prevents further progression and forces the oocyte into second meiosis where it re-arrests in MII (Dekel, 2005). The arrest in MII is sustained by cytostatic factor (CSF), where the loss of CDK1 and cyclin B is prevented, and MPF remains stable (Madgwick & Jones, 2007). The inhibition of APC/C prevents cyclin B degradation. Early mitotic inhibitor (EMI) 2 (mammalian orthologue of *Xenopus* Emi1) has been found to directly inhibit APC/C (Liu & Maller, 2005) and may establish the MII arrest (Madgwick & Jones, 2007). However, there are other pathways that may maintain CSF (Madgwick & Jones, 2007). The major pathway involves MOS, which activates an MAPK kinase (referred to as a MEK). MOS protein synthesis results in the phosphorylation of MEK, which subsequently phosphorylates MAPK, which induces a phosphorylation cascade that may stabilize MPF (Madgwick & Jones, 2007). The MOS-MEK-MAPK pathway is involved in MII arrest in mouse oocytes (Phillips *et al.,* 2002), however how it acts on MPF is not fully

elucidated. Both MOS and EMI2 likely contribute to CSF that ultimately keeps the oocyte arrested in the MII stage. The MII oocyte completes meiosis after fertilization occurs.

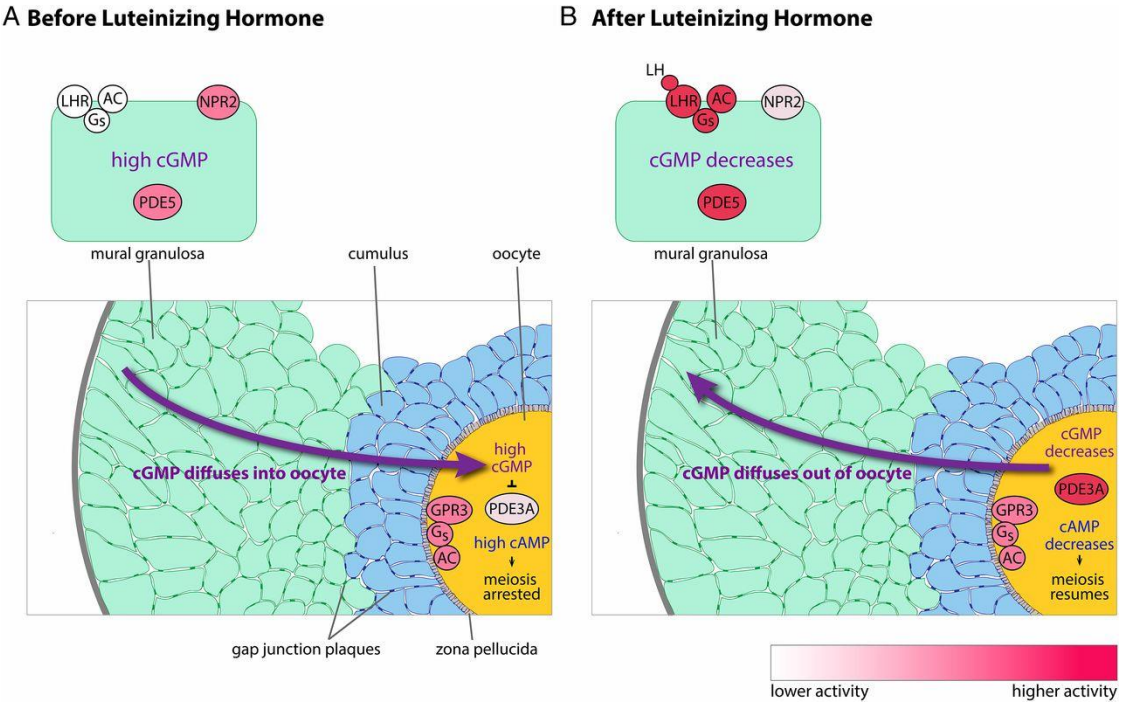


**Figure 2. Meiotic arrest and resumption.**

**A)** Prior to LH exposure, cGMP diffuses into the oocyte via gap junctions and is maintained at a high level through production by the NPR2 guanylyl cyclase located in the cumulus and mural granulosa cells. High levels of cGMP inhibit the phosphodiesterase (PDE) 3A, which prevents cAMP hydrolysis and maintains cAMP at a level sufficient to maintain arrest. cAMP is synthesized from adenylyl cyclase 3 which is kept active via the constitutive activity of the Gs-coupled receptor GPR3**. B)** After LH exposure, $G_s$ activates and induces the dephosphorylation of NPR2, effectively decreasing cGMP. Activity of the cGMP phosphodiesterase, PDE5, increases and degrades cGMP. These two processes cause cGMP to diffuse down its concentration gradient and the decrease of cGMP in the oocyte allows PDE3A to re-activate and hydrolyze cAMP. The low level of cAMP within the oocyte induces meiotic resumption. This image was obtained with permission from: Shuhaibar L.C., Egbert J.R., Norris, R.P., Lampe P.D., Nikolaev V.O., Thunemann M., Wen L., Feil R., and Jaffe L.A. (2015). Intercellular signaling via

cyclic GMP diffusion through gap junctions restarts meiosis in mouse ovarian follicles. PNAS; 112:5527-5532.

## 1.5 Ovulation

Ovulation is the rupture of the mature antral follicle and the release of the meiotically competent oocyte with its surrounding cumulus cloud. The COC is swept into the oviduct where the oocyte may be fertilized. Prior to ovulation, follicular cells break contact with the oocyte and increase the synthesis of high molecular weight proteoglycans and tissue plasminogen activator (Hogan *et al.,* 1994). The amount of follicular fluid increases and the mature follicle moves to the periphery of the ovary. In the follicle, baseline levels of LH stimulate androgen production from theca cells, and FSH stimulates granulosa cells to convert androgens into oestrogens (Marchais *et al*., 2022). When oestrogens reach a certain level, an LH surge is triggered and a positive feedback signal initiates both meiotic maturation and ovulation (Marchais *et al.,* 2022). The LH receptor is localized to mural GCs and is stimulated when pre-ovulatory follicles are growing, which allows only the selected follicles to respond to the LH surge (Peng *et al*., 1991). When LH binds to its receptors, $G_s$ is activated, which in turn activates adenyl cyclase and causes an increase in cAMP (Jaffe & Egbert, 2017). cAMP-dependent protein kinase activation leads to a cascade of signalling that activates proteolytic enzymes that break down the follicle wall (Takahashi *et al.,* 1995; Rose *et al*., 1999). The increase of prostaglandins changes the regional blood flow of the follicle, which heightens intrafollicular pressure and contributes to the release of an oocyte (Brännström *et al*., 1998). The release of EGF-like growth factors from LH-stimulated GCs stimulates further intracellular signalling and gene transcription of products required for successful ovulation, such as hyaluronic acid (HA) secretion for cumulus cell expansion (Park *et al.*, 2004).

Expansion of cumulus cells, or mucification, occurs when HA is synthesized from the cumulus GCs after stimulus by FSH. HA binds to cumulus cells and embeds them in a gelatinous

matrix to aid oocyte rupture from the follicle and subsequent fertilization (Vanderhyden *et al*., 1990; Eppig *et al*., 2001; Zhuo & Kimata, 2001). The fully grown oocyte has a role in cumulus expansion and ovulation, through the secretion of cumulus expansion-enabling factors (CEEFs) that induce GCs to produce HA through the transcription of hyaluronic synthase 2 (HAS-2) enzyme (Eppig *et al*., 2001; Richards, 2005). It has been suggested that GDF-9 is a CEEF (Elvin *et al.,* 1999) and may have a role in inducing preovulatory signalling cascades required for mucification. Other factors upregulated for mucification include the enzyme cyclooxygenase 2 (COX-2) enzymes and the tumor necrosis factor-inducible gene 6 protein (TSG-6). HAS-2 and COX-2 interact synergistically to produce hyaluronic acid (HA) and induce the production of prostaglandins that change gene expression and influence cumulus-oocyte-complex expansion (Hizaki *et al*., 1999). TSG-6 is a hyaluronic acid binding protein expressed in cumulus GCs that has a role in cumulus matrix formation, cell differentiation and cumulus expansion (Freitas de Medeiros *et al.,* 2021).

Ovulation requires the coordinated response of both the oocyte and follicular cells. In mice, ovulation can occur approximately every four days under the optimal conditions (Hogan *et al.,* 1994). Once ovulated, the oocyte and its surrounding cloud of cumulus cells are swept into the infundibulum of the oviduct and await to be fertilized.

### 1.6 Preimplantation embryo development

The ovulated MII oocyte travels toward the expanded ampulla in the oviduct for fertilization. The oocyte reactivates following the sperm-egg fusion, that triggers $Ca^{2+}$ oscillations. The initial $Ca^{2+}$ release is stimulated by the testis-specific sperm factor, phospholipase C zeta (PLCζ) (Saunders *et al*., 2002), that catalyzes the generation of inositol

1,4,5-triphosphate ($IP_3$). $IP_3$ binds to its receptor in the endoplasmic reticulum (ER) membranes and triggers $Ca^{2+}$ release from $IP_3$-sensitive ER stores (Miao & Williams, 2012; Xu *et al*., 1994). The intracellular $Ca^{2+}$ oscillations activate APC/C and lead to APC/C-dependent cyclin B degradation, that allows the egg to complete the second meiosis (Nixon *et al*., 2002). Following the penetration of the egg plasma membrane, the second polar body is emitted and the zygote, or one-cell embryo, is formed. The one-cell embryo contains two distinct pronuclei (PN) with the maternal and paternal genetic material that will migrate to the center of the embryo and align on the first mitotic spindle (Scheffler *et al*., 2021). The destruction of most of the maternal mRNA coincides with the onset of the zygotic genome activation (ZGA) process that persists until the end of the two-cell stage (Schultz, 1993; Mihajlovic & Bruce, 2017). After ZGA, the embryo is able to rely on its own zygotic genome, through the production of its own mRNA.

The one-cell embryo undergoes a series of asynchronous cell cleavage divisions without increasing in volume (Tscherner *et al.,* 2021). At the two- and four-cell stages, the mouse embryo is totipotent (Maemura *et al.,* 2021) and the individual cells are referred to as blastomeres (Gilbert, 2000). The cells undergo compaction from the 8- to 16-cell stages, a process involving intracellular and intercellular reorganization (Pratt *et al*., 1982). Surface adhesion molecules are expressed and tight junctions form between blastomeres to form the morula (Mihajlovic & Bruce, 2017). Late-stage morulae undergo cavitation, which is the formation of the fluid-filled blastocoel. The embryonic cells differentiate into two distinct lineages at this stage, based on their location and polarity. Outer, polarized blastomeres will give rise to the trophectoderm, and non-polarized inner blastomeres will become the inner cell mass (ICM) (Mihajlovic & Bruce, 2017). The trophectoderm encloses the blastocoel cavity and eventually becomes the fetal portion of the placenta, whereas the ICM lies inside the blastocoel and is made up of epiblast and

primitive endoderm progenitors that promote fetal tissue formation, and extraembryonic membranes, respectively (Gasperowicz & Natale, 2011). In mice, the blastocyst implants in the uterine wall approximately five days after fertilization.

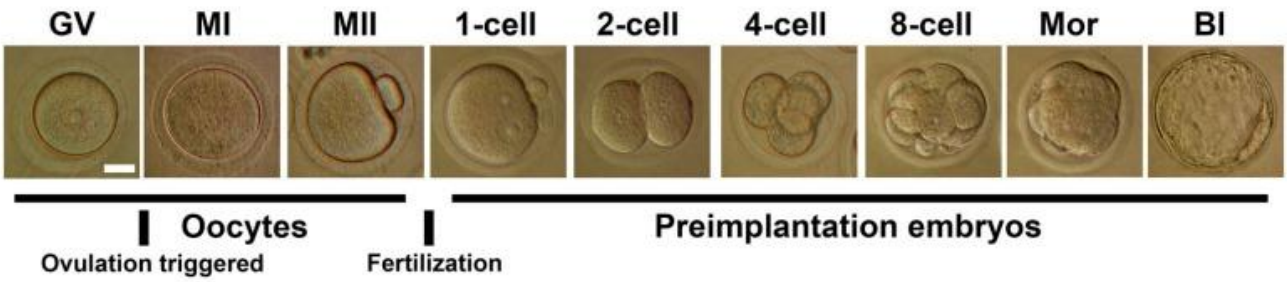


**Figure 3. Oocyte and preimplantation embryo development.**

GV oocytes arrested in prophase I undergo meiotic maturation when ovulation is triggered with a surge in LH. The oocytes proceed through metaphase I (MI) and re-arrest at metaphase II (MII) during meiotic maturation. Following fertilization, the one-cell embryo forms and undergoes a series of cleavages until it begins to compact at the 8-cell stage and eventually forms the morula (Mor). Late-stage morula undergo cavitation and form the fluid-filled blastocoel. The blastocyst (Bl) stage is characterized by the formation of the trophectoderm lining the blastocoel, and the inner cell mass (lower right). This image was obtained and adapted with permission from Tscherner, A.K., Macaulay, A.D., Ortman, C.S., & Baltz., J.M. (2021). Initiation of cell volume regulation and unique cell volume regulatory mechanisms in mammalian oocytes and embryos. *Journal of Cellular Physiology.* DOI:10.1002/jcp.30352.

### 1.7 The development of embryo culture media and in vitro maturation

Mouse preimplantation embryo culture media have drastically changed and been improved over the years, due to a better understanding of the physiological processes that take place in *in vitro* culture conditions. The transfer of rabbit embryos in 1891 was the first successful embryo transfer that resulted in live offspring (Heape, 1891). The first successful culture of rabbit blastocysts followed in 1912 (Brachet, 1912). These foundational experiments led to a series of advancements in embryo culture media that would eventually result in ideal conditions for complete embryo development *in vitro.* The first successful human embryo culture, fertilization and transfer *in vitro* took place in 1978, and resulted in a live birth (Steptoe & Edwards, 1978).

Undefined complex biological fluids such as blood plasma and serum were among the first attempts of culture media for embryos developing *in vitro* (Alexandre, 2001). Simple balanced salt solutions such as Krebs-Ringer, Tyrode's and Gey's were later determined to be best for maintaining preimplantation embryo development (Adams, 1956; Brinster, 1963; Whitten, 1956). Modifications to the balanced salt solutions eventually led to the development of the staple mouse embryo culture medium, M16 (Whittingham, 1971). The first modifications were bovine serum albumin and glucose which allowed eight-cell mouse embryos to develop into viable blastocysts (Whitten 1956), followed by the addition of lactate as a metabolic substrate that extended embryo culture from the two-cell stage to blastocyst (Whitten, 1957). Lastly, the addition of pyruvate was the pivotal modification that supported cleavage to the two-cell embryo stage (Biggers *et al.,* 1967). A fundamental problem still existed in which mouse one-cell embryos could not progress to the blastocyst stage, and instead arrested at the late two-cell stage (Goddard & Pratt, 1983). As discussed below, potassium simplex optimized medium

(KSOM) was designed, and the "two-cell block" could be surmounted. KSOM is the most widely used embryo culture media for mouse oocytes and embryos, which supports development from fertilized eggs through blastocysts (Lawitts & Biggers, 1991; Lawitts & Biggers, 1993).

### 1.8 Overcoming the "2-cell block"

Culturing mammalian embryos from fertilization to the blastocyst stage was still unsuccessful in the classic embryo culture media, M16, and similar media due to the developmental block that occurred in the late $G_2$ stage of the second embryonic cell division (Wang *et al*., 2011). The contributions of the National Cooperative Program on Non-Human *In Vitro* Fertilization and Preimplantation Development, or "Culture Club", implemented by the US National Institute of Child Health and Human Development of the National Institutes of Health accelerated progress on overcoming developmental blocks (Baltz, 2013) by leading to the development of Chatot Ziomek Bavister embryo culture medium (CZB) (Chatot *et al*., 1989) and KSOM (Lawitts & Biggers, 1991). The most significant difference between contemporary and earlier culture media was that KSOM and CZB had lower osmolarities of 250 mOsM and 275 mOsM, while M16 was closer to physiological range at 290 mOsM (Baltz, 2013). Mouse oviductal fluid has an osmolarity of about 300 mOsM (Collins & Baltz, 1999), which suggested that the two-cell block was due to imbalances or deficiencies in the media that elicited a stress response in the embryos and prevented further development (Baltz & Tartia, 2010). It was discovered that the addition of amino acids such as glutamine (Lawitts & Biggers, 1992), and glycine (Van Winkle *et al.,* 1990) improved development from fertilized oocytes, and protected against increased NaCl *in vitro*. With the addition of glycine to culture media, embryos could progress past the two-cell stage even at an osmolarity of 340 mOsM (Wang *et al*., 2011). Betaine

(*N, N, N*-trimethylglycine), a major organic osmolyte in the mammalian kidney, also displayed protective abilities against increased osmolarity when added to culture media (Biggers *et al*., 1993). The accumulation of these amino acids and the development of an embryo culture media at a lower osmolarity were therefore key elements in overcoming the two-cell block (Lawitts & Biggers, 1992; Biggers *et al.,* 1993; Biggers, 1998).

### 1.9 Osmolarity, osmolality and tonicity

Osmosis is the net movement of water flowing from an area of low solute concentration to an area of high solute concentration to achieve equilibrium on both sides of a semi-permeable membrane (Strange, 2004). Osmolarity is the measure of the osmotic pressure exerted by a solution and is expressed as osmoles per liter (OsM). Osmolality (osmoles per kilogram) and osmolarity are similar and used interchangeably in a physiological context where solutions are relatively dilute (Baltz, 2001), but are conceptually different from tonicity. Tonicity is the osmotic pressure of one solution relative to another across a semi-permeable membrane (Baltz, 2001). Tonicity influences cell volume due to the semi-permeability of the membrane, that permits the movement of water through the aquaporin channels but prevents the movement of most other molecules. Osmotic pressure is generated as a result of the inhibited transport of the other solutes (Baltz, 2001).

### 1.10 Cellular responses to fluctuations in tonicity in preimplantation embryos

An isotonic cellular environment keeps the cell in homeostasis and the cell volume stable, as water does not flow into or out of the cell. The volume of a cell changes via water loss or

water gain, as induced by changes to internal or external solute concentrations. Changes in tonicity drive a difference in osmotic pressure between the intracellular compartment and the external environment, resulting in either cell swelling in a hypotonic solution, or cell shrinking in a hypertonic solution (Argyropoulos *et al*., 2016). Cells must be able to independently regulate their volume for survival and proper physiological functioning. Long-term exposure to unsuitable osmotic conditions can negatively influence cell growth and cell proliferation and can cause cell death (Hoffman *et al*., 2009). Cells have therefore evolved physical mechanisms and signalling pathways that are upregulated in response to fluctuations in tonicity. MAPK pathways are vital in mediating cell volume responses in somatic cells, oocytes, and preimplantation embryos. p38 MAPKs are present all throughout mouse oocyte and preimplantation embryo development (Natale *et al.,* 2004), and are specifically activated in blastocysts when the osmolarity increases and the cell shrinks (Sheikh-Hamad & Gustin, 2004). A second MAPK pathway, stress-activated protein kinase/Jun-amino-terminal kinase (SAPK/JNK), is also present in blastocysts and is upregulated in response to hypertonicity (Xie *et al.,* 2007; Bell *et al.,* 2009; Hoffman *et al.,* 2009).

Cells have developed membrane transport mechanisms to avoid osmotic stress induced by perturbations to cell volume. The volume recovery processes generally fall under two categories: acute and long-term adaptations for cell volume recovery. Cells will either undergo a regulatory volume increase (RVI) that involves the import of inorganic ions into the cell, or a regulatory volume decrease (RVD) that drives the efflux of nonessential ions and osmolytes out of the cell. The influx or efflux of water that accompanies RVI and RVD restores the cell to its homeostatic volume. In murine preimplantation embryos, mRNAs for aquaporins (AQPs) 1, 3, 5,

6, 7, 8, and 9 are expressed throughout development (Offenberg et al., 2000), and allow water to flow across the membrane in the direction of osmotic gradients (Shiels & Griffin, 1993).

### 1.11 Mechanisms of acute cell volume recovery

When the volume of a cell decreases, the first response involves the accumulation of inorganic ions accompanied by an osmotically driven influx of water to increase the cell volume, otherwise known as RVI (Hoffman et al., 2009). This mechanism occurs primarily via the coupled activation of $Na^+/H^+$ (NHE) antiporters and $Cl^-/HCO_3^-$ (AE family) exchangers, that import $Na^+$ and $Cl^-$. NHE1 (*Slc9a1* gene) is activated when the cell shrinks, causing an increase in intracellular pH ($pH_i$), from the influx of $Na^+$ and efflux of $H^+$ (Orlowski & Grinstein, 2004). AE2 (*Slc4a2* gene) is subsequently activated by the increase in $pH_i$ (Humphreys *et al*., 1995; Jiang *et al*., 1997), and decreases the $pH_i$ by driving the influx of $Cl^-$ and the efflux of $HCO_3^-$ (Zhou & Baltz, 2013). The coaction of the exchangers results in no net change in $pH_i$, and the import of both $Na^+$ and $Cl^-$ rapidly restores cell volume equilibrium. NHE1 has been extensively studied, though the mechanism by which it is activated is not fully understood. NHE1 is ubiquitous, and it has been suggested that NHE1 is activated through regulation by protein kinases occurring upstream (Zhou & Baltz, 2013). The non-receptor tyrosine kinase, Janus kinase 2 (Jak2), is also upregulated when the cell volume decreases and may phosphorylate calmodulin (CaM), that binds to and activates NHE1 (Garnovskaya *et al.,* 2003; Zhou & Baltz, 2013). The NHE1 isoform is the primary $pH_i$ regulatory mechanism in mouse preimplantation embryos, (Siyanov & Baltz, 2013) and has the most robust activity in two-cell embryos (Zhou & Baltz, 2013).

While accumulating ions is essential for regulating cell volume decreases, preimplantation embryos also require a mechanism of osmolyte release when cells swell. This

mechanism is referred to as RVD, that is mediated through the activity of functionally coupled $K^+$ and $Cl^-$ channels. There are multiple $K^+$ channels that mediate cell swelling, such as those activated from elevated levels of intracellular $Ca^{2+}$ in certain cell types (Hoffman & Dunham, 1995; Seguin & Baltz, 1997). The $Cl^-$ channels are known as volume-regulated anion channels (VRACs), or volume-sensitive organic osmolyte and anion channels (VSOACs). These channels are nearly ubiquitous and activate upon cell swelling to mediate the efflux of both inorganic and organic osmolytes (Strange *et al*., 1996; Okada *et al*., 1997). VRAC/VSOACs are composed of five members of the LRRC8 protein family (LRRC8A-E) that form multimeric complexes to produce functional channels. LRRC8A, also known as SWELL1, is essential for physiological functions and forms a heteromeric complex with any of the other isoforms. The subunit composition determines the substrate selectivity and biophysical properties of the channel (Qiu *et al*., 2014).

Like somatic cells, oocytes and preimplantation embryos possess swelling-activated channels with permeability to taurine, glycine, and β-alanine (Van Winkle *et al.,* 1994; Dawson *et al*., 1998; Kolajova & Baltz, 1999; Sonoda *et al.,* 2003). Swelling-activated whole-cell currents were detected in one-cell embryos (Kolajova *et al*., 1999), and permeability to taurine and glycine increased as a result of cell swelling (Kolajova *et al.,* 1999; Kolajova *et al*., 2001), providing evidence of VRAC/VSOACs in mouse preimplantation embryos. However, the composition of VSOAC in preimplantation embryos remains to be elucidated, as well as whether VRAC/VSOACs have a role in regulating betaine levels during preimplantation embryo development.

### 1.12 Mechanisms of long-term cell volume equilibrium

Significant accumulation of inorganic ions can increase intracellular ionic strength to a level that can be harmful for cell homeostasis. For oocytes and preimplantation embryos that exist in hypertonic conditions, organic osmolytes are taken up to replace a portion of intracellular inorganic ions and mitigate the effects of high intracellular ionic strength (Baltz & Tartia, 2010).

The uptake of organic osmolytes is a mechanism of ensuring long-term cell volume equilibrium in hypertonic conditions. Organic osmolytes are small, neutrally charged organic compounds that can be accumulated at high concentrations to provide intracellular osmotic support without disrupting cell function (Yancey *et al.,* 1982; Garcia-Perez & Burg, 1991). Most organic osmolytes are transported into the cell via specialized transporters. In mammalian somatic cells, the $Na^+$/myo-inositol transporter (SMIT), betaine/GABA transporter (BGT1), taurine/β-amino acid transporter (TAUT), and the System A amino acid transporter are the four major organic osmolyte transporters (Garcia-Perez & Burg, 1991; Kwon & Handler, 1995; Pastor-Anglada *et al.,* 1996). Glycine, glutamine, betaine (Van Winkle *et al*., 1990; Lawitts & Biggers, 1992; Biggers *et al*., 1993), proline, and β-alanine (Dawson & Baltz, 1997) all have documented osmoprotective effects in mouse preimplantation embryos. The transporters expressed in both somatic cells and preimplantation embryos are TAUT, which transports β-alanine (Van Winkle et al., 1994; Hammer & Baltz, 2003) and System A, which transports all the aforementioned compounds but is present only in blastocysts during preimplantation embryo development (Jamshidi & Kaye, 1995).

Another transporter expressed both in somatic cells and preimplantation embryos is GLYT1. GLYT1 is a high affinity $Na^+/Cl^-$ dependent member of the neurotransmitter transporter (NTT) family (Nelson, 1998; Steeves *et al*.,2003). The activation of GLYT1 and meiotic

resumption occur simultaneously, although the two processes are not coupled (Tartia *et al.,* 2009). The activity of GLYT1 and glycine accumulation is greatest in early cleavage stage preimplantation embryos, and gradually declines in later preimplantation embryos until it becomes inactive by the blastocyst stage (Steeves *et al.,* 2003; Tartia *et al.,* 2009). In contrast to other organic osmolyte transporters that require hours to days to synthesize the necessary mRNA and proteins to respond to increased osmolarities, (Garcia-Perez & Burg, 1991; Kwon & Handler, 1995; Pastor-Anglada *et al.,* 1996), GLYT1 induces immediate glycine accumulation at high osmolarities (Steeves *et al.,* 2003). GLYT1 therefore has a crucial role in cell volume regulation during mouse embryogenesis.

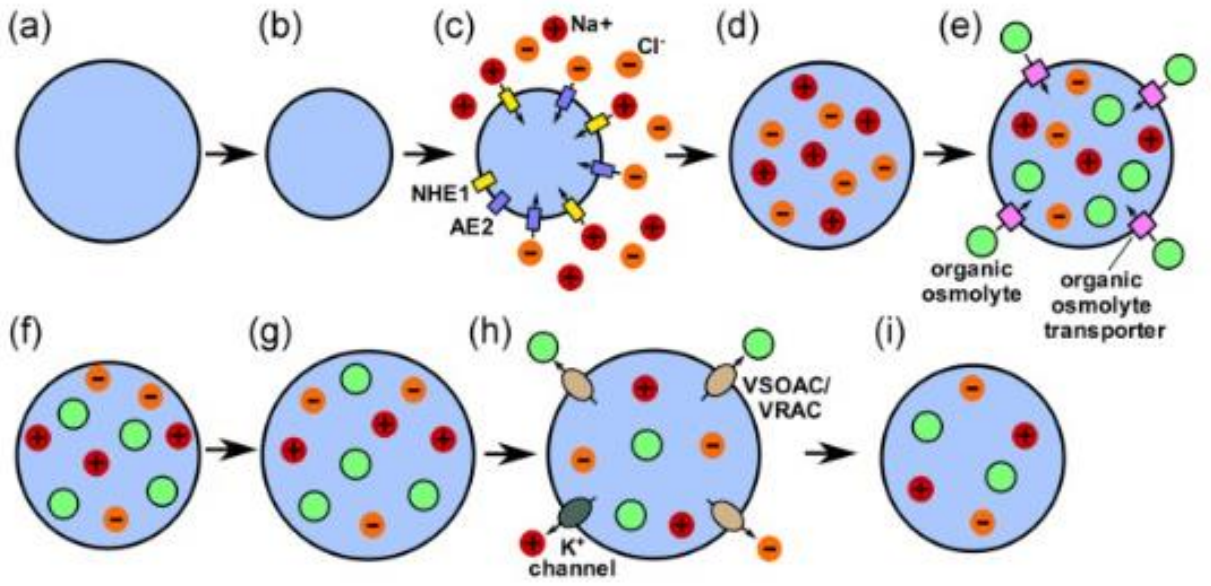


**Figure 4. Schematic representation of mechanisms of cell volume regulation.**

For a cell (a) to recover from a decrease in volume (b), $Na^+/H^+$ (NHE1) and $HCO_3^-/Cl^-$ (AE2) coupled exchangers activate (c) and mediate the influx of inorganic ions to restore the cell to its normal volume and increase intracellular osmolarity (d). The resulting elevated ionic strength can be damaging long term, so some cells have developed the ability to import organic osmolytes into the cell via organic osmolyte transporters (e). The organic osmolytes accumulated replace a portion of the inorganic ions in the cell but still maintain intracellular osmolarity. When a cell (f) increases in volume (g), volume sensitive organic osmolyte and anion channels (VSOACs, also referred to as volume-regulated anion channels (VRACs)) activate and drive the efflux of both inorganic and organic ions (h). This effectively restores the cell to its normal volume (i). This figure was obtained with permission from Tscherner, A.K., Macaulay, A.D., Ortman, C.S., & Baltz., J.M. (2021). Initiation of cell volume regulation and unique cell volume regulatory mechanisms in mammalian oocytes and embryos. *Journal of Cellular Physiology.* DOI:10.1002/jcp.30352.

### 1.13 Betaine as an organic osmolyte

Betaine is a naturally occurring, zwitterionic amino acid derivative that carries a neutral charge at physiological pH. Betaine was first identified in the sugar beet (*Beta vulgaris*) and has since been found at high concentrations in wheat, spinach, and shellfish (Craig, 2004). In humans, a large source of betaine is obtained through the diet and is concentrated to the kidneys, liver, and brain (Craig, 2004), but can also be synthesized *de novo* from choline. Betaine possesses anti-inflammatory mechanisms and may have a role in treating various diseases. In somatic cells, betaine has a major role as an osmoprotectant, specifically in the kidneys and brain (Kempson *et al.,* 2014). In the kidney, betaine has protective effects against hyperosmotic-induced apoptosis (Horio *et al*., 2001), and can increase the cytoplasmic volume and free water content of the cells in hypertonic conditions (Zhao *et al.,* 2018). Betaine is a key player as a methyl group donor used in liver metabolism and in the whole body (Day & Kempson, 2016).

Two betaine transport systems, BGT1 and System A, have been identified in somatic cells. BGT1 can transport both γ-amino-n-butyric acid (GABA) and betaine and possesses a similar nucleotide sequence for GABA transporters in the brain (Kempson *et al*., 2014). BGT1 is a member of $Na^+$ and $Cl^-$ coupled transporters in the SLC6 family that allow the transport of amino acids, neurotransmitters and osmolytes (Chen *et al*., 2004). In hypertonic conditions, BGT1 gene expression increases, and transport activity is upregulated to mitigate osmotic stress in renal cells (Chen *et al.,* 2004). The upregulation of BGT1 is induced by transcriptional activation via tonicity enhancer binding protein (TonEBP), that is synthesized in hypertonic conditions and induces the transcription of genes encoding organic osmolyte transporters (Miyakawa *et al.,* 1999; Woo *et al*., 2002).

In mammalian cells, System A is upregulated in response to hypertonic stress (Ruiz-Montasell *et al*., 1994). Increased betaine uptake through System A in response to hyperosmotic conditions has been documented in syncytiotrophoblasts (Nishimura *et al*., 2010) and hepatic stellate cells (Peters-Regehr *et al*., 1999). Among the subtypes for System A are three SNATs ($Na^+$-dependent, neutral amino acid transporters), referred to as SNAT1, SNAT2, and SNAT4 (Nishimura *et al*., 2014). The substrate selectivity of the System A subtypes are fairly similar, however, betaine uptake appears to be specific to SNAT2 (Nishimura *et al*., 2014). The expression of SNAT2 has been proposed to be regulated by TonEBP (Trama *et al*., 2002). SNAT2 may also be upregulated through the integrated stress response (ISR) pathway, through the osmoadaptation functions of the GADD34 (growth arrest and DNA damage-inducible protein-34) subunit of protein phosphatase 1 (PP1) (Krokowski *et al*., 2017).

### 1.14 Betaine and cell volume regulation in oocytes and embryos

As mentioned above, organic osmolytes are utilized by oocytes and embryos to correct unwanted cell volume decreases and protect against hypertonic stress. Betaine in particular is one of the most effective osmoprotectants in mouse embryos. Betaine added to culture media has been found to support the development of fertilized eggs to preimplantation embryos (Biggers *et al*., 1993; Hammer & Baltz, 2002), and induces a pattern of protein synthesis that more closely resembles that of *in vivo*-produced embryos (Anbari & Schultz, 1993). Further studies showed that adding betaine to the culture media restored blastocyst development (Biggers *et al.,* 1993), and rescued development past the one-cell stage when the osmolarity of the media was increased with either NaCl, or with the trisaccharide, raffinose (Dawson & Baltz, 1997). Betaine has been detected at a concentration of 300-500 μM in murine whole oviducts (Anas *et al*., 2007), which

suggests that it may be available to provide osmoprotection *in vivo,* while the mouse embryo develops prior to implantation. The osmoprotective effects of betaine *in vivo* may translate to added support in culture media for oocytes and preimplantation embryos developing *in vitro.*

### 1.15 Betaine transporters in mouse oocytes and preimplantation embryos

It was initially proposed that organic osmolytes in preimplantation embryos could be divided into substrates of System β, the β-amino acid transporter, and substrates of GLY, the glycine transporter (Dawson & Baltz, 1997). It was assumed that betaine would be transported via the GLY system, given that it is a methylated glycine derivative, and GLY could transport other methylated substrates such as sarcosine (*N*-methylglycine). However, betaine was not transported by GLYT1 (Hammer & Baltz, 2002; Anas *et al*., 2007). The other betaine transporters System A and BGT1 were also ruled out in embryos. System A activity was absent prior to the blastocyst stage (Van Winkle *et al*., 1988), and was not upregulated in early embryos in response to prolonged exposure to hypertonicity (Hammer & Baltz, 2002). Betaine uptake was not inhibited with GABA, excess betaine did not inhibit GABA uptake, and BGT1-like activity was not upregulated in response to increased tonicity in one-cell embryos (Hammer & Baltz, 2002). The amino acid proline also protects preimplantation embryos against increased osmolarity, and a betaine/proline transporter with kinetic and inhibition profiles unique to other transporters in mouse embryos was identified (Baltz, 2001; Anas *et al*., 2007). This unidentified transporter was determined to be $Na^+$ and $Cl^-$ dependent, which gave rise to two candidates; the brain proline transporter (PROT, encoded by *Slc6a7*) and the intestinal imino acid transporter (SIT1, encoded by *Slc6a20a*). SIT1 was identified as the betaine transporter in early embryos, activating shortly after fertilization and becoming quiescent by the four-cell stage (Anas *et al*.,

2008). The measured amounts of endogenous betaine in one- and two-cell embryos corresponds to 6-7 mM, compared to ~0.5 mM in mouse whole oviducts (Anas *et al.,* 2007), and ~4 mM in the liver (Slow *et al*., 2009). SIT1 appears to have a major role in betaine accumulation *in vivo*, but only in early preimplantation embryo development (Anas *et al.,* 2008).

There is no saturable betaine transport in oocytes prior to fertilization and SIT1 activation (Anas *et al*., 2008), however, endogenous betaine was detected in MII oocytes at a level similar to that of one-cell embryos (Corbett *et al.,* 2014). It was hypothesized that COCs possessed a betaine transport system that supplied the enclosed oocyte with betaine through gap junctions, before they became uncoupled during meiotic maturation (Corbett *et al*., 2014). The kinetics, inhibition profile, and $Na^+$ and $Cl^-$ dependency was elucidated for the unknown transporter, which ruled out BGT1, System A, and SIT1. System $y^+$L transport, specifically $y^+$LAT2 (*Slc7a6* gene), was confirmed with mRNA expression and western blot analysis in COCs (Corbett *et al.,* 2014). In addition, the presence of cumulus cells significantly enhanced betaine uptake in the enclosed GV oocyte, illustrating metabolic coupling and a requirement for gap junctions between cumulus cells and the oocyte (Corbett *et al.,* 2014).

While $y^+$LAT2 activity may account for some of the accumulated betaine in MII oocytes, it could not account for the large amount of betaine accumulated during meiotic maturation. The cumulus cloud becomes uncoupled from the oocyte during meiotic maturation and arrests metabolite transfer before betaine reaches maximal endogenous levels in the MII egg. Most of the betaine accumulated during meiotic maturation is synthesized *de novo* via the enzyme choline dehydrogenase (CHDH), as described below.

### 1.16 *De novo* betaine synthesis by choline dehydrogenase

In mammals, betaine is synthesized via a two-step oxidation reaction in which choline is first oxidized in the rate-limiting step by the enzyme CHDH to betaine aldehyde, followed by a second oxidation by betaine aldehyde dehydrogenase (BADH) to betaine (Salvi & Gadda, 2013). In mammals, CHDH is localized to the inner and outer membrane of mitochondria (Park *et al*., 2014), and belongs to the glucose-methanol-choline (GMC) enzyme oxidoreductase superfamily (Salvi & Gadda, 2013). It primarily acts to regulate intracellular choline but can influence tissue homocysteine and S-adenosylmethionine (SAM) concentrations, as betaine is required for the synthesis of both compounds (Johnson *et al.,* 2010). CHDH has a role in supporting male fertility, as deletion of the enzyme results in decreased sperm motility, sperm cells with abnormal mitochondrial morphology, and male infertility (Johnson *et al*., 2010).

CHDH activity has been established to be present primarily in the mammalian liver and kidney (Grossman and Herbert, 1989), however our lab determined that CHDH is also transiently expressed in the developing oocyte over the course of meiotic maturation (McClatchie *et al.,* 2017). The window of CHDH activity during meiotic maturation coincides with significant betaine accumulation *in vivo* (McClatchie *et al*., 2017). Choline is taken up by mouse oocytes through cumulus GCs and transported into the enclosed oocyte via gap junctions until the cumulus cells and oocyte become uncoupled (Eppig, 1982; McClatchie *et al*., 2017). This transported choline serves as the supply required for betaine synthesis throughout oocyte maturation. The mechanism of CHDH activation has not been fully elucidated, although it has been suggested that meiotic progression and regulation by MAPK are involved (McClatchie *et al*., 2017).

While most betaine in oocytes is synthesized during meiotic maturation, and possibly adjusted via $y^+$LAT2 and SIT1, low levels of betaine are present in GV oocytes prior to CHDH activation. It has been proposed that betaine may be synthesized by CHDH elsewhere, such as the liver, (Slow *et al.,* 2009; Johnson *et al*., 2010) and delivered to the follicle via circulation, but further research is required (McClatchie *et al*., 2017).

### 1.17 DNA methylation and one-carbon metabolism

Methylation refers to the addition of a single methyl group on a substrate, or the substitution of a methyl containing group to a substrate. DNA methylation is a type of epigenetic modification that involves the addition of a methyl group to a DNA strand. DNA methylation results in modified RNA or DNA processing, gene expression, or protein function. The methyl group transfer is dependent on the conversion of methionine to SAM, the universal methyl donor (Ratriyanto *et al.,* 2009). SAM forms the cellular methyl pool that is used by most methyltransferases to carry out methylation reactions for epigenetic modifications. SAM is synthesized via one-carbon metabolism (OCM), which encompasses integrated pathways of folate metabolism, the trans- and re-methylation of methionine, and the transsulfuration pathways of homocysteine (Ikeda *et al*., 2012a).

Most SAM is generated from the methionine cycle, in which methionine is converted to SAM, and then SAM is subsequently converted to S-adenosyl homocysteine (SAH) (Ratriyanto *et al.,* 2009). SAH is converted to homocysteine, which competes for two different metabolic pathways (Ratriyanto *et al.,* 2009). One of these pathways is the transsulfuration pathway in which homocysteine is used to form molecules for redox regulation, such as glutathione and taurine (Ikeda *et al*., 2012a). In the other pathway, homocysteine is remethylated to form

methionine and then SAM via two methyl donors: 5-methylTHF in the folate cycle, and betaine via the enzyme Betaine Homocysteine Methyltransferase (BHMT).

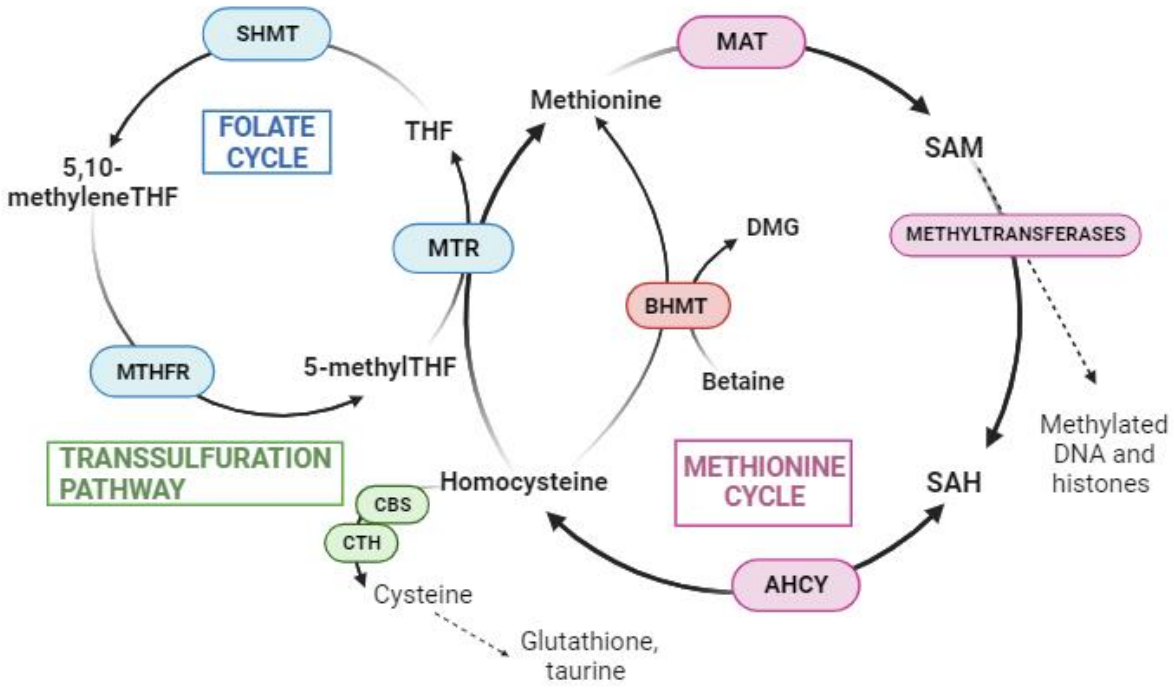


**Figure 5. One-carbon metabolism.**

A schematic representation of the connection between the folate cycle, the methionine cycle, and the transsulfuration pathway. In the folate cycle, tetrahydrofolate (THF) is converted to 5,10-methyleneTHF via serine hydroxymethyltransferase (SHMT), and then reduced to 5-methylTHF via 5,10-methylenetetrahydrofolate reductase (MTHFR). 5-methylTHF is demethylated by 5-methyltetrahydrofolate-homocysteine methyltransferase (MTR) to form THF. The methyl group of 5-methylTHF is donated to homocysteine to produce methionine. In the methionine cycle, methionine adenosyltransferase (MAT) generates S-adenosylmethionine (SAM), which donates methyl groups to methyltransferases for DNA and histone methylation. De-methylated SAM becomes S-adenosylhomocysteine (SAH), which is then hydrolyzed to homocysteine via adenosylhomocysteinase (AHCY). Homocysteine can be converted back to methionine via two methyl donors: 5-methylTHF and betaine. Betaine homocysteine methyltransferase (BHMT) takes a methyl group from betaine to form dimethylglycine and methionine. In the

transsulfuration pathway, homocysteine is converted to cystathionine via cystathionine beta synthase (CBS), and then to cysteine via cystathionine (CTH). Cysteine is used to produce glutathione and taurine. This figure was created with Biorender.com.

### 1.18 DNA methylation patterns in oogenesis and preimplantation embryo development

DNA methylation patterns are erased and re-established over the course of embryogenesis in mammals. Maternal mRNA transcription takes place in growing oocytes during prophase of the first meiosis, when the oocyte genome is globally undermethylated. Nearly all gamete-specific DNA methylation is erased early in preimplantation embryo development, and the control of development is passed from maternal gene products accumulated in the oocyte, to gene products transcribed from the embryonic genome (Gasperowicz & Natale, 2011). During preimplantation embryo development, methyltransferase-mediated methylation is required for epigenetic regulation and cell fate determination (Lee *et al*., 2012). The second de-methylation of the genome occurs prior to implantation, as evidenced by low methylation in the late morula and early blastocyst in mouse embryos (Zhang *et al*., 2015). Global embryo-specific *de novo* DNA remethylation occurs in the ICM of the blastocyst after implantation (Monk *et al*., 1987; Santos *et al.,* 2002). The de-methylation and re-methylation patterns over the course of embryo development indicates a requirement for methyl group availability, as well as metabolites and nutrients generated from OCM.

Mammalian oocytes and preimplantation embryos have a complete set of OCM enzymes (Ikeda *et al*., 2012a). In preimplantation embryos, a deficiency or excess of OCM products may disrupt development and induce unwanted changes to DNA synthesis, epigenetics, protein synthesis and amino acid synthesis (Ikeda *et al.,* 2012a). Homocysteine metabolism is correlated with folate and B vitamins, where deficiencies of either can lead to elevated plasma homocysteine (Ikeda *et al.,* 2012a). A high concentration of homocysteine in culture medium is harmful to preimplantation embryos and decreases the number of embryos cultured to the blastocyst stage (Ikeda *et al*., 2010), potentially from homocysteine's pro-oxidative properties

and the resulting oxidative stress (Guerin *et al*., 2001; Ikeda *et al*., 2012a). Methionine metabolism is crucial during the morula to blastocyst transition, in part due to the requirement of SAM. Inhibiting methionine metabolism decreases DNA methylation in morulae (Ikeda *et al*., 2012b), and suppresses blastocyst development *in vitro* (Menezo *et al*., 1989). Preimplantation embryos also require a specific concentration of reduced folate for their development, as the addition of methotrexate (MTX), an antimetabolite of reduced folate, suppressed development from the one- to two-cell stage, as well as the two- and eight-cell stage to the blastocyst stage (O'Neill, 1998)

### 1.19 The metabolic pathway of betaine and betaine as a methyl donor

Betaine is metabolized to form methionine, which ultimately contributes to the pool of SAM required for DNA methylation reactions. Here, betaine donates a methyl group to homocysteine and is catabolized into dimethylglycine. Homocysteine is converted to methionine via the donation of the methyl group from betaine. Betaine metabolism and homocysteine methylation is carried out by the zinc-dependent cytosolic enzyme BHMT (Teng *et al.,* 2011). BHMT activity has been documented in human liver and kidney (Teng et al., 2011), mammalian GV oocytes (Benkhalifa *et al.,* 2010), preimplantation embryos, and blastocysts (Lee *et al.,* 2012).

### 1.20 Betaine homocysteine methyltransferase

BHMT is an important enzyme in OCM, and the inhibition or absence of the enzyme can impact the levels of several OCM products. In mice, inhibiting BHMT can cause

hyperhomocysteinemia and lead to other homocysteine-related diseases (Collinsova *et al*., 2006). In the mouse liver, deleting BHMT induces a significant increase in homocysteine concentrations, a reduction of SAM, an increase in SAH, and an increase in betaine, all of which contribute to a 75% reduction in methylation potential (Teng *et al*., 2011).

BHMT is in part required for preimplantation embryo development, as knocking down or pharmacologically inhibiting BHMT results in fewer embryos reaching the blastocyst stage *in vitro*, and a reduction in ICM number (Lee *et al*., 2012). In addition, there is a synergy between BHMT and folate metabolism in generating methyl groups. Total SAM levels in blastocysts decreased significantly, and DNA methylation was also significantly affected only when both pathways were inhibited (Zhang *et al.,* 2015). Therefore, both betaine metabolism by BHMT and the folate cycle contribute to the methyl pool required for DNA methylation.

At the blastocyst stage, during which remethylation of the genome begins, endogenously accumulated betaine may be used as a methyl source (Lee *et al*., 2012). The onset of BHMT activity corresponds to a decrease in endogenous betaine, however it has not yet been confirmed that this decrease in betaine is occurring because of metabolism by BHMT.

### 1.21 Endogenous betaine content from the developing oocyte to the blastocyst

Our laboratory has previously determined that endogenous betaine can be detected in all stages from developing oocytes to blastocysts. Betaine was detected in postnatal day 11 preantral follicles at ~0.5 pmoles/oocyte, slightly lower than what was observed in GV oocytes and COCs, which contain ~1 pmoles/oocyte (McClatchie *et al*., 2017). Betaine levels then significantly increase at the MII oocyte stage as a result of CHDH activation during meiotic maturation, and reach 1.45-2.5 pmoles/oocyte (Corbett *et al*., 2014; McClatchie *et al*., 2017). The source and

onset of betaine accumulation in growing oocytes prior to synthesis by CHDH has not yet been elucidated. It can be suggested that betaine may be synthesized elsewhere and transported into the oocyte during oogenesis.

At the one-cell stage, betaine has been detected at 1.4-3.0 pmoles/oocyte (Lee *et al*., 2012; McClatchie *et al*., 2017). As mentioned above, SIT1 activity persists until the four-cell stage, and uptakes betaine at the one- and two-cell stage. Across preimplantation embryo development, betaine levels are conserved and do not significantly fluctuate from the one- to eight-cell stage (Lee *et al*., 2012). At the morula stage, betaine levels begin to decrease until they significantly drop at the blastocyst stage. The morula to blastocyst stage transition coincides with the onset of BHMT activation, highlighting a possible cause of this decrease in betaine.

**1.22 Summary**

Betaine is an important organic osmolyte during mouse oocyte and preimplantation embryo development, with key roles as a cell volume regulator and methyl pool supplier. A significant amount of endogenous betaine is accumulated during meiotic maturation due to *de novo* synthesis by CHDH, but the onset and mechanism of betaine accumulation in growing oocytes remains to be determined. SIT1 activates shortly after fertilization and adjusts betaine levels during the one- and two-cell stages in response to changes in osmolarity but inactivates at the four-cell stage. Betaine levels appear to be retained during the remainder of preimplantation embryo development, while $Cl^-$ channels such as VSOAC are active and directing the efflux of inorganic and organic osmolytes. Global remethylation of the embryo genome occurs in the blastocyst, where SAM is generated for methylation reactions. Betaine supplies the methyl pool

for SAM synthesis and is metabolized by BHMT in the liver, but it is unknown whether the decrease in betaine observed in blastocysts is a result of metabolism by BHMT.

## 2. Significance and Overall Objective

In recent decades, Assisted Reproductive Technologies (ART) have become increasingly prevalent in response to rising human infertility rates. ART involves the manipulation of eggs or embryos outside of the body and encompasses procedures required for fertility-related treatments, as well as procedures for domestic, commercial and research purposes with an animal model. Successful outcomes from ART require a complete understanding of the physiology of the developing oocyte and preimplantation embryo, and an ability to obtain healthy oocytes or embryos and support development *in vitro.*

*In vitro* maturation (IVM) is a method of ART that involves the culture of immature GV oocytes until the MII oocyte stage, where they are then used for standard *in vitro* fertilization (IVF) procedures (Vuong *et al*., 2018). There is conflicting data about the efficacy of IVM, with clinical pregnancy rates appearing comparable to rates observed with IVF (Ellenbogan *et al*., 2014), but a risk of low oocyte maturation and embryo development rates (Blanco *et al*., 2011). Early embryos are highly sensitive to fluctuations in cell volume and are subject to osmotic stresses during preimplantation embryo development (Baltz, 2001). Such stresses may induce changes in gene methylation patterns that may impact embryo physiology and affect the overall health of the offspring (Zhang *et al*., 2015). Therefore, appropriate osmotic culture conditions are crucial in ART.

Preimplantation embryo development has been rescued with the addition of organic osmolytes to culture media. Betaine in particular has been found to support the development of fertilized eggs to preimplantation embryos (Biggers *et al*., 1993; Hammer & Baltz, 2002), highlighting a major role for osmoprotection. Betaine is also instrumental in supplying the methyl pool in blastocysts which may be used to establish the embryonic epigenome (Lee *et al.,*

2012). The importance of betaine is implied by the elevated levels of intracellular betaine (~10 mM) in mouse eggs and embryos (Lee *et al*., 2012; McClatchie *et al*., 2017), as well as the availability of betaine in the female reproductive tract (~0.5 mM) (Lee *et al*., 2012). However, betaine is not included in standard oocyte maturation or embryo culture media.

Maintaining healthy, fertilizable oocytes is the ultimate goal of infertility treatments and oocyte preservation. The *in vivo* maturation process of the GV oocyte is not completely understood, and the maturation process *in vitro* adds a further complicated element in ART. Further investigating the changes in endogenous betaine levels over the course of oocyte and preimplantation embryo development would increase overall knowledge of oocyte and embryo physiology. We know that significant levels of betaine accumulate over meiotic maturation, are slightly adjusted by SIT1 during the one- and two-cell stage and are conserved until they decrease at the blastocyst stage. It is unknown where the low levels of betaine originate from in immature GV oocytes, whether VSOAC has a role in conserving betaine levels by remaining closed and preventing betaine efflux during preimplantation embryo development, and if betaine decreases at the blastocyst stage because of metabolism by BHMT.

**The overall objective of my thesis was to elucidate the mechanisms of intracellular betaine regulation from oogenesis to the blastocyst stage.** I have investigated betaine accumulation and transport during oogenesis and folliculogenesis, and the changes in endogenous betaine levels in preimplantation embryos and blastocysts using the mouse as an animal model and a combination of functional studies and molecular biology techniques. The findings from my research provide a further understanding of the requirement of betaine at various times during oocyte and embryo development, which can be applied to both *in vivo* and *in vitro* contexts. A more complete understanding of the necessity of organic osmolytes and

independent cell volume regulation may improve oocyte maturation and embryo development *in vitro* and improve the outcomes of human IVM. In conclusion, the overall hypothesis for my thesis is that betaine accumulation begins during oogenesis via a transporter in the follicular cells surrounding the oocyte. The betaine synthesized during meiotic maturation and transported by SIT1 is retained in the preimplantation embryo where there is no significant release via VSOAC until the blastocyst stage where it is metabolized by BHMT.

## 3. Specific Aims and Hypotheses

### Specific Aim 1: Identify the onset of betaine accumulation in growing oocytes and determine how much is accumulated during oogenesis

Most betaine in mature MII eggs is synthesized *de novo* via the CHDH enzyme. CHDH is active only during meiotic maturation and mediates betaine synthesis during the transition from GV to MII oocyte (McClatchie *et al*., 2017). Lower levels of betaine have been detected in GV oocytes prior to CHDH activation (Corbett *et al*., 2014; McClatchie et al., 2017). The point in oogenesis of initiation of betaine accumulation and the amount accumulated over oogenesis is unknown. It is possible that transporters may exist either in the developing oocyte itself or in the follicular cells that are connected to the oocyte via gap junctions. Therefore, I hypothesized that betaine accumulation begins in early oogenesis.

### Specific Aim 2: Measure the amount of betaine transported in growing oocytes and follicles during oogenesis

The y+LAT2 transporter is present in cumulus cells surrounding the fully grown GV oocyte in COCs (Corbett *et al.,* 2014). If, as hypothesized above, betaine is present during oogenesis, a transporter may be present in the follicular cells of the developing oocyte that mediates intracellular betaine accumulation prior to becoming a full grown GV oocyte. Therefore, I hypothesized that a transporter exists in follicular somatic cells that takes up betaine and transfers it to the enclosed growing oocyte.

**Specific Aim 3: Elucidate the mechanism of betaine retention and classify *Lrrc8a-e* expression from the preimplantation embryo to blastocyst stage**

VSOACs activate upon cell-swelling to mediate the efflux of organic osmolytes in preimplantation embryos (Kolajova et al., 1999). Endogenous betaine levels are conserved during preimplantation embryo development, but it is unknown if VSOAC is permeable to betaine. VSOACs are composed of five members of the LRRC8 protein family (LRRC8A-E) that form complexes to produce functional channels. The composition of LRRC8 proteins has not been defined in preimplantation embryos, and the link between betaine content and VSOAC activity has not been elucidated. Therefore, I hypothesized that VSOAC regulates betaine levels in preimplantation embryos to conserve betaine until the blastocyst stage.

**Specific Aim 4: Determine if the betaine decrease during the morula to blastocyst stage transition is mediated by BHMT**

Betaine levels remain at a consistent concentration before decreasing at the blastocyst stage. This change in betaine content coincides with the onset of BHMT activity in the ICM of blastocysts. BHMT generates the universal methyl donor, SAM, by removing a methyl group from betaine forming dimethylglycine and methionine, which is subsequently converted to SAM (Zhang *et al*., 2015; Ikeda *et al*., 2012a; Garrow, 1996). Therefore, I hypothesized that endogenous betaine levels decrease in blastocysts due to direct metabolism by BHMT.

## 4. Materials and Methods

### 4.1 Chemicals and Pharmaceutical Agents

The chemicals and solutions used in experiments were embryo tested or cell culture grade where available. All chemicals, compounds and pharmaceutical agents were obtained from the sources listed in Table 1.

**Table 1: Summary of chemicals and compounds used**

| Name of Chemical or Compound | Source |
|---|---|
| 4-(2-butyl-6,7-dichlor-2-cyclopentylindan-1-on-5-yl (DCPIB) | Sigma Aldrich (St. Louis, MO, USA) |
| 4-4'-Diisothiocyano-2, -2'-stilbenedisulfonic acid (DIDS) | TOCRIS, Bio-Techne (Toronto, ON, CA) |
| 4-(2-hydroxyethyl)-1-piperazineethane-sulfonic acid (HEPES) | Sigma Aldrich (St. Louis, MO, USA) |
| [$^3$H]-betaine; 20 mCi/mmol | American Radiolabeled Chemicals (ARC) (St. Louis, MO, USA) |
| $\beta$-mercaptoethanol | Sigma Aldrich (St. Louis, MO, USA) |
| Alanine | Sigma Aldrich (St. Louis, MO, USA) |
| Agarose | Sigma Aldrich (St. Louis, MO, USA) |
| Arcturus Picopure RNA Isolation System | Applied Biosystems (Foster City, CA, USA) |
| Arginine | Sigma Aldrich (St. Louis, MO, USA) |
| Betaine | Sigma Aldrich (St. Louis, MO, USA) |
| Calcium Chloride ($CaCl_2$) | Sigma Aldrich (St. Louis, MO, USA) |
| Collagenase Type 1 | Worthington Biochemical Corp. (Lakewood, NJ, USA) |
| Deoxyribonuclease Type 1V (DNase) | Qiagen (Toronto, ON, CA) |
| Dimethyl Sulfoxide (DMSO) | Calbiochem (La Jolla, CA, USA) |

| | |
|---|---|
| Ethanol | Sigma Aldrich (St. Louis, MO, USA) |
| Ethidium bromide | Sigma Aldrich (St. Louis, MO, USA) |
| Glucose, D- (+) | Sigma Aldrich (St. Louis, MO, USA) |
| Glycine | Sigma Aldrich (St. Louis, MO, USA) |
| Human Chorionic Gonadotropin | Prospec (Sturgeon County, AB, Canada) |
| Hyaluronidase | Sigma Aldrich (St. Louis, MO, USA) |
| Lysine | Sigma Aldrich (St. Louis, MO, USA) |
| Magnesium sulfate heptahydrate ($MgSO_4$) | Sigma Aldrich (St. Louis, MO, USA) |
| Mass Ruler DNA Ladder Mix | ThermoFisher scientific (Rockford, IL, USA) |
| MassRuler DNA Loading Dye (6X) | ThermoFisher scientific (Rockford, IL, USA) |
| Mineral Oil | Sigma Aldrich (St. Louis, MO, USA) |
| Penicillin G potassium salt | Sigma Aldrich (St. Louis, MO, USA) |
| Potassium chloride (KCl) | Sigma Aldrich (St. Louis, MO, USA) |
| Polyvinyl alcohol (PVA) | Sigma Aldrich (St. Louis, MO, USA) |
| Potassium phosphate monobasic ($KH_2PO_4$) | Sigma Aldrich (St. Louis, MO, USA) |
| PowerUp SYBRGreen Master Mix | Applied Biosystems (Foster City, CA, USA) |
| Pregnant Mare Serum Gonadotropin | Prospec (Sturgeon County, AB, Canada |
| Proline | Sigma Aldrich (St. Louis, MO, USA) |
| QIAquick Gel Extraction Kit | Qiagen (Toronto, ON, CA) |
| QIAquick PCR Purification Kit | Qiagen (Toronto, ON, CA) |
| Raffinose pentahydrate, D- (+) | Sigma Aldrich (St. Louis, MO, USA) |
| RNeasy Micro Kit | Qiagen (Toronto, ON, CA) |
| Sarcosine | Sigma Aldrich (St. Louis, MO, USA) |

| | |
|---|---|
| Scintillation fluid | Scintiverse, BD, Fisher Scientific (Pittsburgh, PA, USA) |
| Sodium bicarbonate ($NaHCO_3$) | Sigma Aldrich (St. Louis, MO, USA) |
| Sodium chloride (NaCl) | Sigma Aldrich (St. Louis, MO, USA) |
| Sodium lactate | Sigma Aldrich (St. Louis, MO, USA) |
| Streptomycin sulfate salt ($SO_4$) | Sigma Aldrich (St. Louis, MO, USA) |
| Superscript IV | Invitrogen (Carlsbad, CA, USA) |
| Taq DNA Polymerase | Invitrogen (Carlsbad, CA, USA) |
| Tetrasodium ethylenediaminetetra-acetic acid (EDTA) | Sigma Aldrich (St. Louis, MO, USA) |

### 4.2 Oocyte and Preimplantation Embryo Culture Media

Oocytes and preimplantation embryos were cultured in a modified potassium simplex optimized medium (mKSOM), which was altered from standard KSOM by replacing bovine serum albumin (BSA) with polyvinyl alcohol (PVA, 1 mg/ml, cold-water soluble). Glutamine was also omitted. mKSOM was composed of: NaCl (95 mM), KCl (2.5 mM), $KH_2PO_4$ (0.35 mM), $MgSO_4•7H_20$ (0.2 mM), Na lactate (10 mM), Glucose (0.2 mM), Na pyruvate (0.2 mM), $NaHCO_3$ (25 mM), $CaCl_2•2H_2$ (1.7 mM), Tetrasodium ethylenediaminetetraacetic acid (EDTA) (0.01 mM), K penicillin G (0.16 mM), Streptomycin $SO_4$ (0.03 mM) and 1 mg/ml PVA. Hepes-mKSOM (or KFHM) was the medium used for oocyte and preimplantation embryo isolation and handling. Hepes-mKSOM was prepared identically to mKSOM, except for the addition of 21 mM of Hepes (4-(2-hydroyethyl)-1-piperazineethanesulfonic acid) and $NaHCO_3$ reduced to 4 mM (pH adjusted with NaOH to 7.4). The osmolarities of mKSOM and Hepes-mKSOM were 250 and 240 (± 5 mOsM), respectively, and were measured with a Vapro 5520 osmometer (Wescor, Logan, UT). mKSOM osmolarity was adjusted by decreasing the amount of NaCl to achieve a lower osmolarity or by using D (+) raffinose to achieve a higher osmolarity. The desired osmolarity was confirmed by osmometer as previously described (Dawson & Baltz 1997).

### 4.3 Animals

All animal protocols were approved by the Animal Care Committee of the University of Ottawa Faculty of Medicine and comply with the Canadian Council on Animal Care guidelines. Female CD1 strain mice were acquired from Charles River (St-Constant, QC, Canada) and were

euthanized by cervical dislocation at 4-7 weeks to collect fully-grown oocytes or mated with BDF1 males to produce preimplantation embryos. Female CD1 and male BDF1 mating pairs were set up to collect oocytes and follicles from female neonates over the first wave of oogenesis, ranging from postnatal day 5 to 21. The CD1 strain has been used as a model system in the Baltz laboratory as it produces oocytes and embryos that are sensitive to *in vitro* conditions and osmolarity (Biggers, 1998; Hadi *et al*., 2005), and therefore are suited to study culture manipulations. The University of Ottawa Animal Care and Veterinary Services (ACVS) facility provided animal care. All adult animals were kept on a 12-hour light-dark cycle and were provided unrestricted access to water and Tekland Global 18% protein rodent diet 2018 (Envigo, Indianapolis, IN). Lactating female mice were given Tekland Global 19% Protein Extruded Rodent Diet 2019 (Envigo, Somerset, NJ). Neonatal mice were weaned on postnatal day 21 and transferred to a separate cage with their own food and water supply.

The *Bhmt* null mouse line was obtained from Dr. Steven H. Zeisel (University of North Carolina) and was derived from the C57Bl/6 strain as previously described (Teng *et al.,* 2011). Deletion of both *Bhmt* alleles results in the absence of BHMT activity (Teng *et al.,* 2011). The colony was maintained using heterozygous ($Bhmt^{+/-}$) pairs. $Bhmt^{-/-}$ blastocysts were obtained by mating $Bhmt^{-/-}$ males and females, and $Bhmt^{+/+}$ blastocysts were obtained from mating wildtype males and females. The animals were kept under identical conditions to CD1 mice and were sacrificed by cervical dislocation at 4-5 weeks of age.

## 4.4 Superovulation and hCG injection

A standard superovulation protocol was followed to achieve enough oocytes for experimental use (Hogan *et al*., 1994; Dawson & Baltz, 1997). To stimulate ovarian folliculogenesis, 4–7-week-old female mice received an intra-peritoneal (i.p.) injection of 5 IU of an FSH-like hormone, pregnant mare serum gonadotropin (PMSG). For preimplantation embryo collection, ovulation was triggered using an LH-like hormone, and female adult mice received an i.p. injection of 5 IU human chorionic gonadotropin approximately 48 hours after PSMG, and immediately mated with male mice.

## 4.5 Follicle, oocyte and preimplantation embryo isolation and collection

### *4.5.1 Growing follicles and oocytes from neonatal mice*

A synchronized wave of primordial follicles initiates follicular development during the immediate postnatal period, allowing for relatively homogenous populations of growing oocytes and follicles to be collected at a desired stage. Growing follicles and oocytes earlier than P14 were isolated enzymatically as they were too small to be isolated mechanically. To collect growing oocytes and follicles on postnatal days 5 and 10, ovaries from female neonates were surgically excised and cultured in mKSOM ($MgSO_4•7H_20$ and $CaCl_2•2H_2$ omitted), with the addition of 0.01 mg/ml DNase Type IV and 2 mg/ml Collagenase Type 1 (Worthington Biochemical Corp., Lakewood, NJ, USA). Ovaries were incubated for up to 20 or 30 minutes to release follicles or oocytes, respectively. Ovaries were vigorously pipetted every 10 minutes to facilitate tissue digestion. Oocytes and follicles were washed through five drops of Hepes-mKSOM to remove residual enzymes.

Growing follicles on P15, P17, and P21 were collected by carefully prying the ovary apart with tweezers and isolating individual follicles that were approximately the same size. Growing oocytes on P15, P17, and P21 were collected by mincing the ovarian tissue with a razor blade and denuding the cumulus cells surrounding the oocytes with a narrow-bore flame-pulled Pasteur pipette.

*4.5.2 Fully grown GV oocytes, MII oocytes and preimplantation embryos*

Fully grown GV stage oocytes were isolated by surgically excising ovaries approximately 44 hours post-PMSG injection. The ovarian tissue was minced with a razor blade to release unexpanded COCs, which were then either collected or gently denuded of cumulus cells using a narrow-bore flame-pulled Pasteur pipette.

Both MII oocytes and one-cell embryos were collected by flushing the oviduct with a blunt-tipped syringe with Hepes-mKSOM and 300 μg/ml hyaluronidase to remove the surrounding cumulus cells. MII oocytes were isolated 15 hours after ovulation was triggered by hCG, and one-cell embryos were collected from females mated overnight with BDF1 males approximately 24 hours after ovulation was triggered. Isolated oocytes and embryos were washed through 5 drops of Hepes-mKSOM to remove residual hyaluronidase. Fertilized one-cell embryos were confirmed by the presence of two pronuclei (Hogan *et al.,* 1994).

Two-cells and four to eight cells were obtained by surgically removing and flushing oviducts with Hepes-mKSOM, 42-44 hours and 56-68 hours after hcG injection, respectively.

Morulae and blastocysts were collected 76 and 93-94 hours after hCG injection by surgically removing the uterine horns and flushing them with Hepes-mKSOM.

### 4.6 Oocyte and preimplantation embryo culture

Oocytes and preimplantation embryos were cultured following the standard protocols used routinely in our laboratory (Dawson & Baltz, 1997; Lawitts & Biggers, 1993). Pools of oocytes or embryos were collected from several female mice for experiment replicates. Three drops of 50 µL mKSOM were placed in a 35 mm culture dish (Falcon, Corning NY, USA) and covered with filter-sterilized embryo culture-grade mineral oil (Sigma Aldrich, St. Louis, MO, USA). Mineral oil was omitted when hydrophobic inhibitors were used, and oocytes and embryos were cultured in 750 µL of mKSOM in 4-well plates (Falcon, Corning NY). Culture media was pre-equilibrated in an incubator at 37°C with 5% $CO_2$ in air and 100% humidity (Lawitts & Biggers, 1993) for a minimum of 2 hours. Oocytes and embryos were washed through three drops of pre-equilibrated culture media to minimize carryover of media from collections or previous treatments and left to culture in the final drop.

### 4.7 Endogenous betaine and choline measurements

All endogenous betaine and choline measurements were accomplished by liquid chromatography with tandem mass spectrometry (LC-MS/MS). All measurements were performed by Jeremy Zhang of the Pharmacokinetics Laboratory of the Clinical Investigations Unit of the Ottawa Hospital. He has provided the following description of the protocol:

"Measurements were obtained using a Thermo Accela HPLC system (0.4 mL/min flow rate) with Thermo TSQ Quantum Access Max Triple Quadrupole mass spectrometer (Thermo Fisher Scientific, Waltham, MA). Separation was by Thermo Accucore HILIC column (100 mm x 2.1 mm, 2.6 um). The mobile phase was Line A: 0.1% Formic Acid and Line B:

Acetonitril+0.1% Formic Acid with a gradient of 10% to 90% B in 2 min and back to 10% B in 5 min, then holding at 10% B for another 2 min, for a total run time of 4.5 min.

Samples were re-suspended in 1 mL of 10% methanol, 90% acetonitrile with deuterated D9-betaine (10 μmol/L) internal standard. The injection volume was 10 μL and the oven temperature was 40°C. Betaine was detected in positive ion mode by electrospray ion source with a mass transition 118 →59 and 127→ 68 for D9-betaine. The betaine content of an equal volume of each final wash drop was also determined to ensure that there was no contamination."

Choline was detected using the same protocol in the same samples by measuring the choline peak that was separate from the betaine peak. The limit of detection was determined by the Clinical Investigations Unit prior to analysis of oocyte samples to ensure that a small magnitude of betaine and choline (down to ~3 pmoles total in the sample) could be accurately measured. Samples with known betaine content were measured as described above. The measured value was compared to the nominal value and plotted, with duplicate measurements taken for every sample (Figure 6). The standard error rate accepted was < 10%.

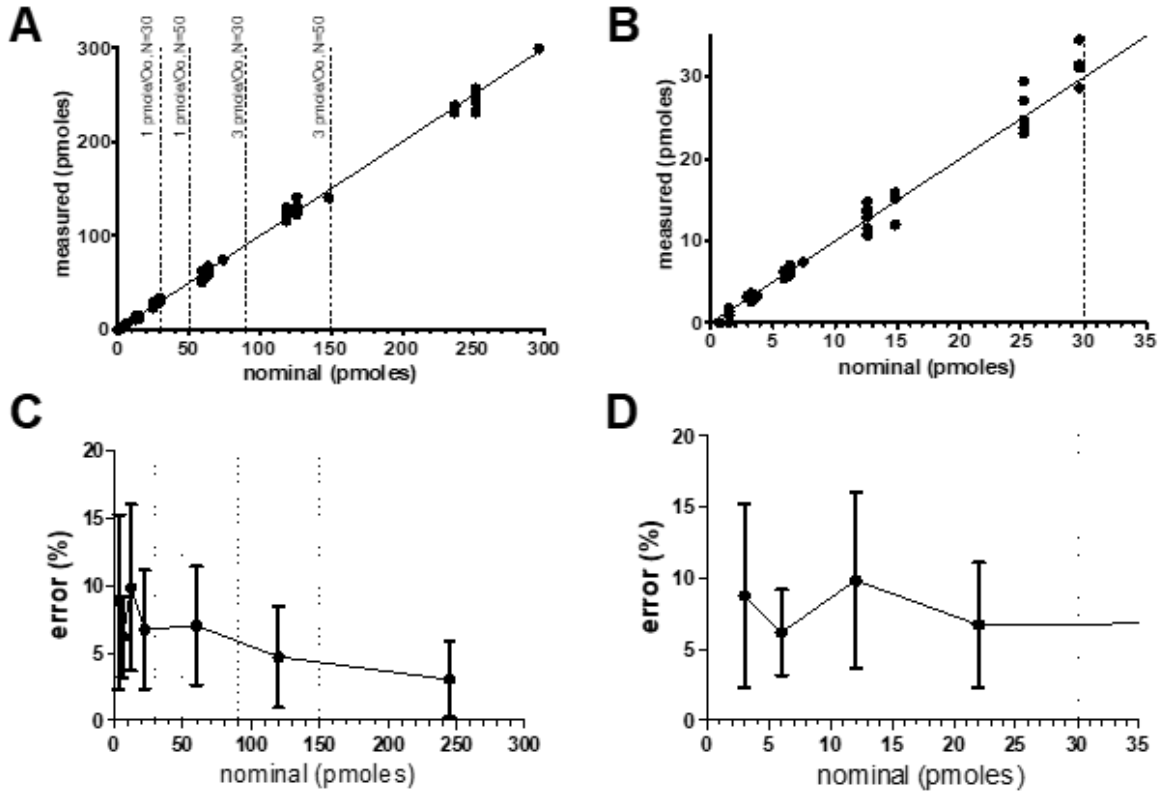


**Figure 6. Limit of detection in measuring endogenous betaine with LC-MS/MS**.

A) Measured betaine levels of nominal samples ranging from 1 to 300 pmoles and measured with LC-MS/MS. Sample sizes of 30 and 50 oocytes with 1 pmole/oocyte and 3 pmole/oocyte are superimposed. Actual endogenous betaine per oocyte ranges between 1 and 3 pmol/oocyte or embryo (McClatchie *et al.,* 2017; Corbett *et al*., 2014; Anas *et al*., 2008). These nominal values represent the equivalent betaine levels expected in sample sizes of 30 or 50 oocytes or embryos. B) Nominal betaine values below 30 pmole demonstrate a linear curve. This is indicative of reasonable accuracy if the betaine content is less than 1 pmole/oocyte from sample sizes with less than 30 oocytes. C) Percent error for nominal values from 0-200 pmole. D) Percent error for nominal values from 3-30 pmole. Error percent ranges from ~10-15. Samples were not tested below 3 pmole.

*4.7.1 Betaine and choline content in growing oocytes and follicles*

Growing oocytes, growing follicles, fully grown GV oocytes and MII oocytes were collected for LC-MS/MS. Growing oocytes and follicles were collected from neonatal mice over the first wave of oogenesis in groups of 100 for P5 and P10, 60 for P15, 50 for P17 and 30 for P21. Fully grown GVs and MIIs were also collected in groups of 30. Growing follicles were collected on P10, P15 and P21, in groups of 50, 30, and 20, respectively. All the groups were washed in Hepes-mKSOM and stored at -20°C in 1.5 mL Eppendorf tubes. Each sample was dried overnight on the benchtop before processing.

*4.7.2 In vivo and in vitro betaine content in two-cell embryos, morulae, and blastocysts*

Two-cell embryos were collected in Hepes-mKSOM and split into two groups. Half were collected for LC-MS/MS for the *in vivo* measurements, and the other half were placed in mKSOM and cultured until the morula and blastocyst stage for the *in vitro* measurements. At the desired stage, the embryos were removed from the culture dish and stored for LC-MS/MS. Freshly isolated morulae and blastocysts were also collected for the *in vivo* measurements.

*4.7.3 Endogenous betaine levels in wildtype vs. BHMT knockout blastocysts*

Blastocysts from both wildtype and BHMT knockout mice were collected and isolated in Hepes-mKSOM by Taylor McClatchie. Each sample was stored and prepared for LC-MS/MS as described above.

### 4.8 [$^3$H]-betaine transport measurements

Betaine transport in follicles, oocytes and embryos was measured following standard laboratory protocols published by the Baltz laboratory (Baltz, 2013). The rate of betaine transport across GV oocyte, COC and preimplantation embryo stages has been previously defined in our lab (Corbett *et al*., 2014; Anas *et al*., 2008). After receiving each bottle of [methyl-$^3$H]-betaine (American Radiolabeled Chemicals, St. Louis, MO; #ART 1903), small volumes were aliquoted in 0.5 mL Eppendorf tubes and stored at -80°C to prevent degradation. All dishes containing [$^3$H]-betaine were prepared the day before. [$^3$H]-betaine aliquots were thawed for one hour with the lid open under the laminar flow hood, and then shaken and resuspended in mKSOM for two hours. The mKSOM used in the incubation drops were more concentrated with 70% of the normal amount of sterilized water (70 mKSOM), 2 μM of [$^3$H]-betaine, and sufficient filter sterilized water to adjust the mKSOM to normal concentrations. 50 μL drops of the [$^3$H]-betaine mKSOM media was placed in dishes under embryo oil and incubated for at least two hours in 5% $CO_2$/air and 37°C. Oocytes, follicles or embryos were isolated as previously described and washed through three drops of pre-equilibrated mKSOM under oil before being placed in mKSOM medium containing 2 μM [methyl-$^3$H]-betaine for a desired time point, typically after 10 or 30 minutes. Oocytes, follicles, or embryos in groups of 5-10 were washed through 6 drops of ice-cold Hepes-mKSOM and transferred to a scintillation vial with minimal excess media. A sample of the same volume of the final wash drop was placed into a separate scintillation vial to measure the background. Each scintillation vial contained 4 mL scintillation fluid (Scintiverse BD, Fisher Scientific, Pittsburgh, PA, USA). The total molar amount of [$^3$H]-betaine was quantified by the scintillation counter (LS 6500, Beckman Coulter, Brea, CA) with a 5-minute counting period for each sample (Dawson *et al.,* 1998). The counts generated from the

background were subtracted from the oocyte, follicle, and embryo samples. To measure the non-saturable rate of transport, oocytes, follicles, or embryos were incubated in 5 mM unlabeled betaine and 2 µM [$^3$H]-betaine, and the amount generated was compared to the control uptake with the absence of unlabeled betaine.

To convert the counts per minute (CPM) generated by the scintillation counter into concentration, standard curves were completed every week. Two 15 mL conical tubes were filled with 5 and 7.5 mL of filter-sterilized water with 1 µL of the stock [$^3$H]-betaine for a 1:5000 and 1:7500 dilution. Five serial twofold dilutions were prepared for each tube and 5 µL from each dilution was added to a scintillation vial. A background measurement was also prepared with 5 µL filter-sterilized water. The rate of transport was then calculated in femtomoles of [$^3$H]-betaine per oocyte/follicle/embryo per minute of incubation.

For each new bottle of [$^3$H]-betaine, an experiment previously established in our lab (Anas *et al*., 2007; Anas *et al*., 2008) was performed to ensure the product received was [$^3$H]-betaine. One-cell embryos were isolated as previously described and incubated in 2 µM [$^3$H]-betaine and mKSOM for 30 minutes. Parallel experiments were performed with the addition of 5 mM unlabeled betaine, proline, or glycine. Unlabeled betaine or proline acted as competitive inhibitors for [$^3$H]-betaine uptake by SIT1. One-cell embryos were selected as the betaine transporter SIT1 is most active during the one-cell stage. SIT1 transports both betaine and proline, but not glycine. Therefore, the same inhibition pattern should be seen with every bottle of [$^3$H]-betaine, that is, betaine uptake inhibited with unlabeled betaine and proline and uninhibited with unlabeled glycine.

## 4.9 Polymerase Chain Reaction (PCR)

### *4.9.1 RNA Extraction*

Total cellular RNA was extracted from tissues using the RNeasy Micro Kit (Qiagen, Toronto, ON, CA #74004) with on-column DNase digestion using RNase-Free DNase Set (Qiagen, Toronto, ON, CA #79254). Liver, kidney, spleen, and ovary were used as the control tissues and excised from CD1 females.

RNA was extracted from oocytes, preimplantation embryos and blastocysts using the Arcturus Picopure RNA isolation system (Applied Biosystems, Foster City, CA #KIT0204) with the same on-column DNase set.

### *4.9.2 Reverse Transcription*

RNA was reverse transcribed to cDNA using the Superscript IV Kit (Invitrogen, Carlsbad, CA #18091050).

### *4.9.3 Primer Design*

The primers used for all PCR experiments are listed in Table 3. Primers were designed for the five isoforms that are found in VSOACs, LRRC8A-E, using the primer designing tool by the National Center for Biotechnology Information (NCBI). Several primers were tested for each isoform and the required annealing temperature was determined using a temperature gradient ranging from 55.5°C-62.4°C. *Hmgb3* (High Mobility Group Box 3) and *Rb1cc1* (RB1 Inducible Coiled-Coil 1, or FIP200, FAK-family Interacting Protein of 200 kDa*)* were selected as reference genes as they exhibited the least variation in expression when assessed from the GV oocyte to the blastocyst stage (Tscherner *et al.*, 2023). *Hmgb3* functions in DNA replication, binding, and

repair (Wen *et al.,* 2021), and *Rb1cc1* is a regulator of autophagy and inflammatory processes (Yeo *et al*., 2020). To confirm the specificity of the primers, amplicons were prepared using the QIAquick Gel Extraction Kit (Qiagen, Toronto, ON, CA #28704) and sent for sequencing to the Ottawa Hospital Research Institute StemCore facilities. Sequences were matched to the predicted region using BLAST provided by NCBI.

**Table 2. Forward and reverse primer sequences used for PCR**

| **Name** | **Forward Sequence** | **Reverse Sequence** | **Size (bp)** |
|---|---|---|---|
| LRRC8A | 5'-AAGTGCCGTGCTCTTCTCTC-3' | 5'-GCTGACCTCTCATGCCCAAT-3' | 436 |
| LRRC8B | 5'-CTCTGCTGTCTTCCCTGCAA-3' | 5'-GGGGAAAAACTTGGCGAACC-3' | 210 |
| LRRC8C | 5'-CCCCCAGAGATTAATGTGGC-3' | 5'-CCACCGAGAGGTAATCCGTG-3' | 184 |
| LRRC8D | 5'-GCTTGTTTGGAAGCGTGGG-3' | 5'-ATGAGCATAGCCACGGTGAG-3' | 441 |
| LRRC8E | 5'-TAGCGTCTGTACTGAGGCGG-3' | 5'-ATGAGCATAGCCACGGTGAG-3' | 290 |
| HMGB3 | 5'-GTGCCAAGGGTCCTGCT-3' | 5'-GTCAATCACAGCGCTCTCCTA-3' | 152 |
| RB1CC1 | 5'-GTGCACCACTGCCAAACAAG-3' | 5'-AGCTCTATTACAAGGCGGAGC-3' | 129 |

*4.9.4 RT-PCR*

cDNA synthesized from the reverse transcriptase reaction was added to a PCR mastermix consisting of 10 mM dNTP mix (made up of equal parts dATP, dCTP, dGTP and dTTP in water), 10 µM primer stock solutions, 10X PCR MgCl2-free buffer, 50 mM MgCl2 and Taq Polymerase (Invitrogen, Carlsbad, CA #2567166). The conditions of the PCR protocol were as follows: 94°C for 3 min, 94°C for 45 sec, 60°C for 30 sec, 72°C for 90 sec (repeated for 36 cycles) and

72°C for 10 min. The PCR program was run at 40 cycles while troubleshooting primers and annealing temperatures. The PCR reactions were run on a Bio-Rad T100 Thermocycler.

*4.9.5 qRT-PCR*

A standard curve was prepared with liver, kidney, spleen, or ovary cDNA to be used as a reference for quantification. Five PCR reactions for each *Lrrc8* primer set was run and compiled into one sample for DNA purification using the QIAquick PCR Purification Kit (Qiagen, Toronto ON, CA #28104). The DNA concentration of each sample was quantified by spectrophotometry using the NanoDrop 2000 (ND-2000 ThermoFisher Scientific). The purified DNA product was diluted to 1 pg/µL, followed by a 1:10 serial dilution five times to obtain six points for a standard curve in femtograms ranging from 1000 fg to 0.01 fg.

A master mix was prepared with Nuclease and RNase-free water, primers, and PowerUp SYBRGreen Master Mix (Applied Biosystems, Foster City, CA #A25742). Quantitative reverse-transcription PCR reactions were carried out on a 7500 FAST Real-Time system (Applied Biosystems, Foster City, CA #A25742) in MicroAmp Fast optical 96-well reaction plates and covered with adhesive film (Applied Biosystems, Foster City, CA #43346907 and #4311971). Primers used in the previous RT-PCR reactions were used again and run alongside *Hmgb3* and *Rb1cc1.* The oocyte and embryo samples were extracted by Dr. Allison Tscherner and diluted so that 0.36 oocyte/embryo equivalents were loaded per well. The mastermix was 10 µl SYBRGreen, 0.4 µl 10 mM forward and reverse primer, 7.6 µl water and 2 µl template. Each sample was loaded in triplicate wells and was averaged for one independent repeat. The qPCR program was 50°C (3 min), 95°C (10 min), followed by 35 cycles of 95°C (15 sec), 60°C (15 sec), and 72 (1min). A melt curve from 60-95-60°C (15 sec each) was performed following amplification to confirm the presence of a single PCR product.

*4.9.6 Gel Electrophoresis*

The products of RT-PCR were visualized by gel electrophoresis. 1.75% agarose gels with ethidium bromide were run and cast with the ThermoScientific Owl EasyCast B2 mini gel electrophoresis system. DNA ladders (ThermoScientific MassRuler #SM0403) were loaded on one side of the samples. The Fisher Scientific FB300 power supply was used to run the gel at 110 V.

**4.10 RNAseq data set**

Dr. Allison Tscherner recently completed a project in which the Gene Expression Omnibus (GEO) was searched for recent RNAseq data sets containing oocytes, preimplantation embryo, and blastocyst stages (Tscherner *et al*., 2023). The data sets were downloaded from the Sequence Read Archive (SRA) and normalized and merged by the Ottawa Bioinformatics Core Facility. Sequences were mapped to transcripts from the GENCODE mouse vM25 annotation release using salmon. Each of the stages and treatments of oocytes, eggs and embryos in the GEO DataSets were confirmed using PubMed identifiers (PMID#) from GEO that allowed access to the associated published studies (Tscherner *et al.,* 2023). Among the sequences included were all five *Lrrc8* transcripts in oocytes and preimplantation embryos, which were extracted from the data set.

### 4.11 Statistical Analysis

Prism 10.0.2 (GraphPad Software, San Diego, CA) was the program used for graphing and statistical analyses. Quantitative data was expressed and plotted as the mean ± the standard error of the mean (SEM). A student's two-tailed *t*-test was used when two sample groups were compared. When there was one independent variable and more than two sample groups were compared, a one-way ANOVA and Tukey multiple comparisons test was used to compare each mean to every other mean. A two-way ANOVA followed by Šidák's multiple comparisons test was used with two independent variables to compare independent means within each row and each column.

## 5. Results

### 5.1 Betaine and choline accumulation over oogenesis

In MII eggs, most of the betaine is synthesized *de novo* via the enzyme CHDH that is active only during meiotic maturation and mediates betaine synthesis during the transition from GV to MII oocyte (McClatchie *et al*., 2017). Betaine has been detected in growing oocytes as early as postnatal day 11 (McClatchie *et al*., 2017), but how early in oogenesis betaine begins to accumulate in growing oocytes is unknown. My objective was to collect oocytes and follicles from neonates during the first wave of oogenesis, and to identify the postnatal day in which betaine accumulation begins.

*5.1a Endogenous betaine content in neonatal and fully grown oocytes is at a consistent level until the MII oocyte stage*

Growing oocytes from postnatal days 5-21, fully grown oocytes, and MII oocytes were isolated from neonatal mice and their betaine and choline was measured by LC-MS/MS, with the amount expressed as picomoles per oocyte.

Endogenous betaine was present in P5 oocytes but did not increase significantly over postnatal days and was not significantly different from betaine in fully grown GV oocytes (Figure 7A). Betaine levels were highest in MII oocytes at 1.60 pmoles/oocyte which was consistent with previous work (McClatchie *et al*., 2017). Endogenous choline increased slightly over postnatal days but was not significantly different between groups (Figure 7B). Choline levels were slightly lower than betaine levels over the postnatal days, with the difference most pronounced at the MII stage.

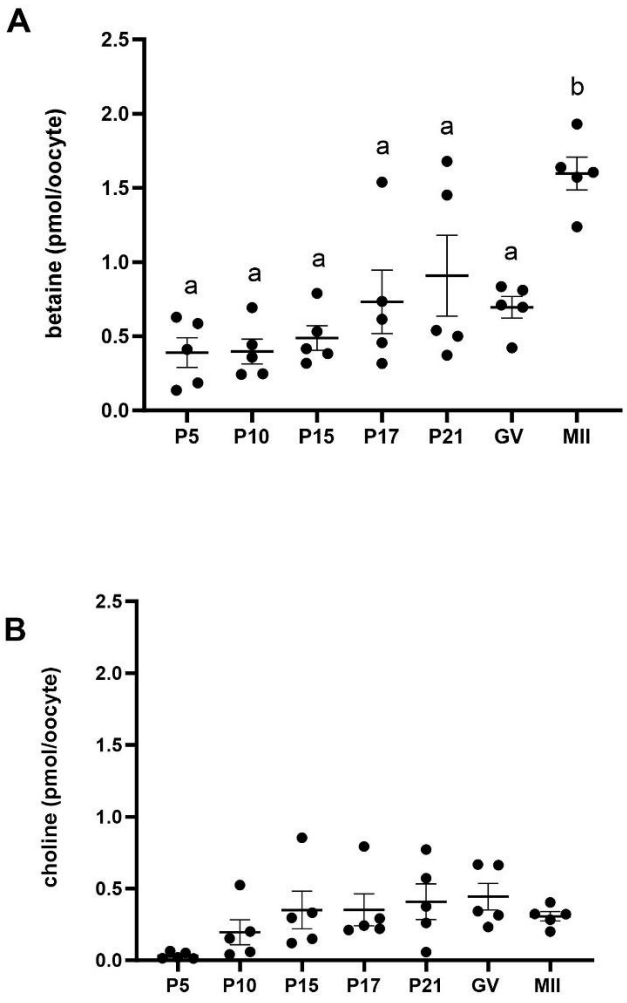


**Figure 7. Endogenous betaine and choline content in growing oocytes, GV oocytes and MII eggs.**

Betaine (A) and choline (B) levels were measured by LC-MS/MS in oocytes collected from neonates during the initial postnatal wave of oogenesis. Oocytes were collected in groups of 100 for P5 and P10, 60 for P15, 50 for P17, and 30 for P21, GV, and MII oocytes for an N=5. Points with different letters are significantly different ($p < 0.0001$ by ANOVA with Tukey test). There was no statistical difference between groups for choline ($p > 0.05$ by ANOVA with Tukey test).

*5.1b Growing follicles have a high reserve of endogenous betaine and choline that increases over postnatal days*

Growing follicles were collected from neonates on postnatal days 10, 15, and 21 and the betaine and choline content were measured with LC-MS/MS, with the amount of betaine or choline expressed in picomoles per follicle. P21 follicles included antral fluid.

Both endogenous betaine and choline increased from postnatal day 10 to postnatal day 21 and were highest in postnatal day 21 (Figure 8). Betaine in P10 and P15 follicles were present at a similarly low level but significantly increased by P21 (Figure 8A). Similarly, choline was lower in P10 and P15 follicles but greatly increased in P21 follicles (Figure 8B). Choline was present at levels approximately ten times greater than betaine in follicles.

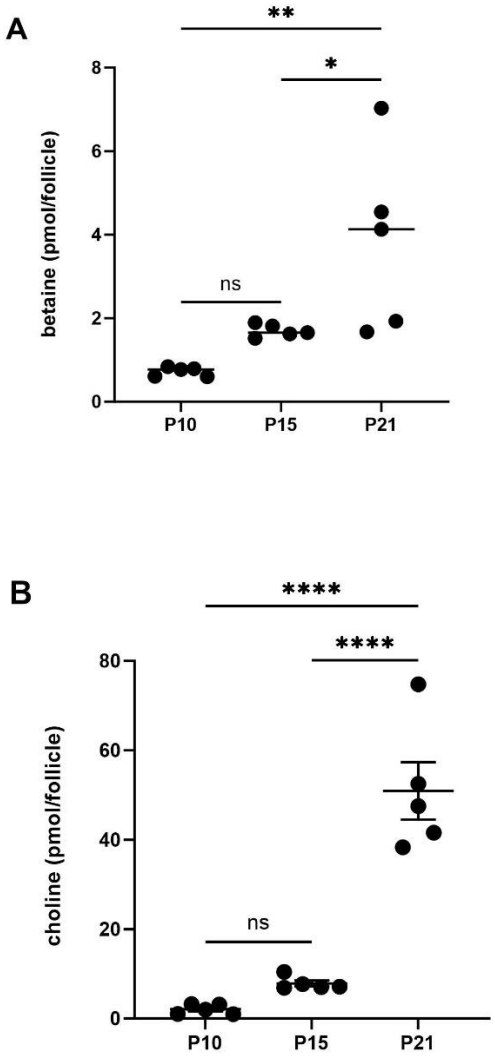


**Figure 8. Endogenous betaine and choline levels in follicles isolated from neonates.**

Betaine (A) and choline (B) levels were measured with LC-MS/MS in follicles collected during the initial postnatal wave of oogenesis. Growing follicles were collected in groups of 50 for P10, 30 for P15, and 20 for P21 for an N=5. Asterisks indicate a significant difference between groups (A: **:p=0.0053, *: p=0.0475 by ANOVA with Tukey test; B: ****:p<0.0001 by ANOVA with Tukey test).

### 5.2 Betaine is transported into follicles via a saturable transporter by postnatal day 17

Betaine is present in oocytes prior to CHDH activation and meiotic maturation but its origin is unknown. It is hypothesized that a betaine transporter exists in the follicular cells of the developing oocyte that mediates intracellular betaine accumulation prior to becoming a fully grown GV oocyte. My objective was to measure the amount of betaine uptake in pre-antral follicles and elucidate the pattern of betaine uptake over the course of folliculogenesis.

Groups of ~10 growing follicles and denuded oocytes were collected on P10, P15, P17 and P21 from neonatal mice. Follicles and oocytes were incubated in [$^3$H]-betaine (2 μM) with or without 5 mM unlabeled betaine for 10 minutes and the total and non-saturable amount of betaine taken up was measured. The amount of betaine is presented as femtomoles per follicle/oocyte per minute.

The amount of total and non-saturable [$^3$H]-betaine taken up was not significantly different in earlier follicles, at P10 and P15 (Figure 9). In P17 and P21 follicles, total [$^3$H]-betaine uptake was significantly higher than non-saturable uptake, indicating some saturable transport on these days. In comparison, denuded oocytes had significantly higher non-saturable uptake on P10, and approximately the same uptake between total and non-saturable groups on P15, P17, and P21 (Figure 10).

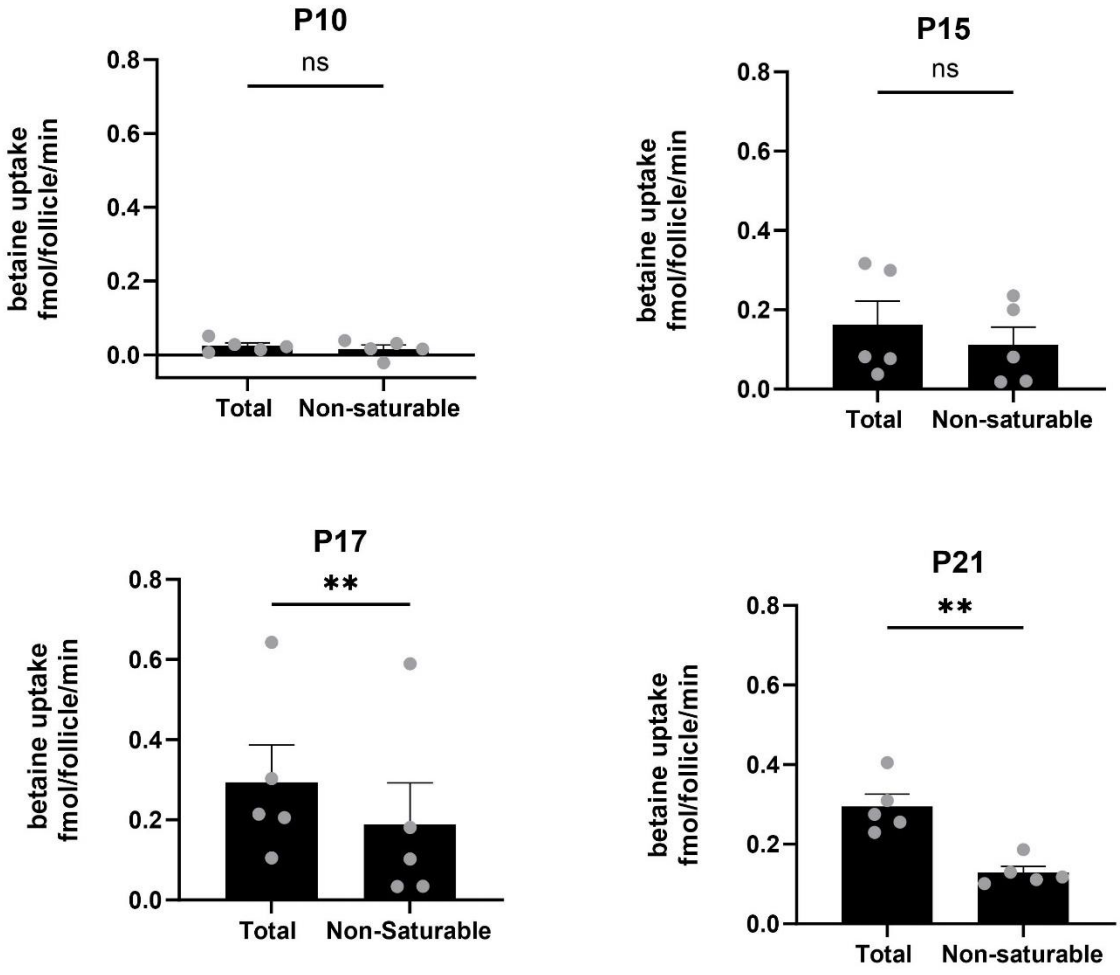


**Figure 9. Total and non-saturable betaine transport in growing follicles.**

Groups of ~10 growing follicles were collected at P10, P15, P17, and P21 and incubated for 10 minutes in 2 µM [3H]-betaine with 5mM unlabeled betaine (labeled non-saturable) or without 5mM unlabeled betaine (labeled total). Asterisks indicate a statistical difference among groups (P17: **: p=0.0088; P21: **: p=0.0061 by t test).

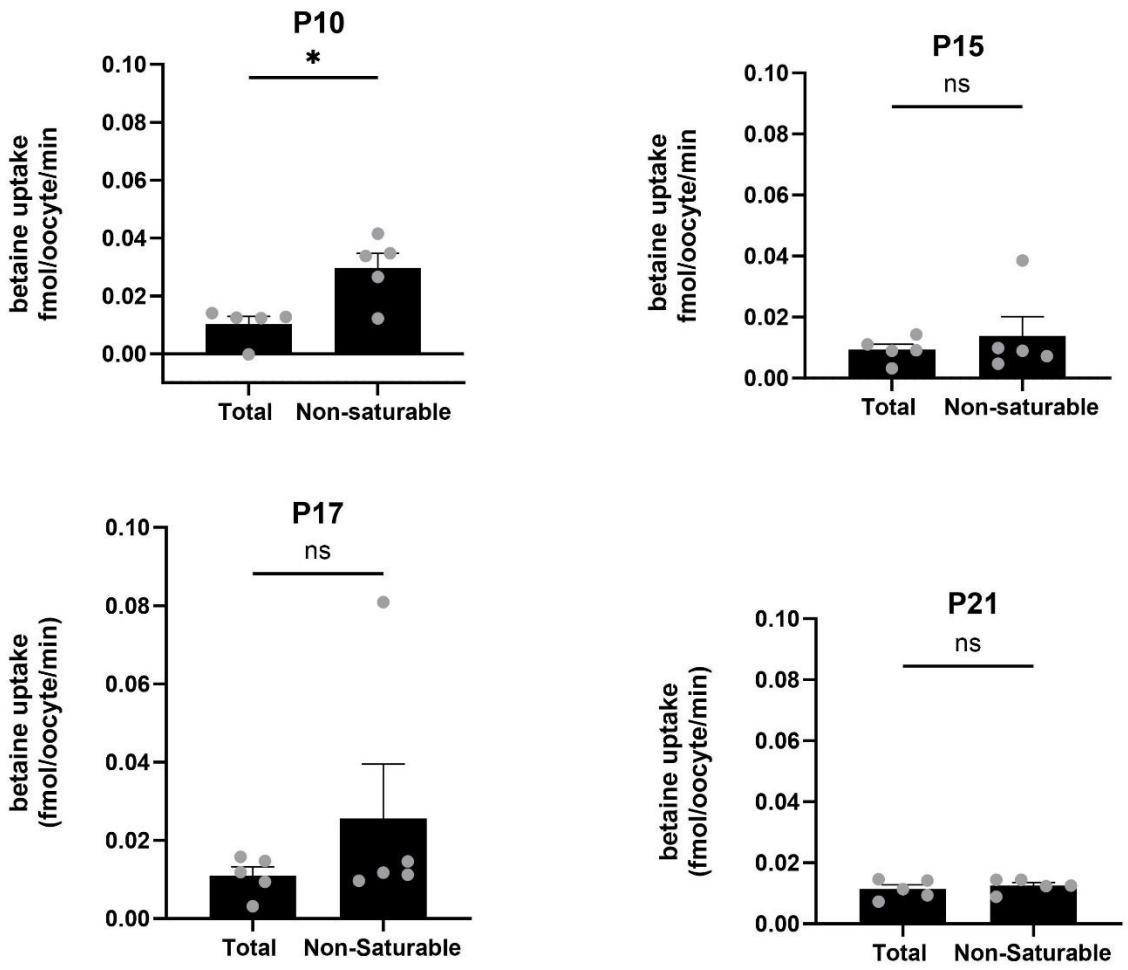


**Figure 10. Total and non-saturable betaine transport in denuded oocytes.**

Groups of ~10 denuded oocytes were collected at P10, P15, P17, and P21 and incubated for 10 minutes in 2 µM [3H]-betaine with 5mM unlabeled betaine (labeled non-saturable) or without 5mM unlabeled betaine (labeled total). Asterisks indicate a statistical difference among groups (*: p= 0.0351 by t test).

The amount of saturable transport in growing follicles and denuded oocytes was calculated by subtracting the non-saturable uptake from the total uptake and is presented in Figure 11A. In growing follicles, the amount of saturable uptake significantly increased between P10 and P21, from a rate of 0.008 to 0.166 fmoles/follicle/min. P15 was also significantly lower than P21 at a rate of 0.051 fmoles/follicle/min. Denuded oocytes exhibited no saturable transporter activity over any of the postnatal days, with the amount of saturable uptake consistently around 0 (Figure 11B).

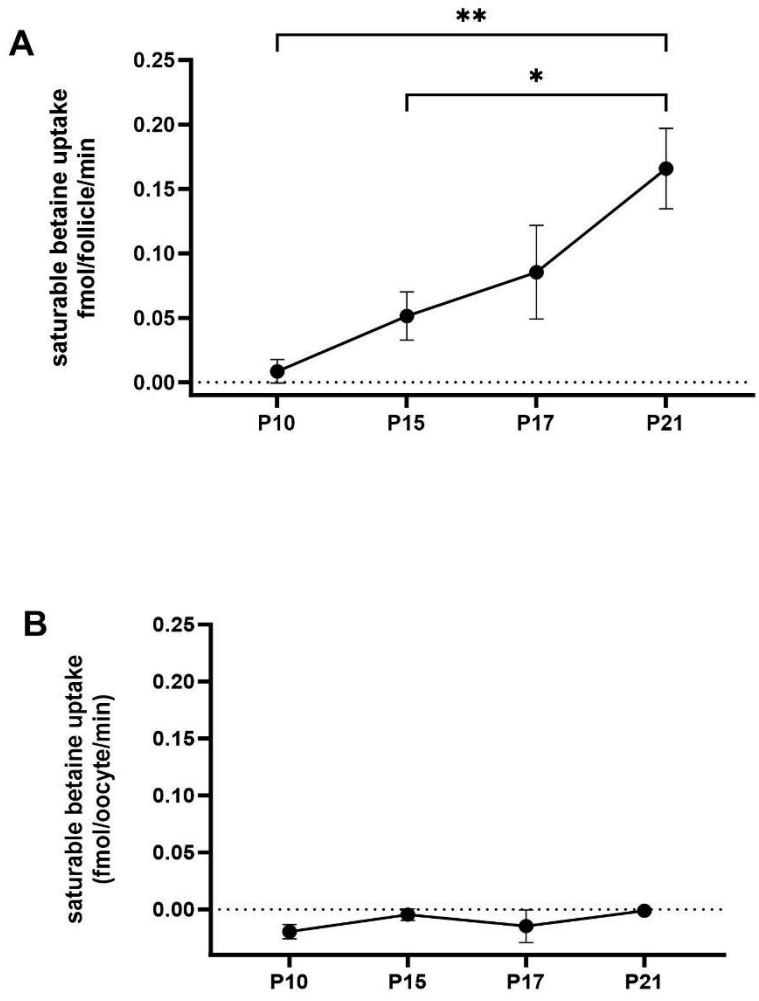


**Figure 11. Saturable transport in neonatal follicles and denuded oocytes.**

Groups of ~10 follicles (A) and oocytes (B) were collected over the first wave of oogenesis and incubated in 2 μM [3H]-betaine +/- 5 mM unlabeled betaine for 10 minutes. The amount of saturable transport was calculated from subtracting the non-saturable transport from the total transport for follicles in Figure 9, and oocytes in Figure 10. Asterisks indicate a significant difference (**: p=0.0030; *: p=0.0317 by ANOVA with Tukey test). N=5.

$Y^+$LAT2 has been previously detected in COCs (Corbett *et al*., 2014), and we hypothesized that the same saturable transporter would also be present in growing follicles. As there was evidence of saturable transport in P21 follicles, the experimental plan was to elucidate the inhibition profile of the unknown transporter using competitive amino acids that have been previously successful in inhibiting betaine uptake in COCs. However, we determined that our supply of [$^3$H]-betaine had degraded and labeled betaine of adequate quality was no longer obtainable from any source, so we could no longer proceed with this experiment (Figures B1-B3 in Appendix B).

### 5.3 Betaine retention, swelling-activated betaine efflux and *Lrrc8* expression across oocyte and preimplantation embryos

VSOACs activate upon cell swelling to mediate the efflux of both inorganic and organic osmolytes. VSOAC currents have been detected in preimplantation embryos and these channels may function in conserving betaine levels over the course of preimplantation embryo development. These $Cl^-$ channels are composed of five members of the LRRC8 protein family (LRRC8A-E) that form complexes to produce functional channels, consisting of LRRC8A and at least one other isoform to produce a heteromer. The composition of LRRC8 proteins from the GV oocyte to blastocyst stage has not been defined in mouse oocytes and preimplantation embryos. My objective was to determine whether betaine was retained over the course of preimplantation embryo development, to elucidate the link between betaine content and VSOAC activity prior to the blastocyst stage, and to measure *Lrrc8a-e* expression across oocyte and preimplantation embryo stages.

*5.3a Betaine levels are retained from two-cell embryos to morulae both* in vivo *and* in vitro

Fresh two-cell embryos, fresh morulae, fresh blastocysts, and morulae and blastocysts cultured *in vitro* from the two-cell stage were collected in groups of 30, and the endogenous betaine content was measured with LC-MS/MS. One repeat for morulae cultured *in vitro* was discarded due to a large contamination in the background. The amount of endogenous betaine is expressed as picomoles per embryo.

As shown in Figure 12A, there was no significant loss of endogenous betaine from the two-cell embryo stage to the morula stage when embryos were cultured in the absence of betaine, as two-cells and *in vivo* morulae had nearly identical betaine levels. *In vitro* morulae had slightly less betaine than two-cell embryos, but the difference was not significant. Freshly collected blastocysts and blastocysts cultured *in vitro* had a significantly lower level of betaine compared to two-cell embryos and *in vivo* morulae, which was consistent to results previously seen (Lee *et al.,* 2012). Endogenous betaine levels were not significantly different between *in vivo* and *in vitro* morulae or blastocysts.

Endogenous choline levels were consistent across preimplantation embryo stages, with no significant difference between two-cell embryos and either set of morulae or blastocysts (Figure 12B). However, choline was significantly higher in *in vivo* morulae compared to *in vitro* morulae, and in *in vivo* blastocysts compared to *in vitro* blastocysts. Betaine in morulae cultured *in vivo* was also significantly higher than blastocysts cultured *in vitro.*

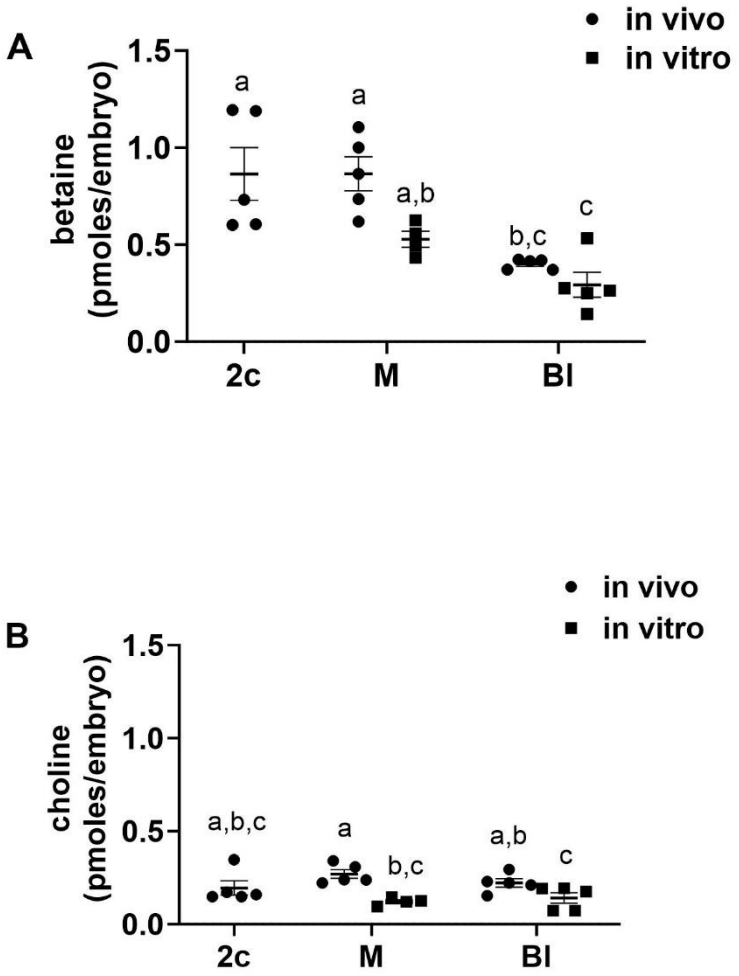


**Figure 12. Endogenous betaine and choline loss from the two-cell to morula and blastocyst stage in *in vivo* and *in vitro* conditions.**

Two-cell embryos, morulae, and blastocysts were freshly isolated and collected in groups of 30. Half of the two-cells first collected were cultured in mKSOM + PVA and collected at the morula or blastocyst stage in groups of 30. Endogenous betaine (A) and choline (B) levels were measured with LC-MS/MS. Different letters indicate a significant difference between groups ($p<0.05$ by two-way ANOVA with Šidák's multiple comparisons test).

*5.3b Swelling-induced betaine efflux out of one-cell embryos*

To determine if cell-swelling induces an efflux of betaine (i.e., if VSOAC as expressed in embryos is permeable to betaine), one-cell embryos were incubated in 2 μM [$^3$H]-betaine in mKSOM with an osmolarity of 250 mOsM for 30 minutes to load them with labelled betaine. Approximately ~10 embryos were removed for liquid scintillation, and the remainder (~10) were transferred to a non-radioactive drop of mKSOM with an osmolarity of 150 (hypotonic) or 250 mOsM (isotonic). After incubating for 30 minutes, the embryos were removed, and the betaine content was measured with liquid scintillation.

The percentage of betaine remaining in one-cell embryos after the second incubation is presented in Figure 13. Approximately 50% of the [$^3$H]-betaine initially accumulated was lost after transfer to the 150 mOsM mKSOM drop. In comparison, one-cell embryos retained approximately the same amount of betaine after the transfer to a drop of 250 mOsM mKSOM.

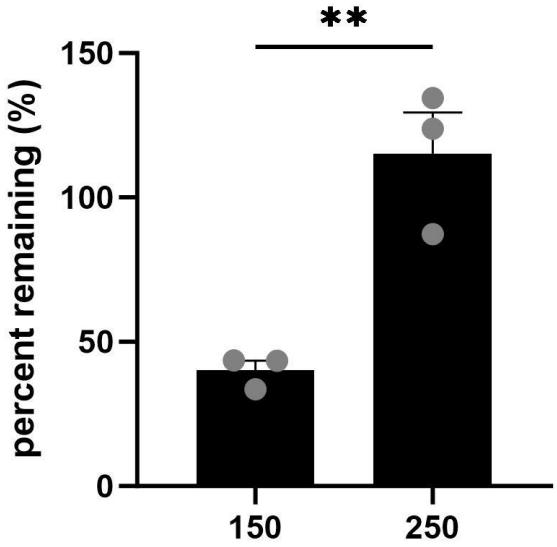


**Figure 13. Percentage of betaine remaining in one-cell embryos after remaining in isotonic media or transfer to hypotonic media.**

One-cell embryos were incubated in 2 μM [$^3$H]-betaine in 250 mOsM mKSOM for 30 minutes, followed by a 30-minute incubation in 150 mOsM or 250 mOsM mKSOM. One-cell embryos were collected in groups of ~10. The percent remaining was calculated by dividing the amount of betaine after the second incubation by the amount of betaine initially accumulated. Asterisks indicate a significant difference between groups ($p = 0.0069$ by *t* test).

An experiment to confirm that betaine efflux required VSOAC activity in preimplantation embryos was attempted with [$^3$H]-betaine in the presence of the VSOAC-specific inhibitor, DCPIB, but ultimately failed. Culture experiments using DCPIB and another $Cl^-$ channel inhibitor, DIDS, were also attempted. These are detailed in Appendix B and C (Figures B4, C1 and C2).

*5.3c* Lrrc8a-e *expression in oocytes and preimplantation embryos*

***5.3c (i) RT-PCR***

Total cellular RNA was isolated from GV oocytes, MII oocytes, two- and eight-cell embryos, morulae, and blastocysts. RNA isolated from liver, kidney, spleen, or ovary was used as the positive control. Several primers were selected using the primer designing tool by the NCBI and tested at various annealing temperatures using a temperature gradient (Figure A1 in Appendix A). A number of primer pairs were assessed for conventional RT-PCR but only one for each isoform was found to produce a single prominent band (not shown).

Amplicons were extracted using the QIAquick Gel Extraction Kit and sent for sequencing to the Ottawa Hospital Research Institute StemCore facilities. Sequences were matched to the predicted region using BLAST by NCBI, and primer specificity was confirmed for each LRRC8 isoform.

*Hmgb3* and *Rb1cc1* were used as reference genes to test the quality of cDNA. mRNA from each gene was present throughout all oocyte and embryo stages (Figure 14). *Lrrc8a* and *Lrrc8b* expression was detected at each stage, whereas *Lrrc8d* and *Lrrc8e* was more prominent in the GV and MII oocyte and one- and two-cell embryo stages. *Lrrc8c* was hardly detectable at any stage (Figure 14).

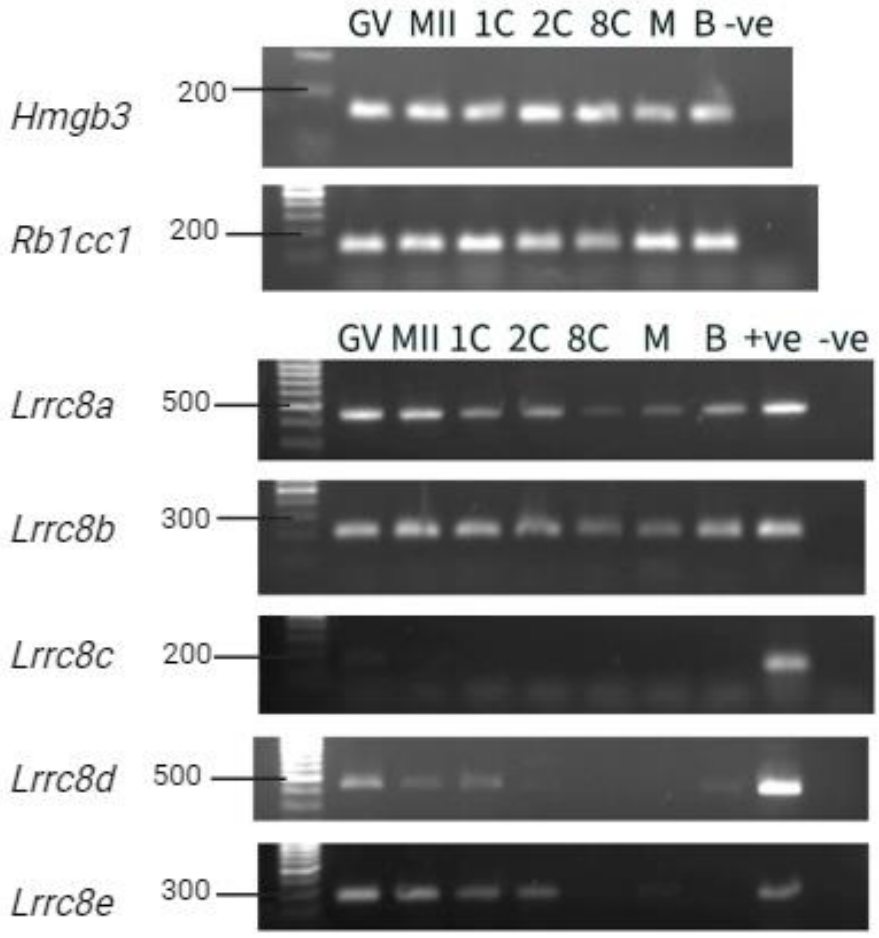


**Figure 14. *Hmgb3, Rb1cc1,* and *Lrrc8a-e* expression across oocyte and preimplantation embryo stages.**

RT-PCR (36 cycles) was performed with 2.5 oocytes or embryos per reaction, and ~20-40 ng of tissue cDNA for the positive control, depicted as +ve. Water was added to the reaction mix as a negative control (-ve). *Hmgb3* and *Rb1cc1* are at 152 bp and 129 bp, respectively. *Lrrc8a-e* bands are at 436 bp, 210 bp, 184 bp, 441 bp, and 290 bp, respectively. The samples were run in a 1.75% agarose gel with ethidium bromide for 1 hour at 110 V. The figure shown is representative of three independent repeats.

### *5.3c (ii) qRT-PCR*

qRT-PCR was performed to measure *Lrrc8a-e* expression quantitatively. All samples used for qRT-PCR were collected and converted to cDNA by Dr. Allison Tscherner. cDNA was diluted so that an equivalent of 0.36 oocytes per 2 µl template were used in each qPCR reaction. The same primers used in the conventional RT-PCR experiments were used again. A standard curve was prepared for *Hmgb3, Rb1cc1* and each *Lrrc8* isoform (other than *Lrrc8c*) and was run along the oocyte and preimplantation embryo samples to measure the amount of RNA in femtograms. A melt curve was also generated to confirm the presence of a single amplified product (Figure A2 in Appendix A). The primers used for *Lrrc8d* and *Lrrc8e* displayed more than one peak in the melt curve, indicating amplification of a secondary product, and could therefore not be used (Figure A3 in Appendix A).

As expected, mRNA for *Hmgb3* and *Rb1cc1* was detected at each oocyte and embryonic stage, with the highest level of expression in the GV oocyte stage, as shown in Figure 15. *Hmgb3* expression did not significantly differ among stages, but *Rb1cc1* expression in GV oocytes was significantly higher than in two- and eight-cell embryos, and blastocysts. mRNA for *Lrrc8a* was also detected, but at levels lower than either of the reference genes, and with no significant difference between oocyte or embryo stages (Figure 15). *Lrrc8a* was expressed in GV oocytes, MII oocytes, one-cell embryos, and two-cell embryos. However, very little mRNA was present in the later embryo stages. The cycle threshold (Ct) values for *Hmgb3, Rb1cc1,* and *Lrrc8a* were approximately 30. There was continuous contamination in the no template control for *Lrrc8b,* so it was also omitted.

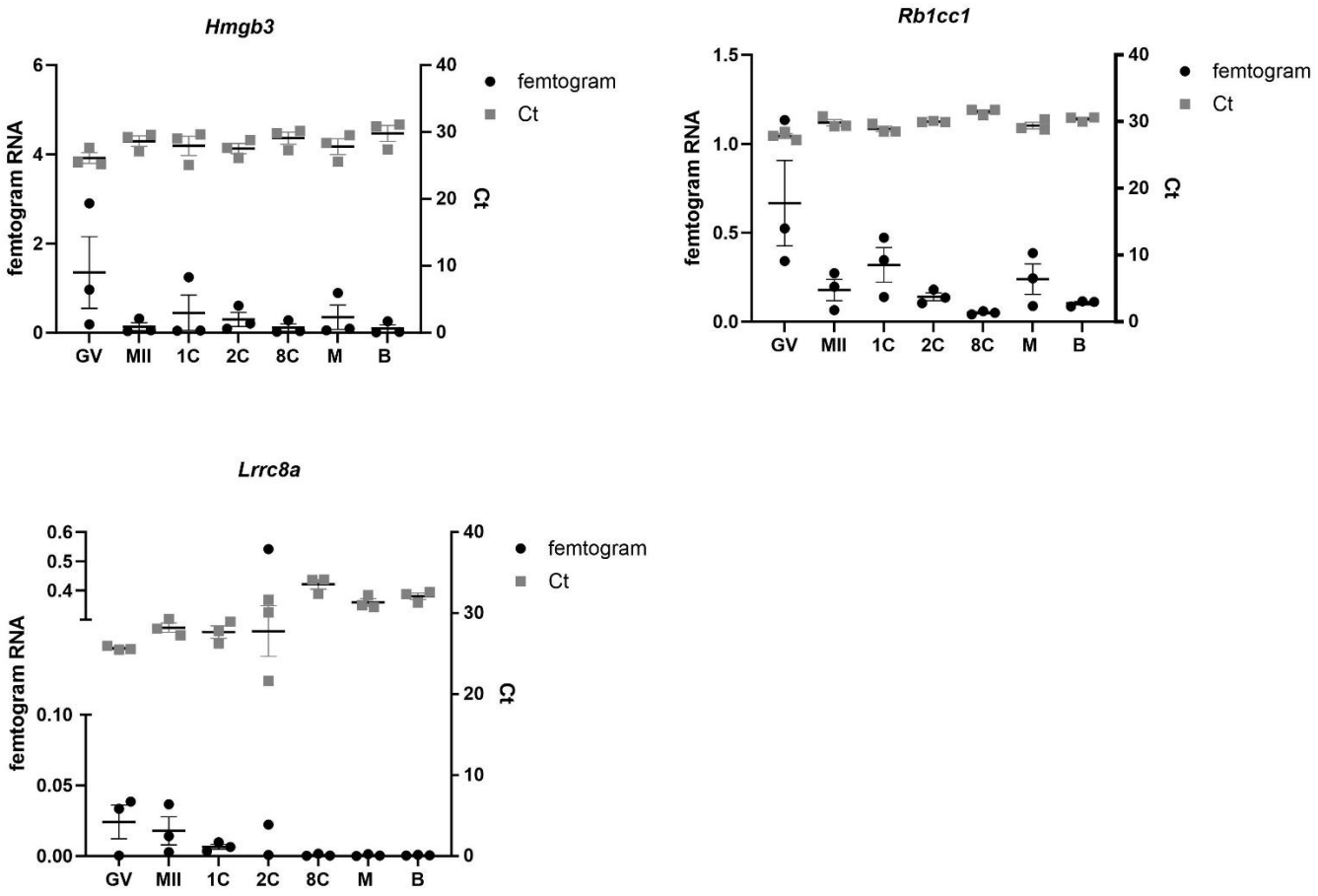


**Figure 15. mRNA quantification of *Hmgb3, Rb1cc1*, and *Lrrc8a.***

qRT-PCR was performed using 0.36 oocytes/embryos per reaction, with the same primers used in conventional RT-PCR. Each sample was loaded in triplicate wells and averaged for one independent repeat. The amount of RNA in femtograms was calculated by preparing a standard curve from 1000 fg diluted to 0.01 fg with a 1:10 serial dilution. Ct = cycle threshold. Bars with different letters indicate a significant difference ($p<0.05$ by one-way ANOVA with Tukey test).

### *5.3c (iii)* **Lrrc8** *expression assessed using RNASeq data sets*

GEO DataSets that contained *Lrrc8* transcripts were extracted from standardized and merged RNAseq data sets (Tscherner *et al*., 2023). The RNAseq data for GV oocytes, MII eggs, and each preimplantation embryo stage are shown in Figure 16. Expression for each of the transcripts changed over development. *Lrrc8c* was hardly expressed across oocyte or preimplantation embryo stages, consistent with the results of conventional RT-PCR. *Lrrc8a, Lrrc8b, Lrrc8d,* and *Lrrc8e* expression was mostly concentrated in GV oocytes, MII oocytes, one- and two-cells, and less expression was observed in four-cells, eight-cells, morulae, and blastocysts. Isoforms were uniformly expressed in GV oocytes and one-cell embryos. In MII oocytes, *Lrrc8a, Lrrc8d,* and *Lrrc8e* were expressed at a level similar to GVs, and *Lrrc8b* was the most highly expressed. Two-cell embryos exhibited some variation in expression, with *Lrrc8a* most prominent, followed by *Lrrc8b*, *Lrrc8d*, and then *Lrrc8e. Lrrc8a* was highest in four-cell embryos, followed by *Lrrc8e, Lrrc8b,* and finally *Lrrc8d.* Eight-cell embryos, morulae, and blastocysts exhibited approximately the same expression for each isoform, but *Lrrc8a* was overall highest, followed by *Lrrc8d, Lrrc8e,* and finally *Lrrc8b.*

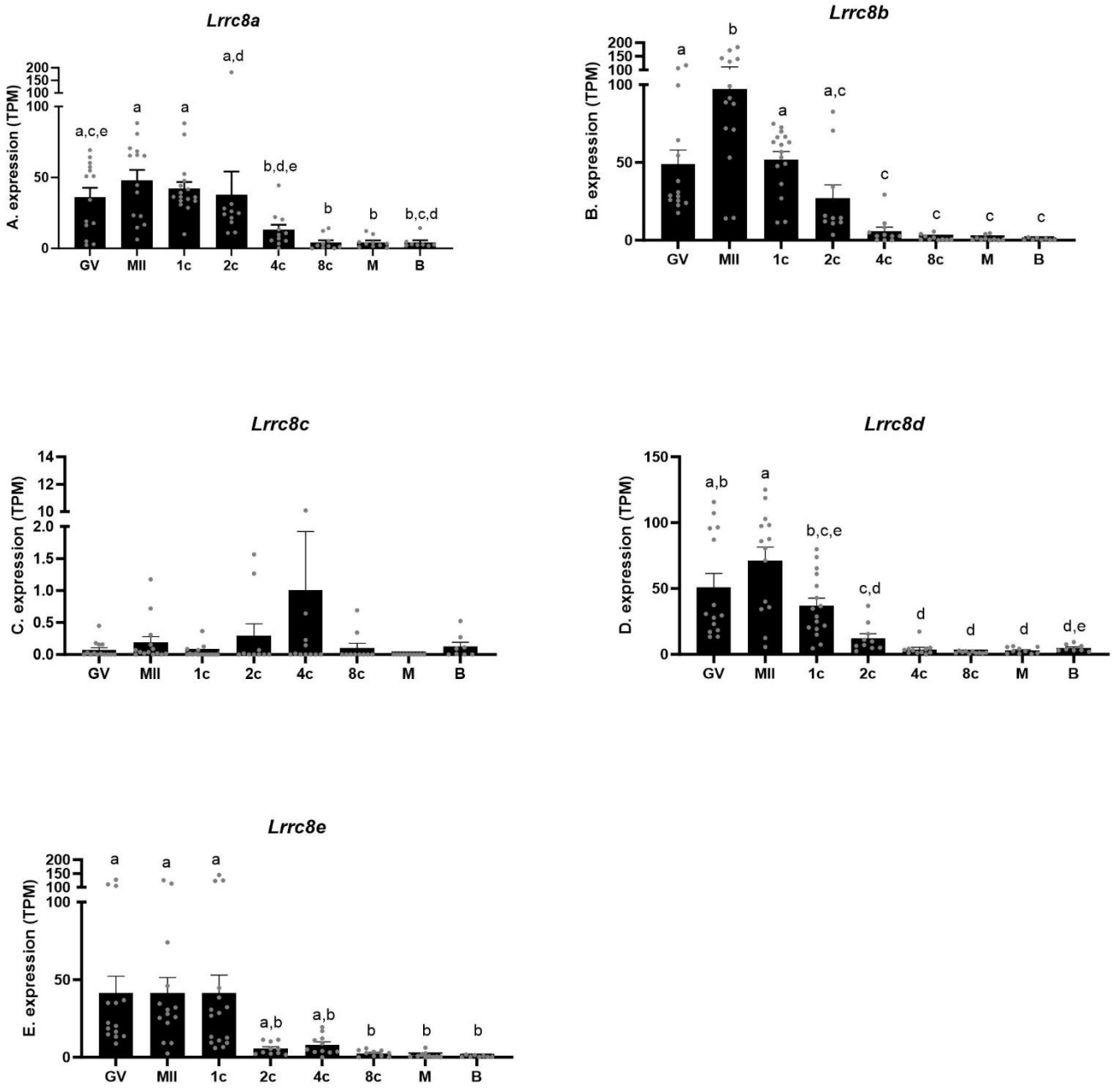


**Figure 16. *Lrrc8a-e* expression in transcripts per million (TPM) across GV, MII, and preimplantation embryo stages.**

The RNAseq data sets were pulled from GEO and mapped to the GENCODE mouse vM25 annotation release of the mouse genome. Bars with different letters are significantly different

($p<0.05$ by one-way ANOVA with Tukey test). GV: GV oocytes; MII: MII oocytes; 1C: one-cell embryo; 2C: two-cell embryo; 4C: four-cell embryo; 8C: eight-cell embryo; M: morula; B: blastocyst.

### 5.4 Endogenous betaine levels in BHMT wildtype and BHMT knockout blastocysts were not significantly different

Betaine has a second role as a methyl donor for methylation reactions in the inner cell mass of the blastocyst. The universal methyl donor, SAM, is derived from BHMT in some cell types (Lee *et al*., 2015; Zhang *et al.,* 2015). BHMT catalyzes the transfer of a methyl group from betaine to homocysteine, which forms dimethylglycine and methionine. The latter is subsequently converted to SAM. The onset of BHMT expression coincides with a decrease in betaine levels at the blastocyst stage. My objective was to determine if metabolism by BHMT is the cause for the decrease in betaine from the morula to blastocyst stage.

Blastocysts from both *Bhmt*$^{+/+}$ and *Bhmt*$^{-/-}$ mice were collected in groups of 30 and their endogenous betaine and choline was measured with LC-MS/MS. Unexpectedly, knocking out BHMT did not increase betaine levels to that observed in morulae. Both endogenous betaine and endogenous choline were not significantly different between *Bhmt*$^{+/+}$ and *Bhmt*$^{-/-}$ blastocysts (Figure 17). There seemed to be a trend toward lower choline, however ($p = 0.0921$).

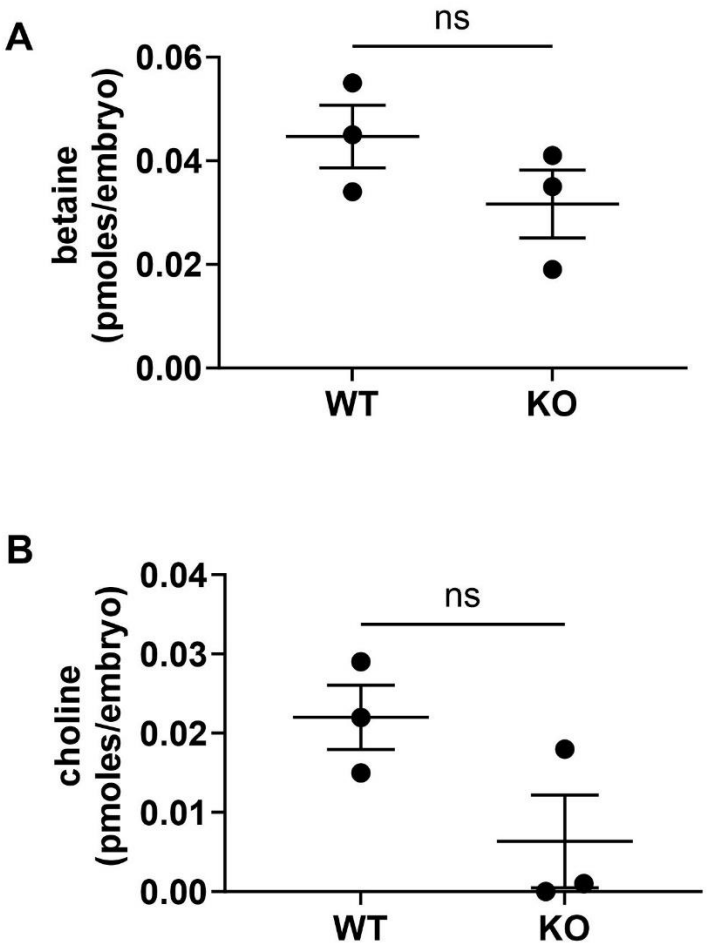


**Figure 17. Endogenous betaine levels in wildtype vs. knockout BHMT blastocysts.**

Blastocysts were collected in groups of 30 and measured with LC-MS/MS. Neither betaine (A) nor (B) choline was significantly different between groups ($p>0.05$ by *t* test).

## 6. Discussion

Betaine has been proposed as a crucial organic osmolyte during oocyte and preimplantation embryo development. It has demonstrated the ability to rescue early cleavage stage embryo growth at high osmolarities *in vitro* (Dawson & Baltz, 1997). It also contributes to both the methyl pool for DNA methylation reactions and the development of the ICM of the blastocyst (Lee *et al*., 2012). The research presented here investigates how intracellular betaine levels are regulated from oogenesis to the blastocyst stage. My results show that intracellular betaine is present early in oogenesis and may be transported into the developing follicle near the end of folliculogenesis. Endogenous betaine levels may be retained by VSOAC during preimplantation embryo development, and the betaine decrease at the blastocyst stage may not be due to metabolism by BHMT.

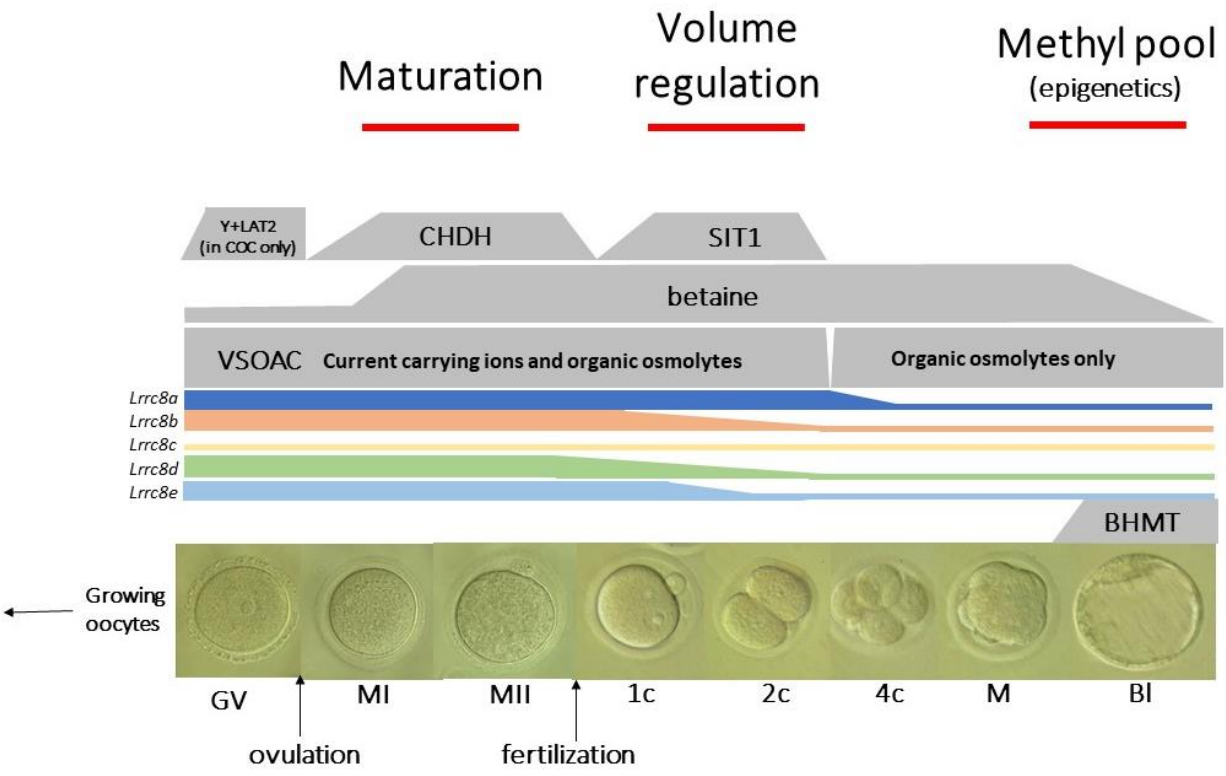


**Figure 18. Schematic representation of processes driving endogenous betaine levels in oocytes and preimplantation embryos.**

Growing oocytes contain a low level of endogenous betaine prior to both y+LAT2 and choline dehydrogenase (CHDH) activation. $Y^{+}$LAT2 is present in the cumulus cells of the COC and uptakes betaine and transports it via gap junctions to the enclosed oocyte, which may contribute to some of the low levels of endogenous betaine observed in GV oocytes. When ovulation is triggered, meiotic maturation occurs, and betaine synthesis via CHDH is activated. After the egg is fertilized, CHDH inactivates and the SIT1 transporter mediates betaine transport until the four-cell stage. Regulatory volume decrease (RVD) occurs throughout oocyte and preimplantation embryo development, via volume-sensitive organic osmolyte and anion channels (VSOACs). VSOACs are permeable to both current carrying ions and organic osmolytes until the four-cell

stage, where the permeability changes to organic osmolytes only. VSOACs are composed of LRRC8 proteins, and *Lrrc8* transcripts are more highly expressed in oocytes, eggs, and early preimplantation embryos. Betaine levels are conserved over preimplantation embryo development but decrease at the blastocyst stage. At the same time, betaine homocysteine methyltransferase (BHMT) activates in the blastocyst and uses a methyl group from betaine to generate S-adenosylmethionine (SAM) to be used in methylation reactions for epigenetic modifications of DNA.

**Endogenous betaine is present at a low, uniform level from early oogenesis through the GV stage**

There appears to be a requirement for endogenous betaine as suggested by the high levels present in mouse eggs and preimplantation embryos (Lee *et al*., 2012; McClatchie *et al*., 2017). There are three potential sources of intracellular betaine: *de novo* synthesis by CHDH within the oocyte or embryo itself, synthesis by CHDH in other tissues, or by supplementation from the diet. The latter two would necessarily require transport of the external betaine into the oocyte or embryo. Our laboratory has previously determined that the high intracellular betaine in mouse eggs is derived from *de novo* synthesis by CHDH that becomes highly active during meiotic maturation (McClatchie *et al.,* 2017). Despite the lack of such high CHDH activity, betaine is present in postnatal day 11 pre-antral follicles, at a level slightly lower than what is observed in GVs and COCs (McClatchie *et al*., 2017). The source of endogenous betaine and onset of betaine accumulation in growing oocytes was a key knowledge gap in mouse oocyte and embryo physiology. Therefore, I aimed to determine the precise stage of growth at which intracellular betaine appears during oogenesis, and how much is present in both denuded oocytes and follicles to determine which compartment(s) betaine may be stored in.

Growing oocytes isolated from neonatal ovaries contained low, essentially constant levels of betaine throughout oogenesis. Contrary to our hypothesis, betaine did not appear during oogenesis and its levels did not increase during oocyte growth but remained at a consistently low level of ~0.5-1.0 pmoles/oocyte from P5 through the GV stage, where they peaked after the onset of CHDH activation.

The endogenous concentration of choline was also examined over the same postnatal days, and we found that intracellular choline stayed nearly constant. The lack of a significant betaine

increase and corresponding choline decrease does not suggest choline conversion to betaine by CHDH, which is consistent with the lack of CHDH activity previously seen in growing oocytes (McClatchie *et al.,* 2017). As endogenous betaine was present in small growing (P5) oocytes, it is possible that betaine accumulates earlier than that stage.

**Growing follicles possess a larger reserve of endogenous betaine and choline that may not be transferred to the enclosed oocyte during oogenesis**

We also sought to measure the endogenous betaine and choline content of growing follicles, to determine if betaine or choline is stored in the follicle and possibly transferred to the enclosed growing oocyte. Growing follicles had a high reserve of betaine, especially when fully grown (P21) at ~4 pmoles/follicle. Endogenous choline was found at an even higher concentration, at ~60 pmoles/follicle in fully grown oocytes at P21.

Given the difference between the concentration of betaine and choline in the follicles and the concentration in the denuded oocytes, it appears that growing follicles do not transfer a significant proportion of their content of either molecule to the enclosed growing oocyte. Choline can be transported into GV oocytes via uptake by cumulus cells and subsequent transfer to the enclosed oocyte (Eppig, 1982; Salustri & Siracusa, 1983). The choline required for metabolism by CHDH is transported into the oocyte via gap junctions, until the cumulus cells and the oocyte become uncoupled at ~6 h post-hCG (McClatchie *et al.,* 2017). My results support this idea, as the choline level observed in both denuded P21 and GV oocytes is still relatively low at ~0.4 pmoles/oocyte. Therefore, choline may only be transferred from cumulus cells to the oocyte between the GV and MI oocyte stage, prior to uncoupling. Betaine may be concentrated in the

GCs or follicular fluid, rather than in the cumulus cells, as COCs and denuded GV oocytes had nearly the same amount of endogenous betaine at less than 1 pmole/oocyte (McClatchie *et al*., 2017).

The source of intracellular betaine in growing oocytes and follicles is likely from synthesis by CHDH in other tissues, such as the liver and kidney (Grossman & Hebert, 1989). The synthesized betaine may be brought to the ovary via circulation, before entering the follicle. Growing oocytes may not have an absolute requirement for betaine, given the low levels observed, however, the higher reserve of endogenous betaine and choline in follicles may be required for follicular growth or other physiological functions during development.

Betaine has demonstrated the ability to enhance the activity of antioxidants in the rat ovary (Alirezaei *et al.,* 2012), and may have a role in protecting cell membranes from reactive oxygen species (ROS) generated as preovulatory follicles develop (Tsai-Turton & Luderer, 2006), and at the time of ovulation (Ebisch *et al*., 2007). Choline is an essential nutrient as a precursor for the synthesis of acetylcholine and membrane phospholipids (Zeisel, 2006). Follicular fluid contains an abundance of certain phospholipids, such as phosphatidylcholine (PC) and lysophosphatidylcholine (LPC), suggesting that PC synthesis is involved in follicular growth (Lai *et al*., 2018), which would ultimately require choline. Overall, further research is required to determine the precise point at which betaine is initially accumulated during oogenesis and the role of choline.

**Growing follicles are capable of saturable betaine transport when they reach the antral stage**

As mentioned above, one of the possible routes through which betaine may enter growing oocytes is via synthesis by CHDH in other tissues, and delivery to the follicle through the circulation. This mechanism likely requires a betaine transporter in the follicular cells, as it has been previously determined that GV oocytes themselves cannot transport betaine (Anas *et al*., 2008). The low levels of betaine detected in GV oocytes is transferred from the cumulus cells of COCs, via the $y^+$LAT2 (*Slc7a6*) transporter (Corbett *et al*., 2014). Thus far, $y^+$LAT2 activity has been reported to be restricted to cumulus cells, and a betaine transporter in growing follicles has yet to be demonstrated. Therefore, I measured how much betaine is transported during folliculogenesis and if there is a saturable betaine transporter present in growing follicles and denuded oocytes.

My results are consistent with previous data in that denuded oocytes were only capable of nonsaturable betaine uptake, likely via passive diffusion (Anas *et al*., 2007; Anas *et al*., 2008; Corbett *et al.,* 2014). Nonsaturable uptake was significantly higher in mid-growth (P10), and approximately the same amount of betaine was observed in the total and nonsaturable groups for the remaining stages of growth. The amount of uptake was overall low, at ~0.01 pmoles/oocyte for oocytes from P10, P15 and P21, and ~ 0.02 fmoles/oocyte/min for P17. As such, the saturable amount of betaine taken up in growing oocytes was negligible and we can likely conclude that growing oocytes lack a betaine transporter, or do not have a requirement for activating a saturable betaine transport during this stage.

As for the growing follicles, preantral follicles collected on P10 and P15 displayed similar transport activity. The betaine taken up was indicative of mostly nonsaturable transport, however

the amount taken up in P15 follicles was much higher than the betaine taken up by denuded oocytes. At P17 and P21, the total amount of betaine taken up was significantly higher than the nonsaturable amount, which suggested some saturable transport over these postnatal days. When the nonsaturable amount was subtracted from the total amount of betaine, it was evident that saturable betaine transport increased over postnatal days, from a rate of 0.008 to 0.166 fmoles/follicle/min from preantral (P10) to antral (P21). These results agree with our hypothesis that there is a saturable betaine transporter present in growing follicles. However, the transporter may only be active towards the end of folliculogenesis.

Given that $y^+$LAT2 has been identified in COCs, it is possible that $y^+$LAT2 is also present in developing follicles. We attempted to identify the transporter in P21 follicles using competitive amino acid inhibition and [$^3$H]-betaine, but betaine that passed quality control tests was no longer available (as shown in Appendix B). Further experiments to demonstrate the likely presence of y+LAT2 without the use of [$^3$H]-betaine could involve conventional RT-PCR and qPCR and/or western blots to assess the expression of the transporter. If $y^+$LAT2 is indeed present in follicular cells, transcription of the transporter may begin at some point during folliculogenesis, but its functional expression may be limited to antral follicles. There is very likely no expression in growing oocytes, consistent with denuded GV oocytes, since they do not transport betaine (Corbett *et al*., 2014).

There are a few possibilities that can be proposed to explain the low levels of endogenous betaine in growing oocytes despite the apparent lack of transporter activity. First, low levels of CHDH activity could be present during all of oogenesis, either in growing oocytes or growing follicles. Secondly, betaine transport by oocytes could occur prior to the beginning of growth, or prior to P5. Betaine transport may occur in oocytes at the time of recruitment for growth, or in

follicular cells at the start of folliculogenesis. Both have yet to be explored and require further research.

**Betaine is retained during preimplantation embryo development**

As shown in Figure 18, after CHDH activity dissipates post-meiotic maturation, and SIT1 inactivates at the four-cell stage, endogenous betaine levels are still retained over preimplantation embryo development until the blastocyst stage, where they then decrease. There has been no significant betaine transporter activity detected during this time (Anas *et al*., 2008). While development is occurring, cell volume regulatory mechanisms are still in place, including VSOAC channels to mitigate cell volume increases. VSOAC can be activated by cell swelling from the oocyte stage to the blastocyst stage and has exhibited increased permeability to several organic osmolytes when hypotonic swelling was induced (Van Winkle *et al*., 1994; Dawson *et al*., 1998; Kolajova *et al*., 1999). It has not been confirmed that VSOAC regulates endogenous betaine levels prior to the blastocyst stage, nor has the expression of *Lrrc8a-e* been determined throughout oocyte and preimplantation embryo development. Therefore, I sought to measure whether endogenous betaine is lost from the two-cell stage to the morula and blastocyst stages, determine if betaine is capable of being lost via swelling-activated channels, and elucidate which *Lrrc8* isoforms are present and at what stage.

Consistent with previous reports (Lee *et al.,* 2012), my results showed that endogenous betaine levels are conserved from the two-cell to morula stage and decrease at the blastocyst stage both in *in vivo* and *in vitro* groups. Endogenous betaine was not significantly different between *in vivo* and *in vitro* morulae or blastocysts, but *in vitro* embryos did have slightly less betaine. Endogenous choline levels were also measured and revealed that choline levels do not

change significantly from the two-cell to morula or blastocyst stage. However, differences in choline levels were apparent between *in vivo* and *in vitro* groups, with *in vivo* morulae and blastocysts having significantly higher levels than *in vitro.* Choline may be present at high concentrations in the oviduct, which may have been reflected in the morulae and blastocysts cultured *in vivo*, or the difference may have been due to variations between the mice. These results confirm that both betaine and choline are retained over preimplantation embryo development.

**VSOAC is capable of mediating swelling-activated betaine loss in preimplantation embryos**

Since the hypothesis had been that betaine might be lost via VSOAC channels during preimplantation embryo development, I sought to show that betaine retention was not due to the inability of VSOAC channels to be permeable to betaine. Therefore, I confirmed that one-cell embryos exhibited swelling-activated betaine efflux. One-cell embryos loaded with [$^3$H]-betaine and placed in a dish with hypotonic medium retained approximately half the amount of betaine initially accumulated. In comparison, one-cell embryos that remained in isotonic media after loading with [$^3$H]-betaine retained nearly all their betaine.

The increased permeability to betaine induced by hypotonic swelling is consistent with previous reports that have shown similar swelling-induced permeability with glycine and taurine in mouse embryos (Van Winkle *et al*., 1994; Dawson *et al*., 1998; Kolajova *et al*., 2001). As VSOAC is activated upon cell-swelling, this experiment suggests that VSOAC is capable of mediating betaine efflux and may induce the release of betaine as a cell volume regulatory mechanism. However, to further confirm that it is VSOAC specifically that induces swelling-

activated betaine loss would include using the VSOAC-specific inhibitor, DCPIB, or other $Cl^-$ channel inhibitors to inhibit betaine efflux.

### *Lrrc8a-e* transcript expression is highest in oocytes and early preimplantation embryos

Looking at *Lrrc8* isoform expression across oocyte and preimplantation embryo development, conventional RT-PCR revealed that *Lrrc8a* and *Lrrc8b* appeared to be expressed at every stage from GV oocyte to blastocyst. *Lrrc8d* and *Lrrc8e* appeared to be restricted to the GV oocyte, MII oocyte, and one-cell embryo. Expression also persisted into the two-cell stage for *Lrrc8e. Lrrc8c* was not expressed at all throughout development. Based on these results, I proceeded with qPCR to quantitatively measure mRNA expression. However, I was only able to obtain data from the reference genes *Hmgb3* and *Rb1cc1*, and *Lrrc8a* since suitable primer pairs could not be identified for the other *Lrrc8* isoforms. *Lrrc8a* mRNA was detected primarily from the GV oocyte to the two-cell embryo stage, after which it decreased.

The data from RNAseq data sets confirmed the lack of *Lrrc8c* expression and showed that *Lrrc8a, Lrrc8b, Lrrc8d,* and *Lrrc8e* were mainly expressed from the GV oocyte to the one-cell or two-cell stages. The expression pattern obtained from RNAseq for *Lrrc8a* was essentially consistent with that obtained by RT-qPCR. However, the values generated from the RNAseq datasets are counted as a proportion while the values from qPCR are absolute, so we can only suggest the relative pattern of *Lrrc8* during oocyte and preimplantation embryo development.

It was previously shown that the properties of VSOAC changes over oocyte and preimplantation embryo development. VSOAC currents carried by anions were present only through the two-cell stage, while swelling-activated permeability to the organic osmolyte glycine persisted from the four-cell stage and on (Kolajova *et al.,* 2001; shown in Figure 18). The

swelling-activated anion current carried by VSOAC (referred to as $I_{Cl,swell}$) is significant in the one-cell stage, becomes inactive at the end of the two-cell stage, and does not re-appear until the blastocyst stage. Swelling-induced permeability to glycine is evident in one-cell embryos and two-cell embryos in the late $G_2$ phase, however, glycine permeability de-activates in two-cell embryos entering metaphase, and then re-appears at the end of the two-cell stage after cytokinesis (Kolajova *et al.,* 2001). It can be suggested that this may be due to differences in isoform composition and selectivity for a particular substrate at a specific developmental stage. Certain LRRC8 family isoforms may therefore be expressed during oocyte and preimplantation embryo development to regulate the efflux of current carrying anions, or the efflux of organic osmolytes.

LRRC8A (or SWELL1) is essential for $I_{Cl,swell}$ (Qiu *et al.,* 2014; Voss *et al*., 2014), and typically forms a heteromer with at least one other isoform. Previous studies have shown that in somatic cells, LRRC8A with either LRRC8C or LRRC8E may be necessary for $I_{Cl,swell}$ (Voss *et al.,* 2014), or LRRC8A with LRRC8D or LRRC8E (Syeda *et al*., 2016). For permeability to organic osmolytes, LRRC8A coupled with LRRC8D may be required for swelling-induced taurine efflux (Planells-Cases *et al*., 2015; Lutter *et al*., 2017). As swelling-induced permeability to glycine was observed in four-cell embryos (Kolajova *et al*., 2001), but *Lrrc8* transcripts were low, it may be possible that LRRC8 proteins required for organic osmolyte efflux are stable and remain present throughout preimplantation embryo development. Whether four-cell embryos and later preimplantation embryos exhibit swelling-activated betaine efflux remains to be determined, as well as which LRRC8 proteins may be required for conducting betaine loss.

Furthermore, maternal mRNA degrades in two cascades, where the first wave occurs during meiotic maturation and is triggered by maternal factors (Walser & Lipshitz, 2011), and the

second occurs alongside ZGA, guided by zygotic factors, and mainly occurs between the two- and four-cell stages (Sha *et al*., 2020) It can be suggested that *Lrrc8* family mRNAs are maternal, and possibly degrades by the four-cell stage, which is represented by the lack of expression in the later preimplantation embryo stages. Vigorous transcription activity in growing oocytes establishes the maternal transcriptome (Tora *et al.,* 2021). At the end of oocyte growth, the stability and the translatability of the maternal transcriptome may be crucial for fertilization, meiotic resumption, and early preimplantation embryo development (Tora *et al.,* 2021; Innocenti *et al*., 2022). Therefore, if *Lrrc8* family mRNAs are maternal, transcripts may be synthesized and stored as the oocyte grows, prior to the onset of transcriptional repression at the GV stage (De La Fuente & Eppig, 2001). If most of the maternal mRNA has degraded by the two-cell stage, it is possible that the composition of VSOAC changes to one that does not allow betaine to permeate through. This could cause endogenous betaine to be retained during preimplantation embryo development.

**Deleting *Bhmt* does not prevent the decrease in endogenous betaine at the blastocyst stage**

Re-methylation of the embryonic genome takes place in the ICM of the blastocyst (Lee *et al*., 2012). At this time, most SAM is generated from the methionine cycle and supplies the methyl pool for DNA and histone methylation reactions. Simultaneously, BHMT generates some SAM through the metabolism of betaine (Zhang *et al*., 2015). In the blastocyst stage, endogenous betaine levels are lower than at any other preimplantation embryo stage. As BHMT becomes active in the blastocyst, it was hypothesized that BHMT metabolizes betaine and causes the decrease in endogenous betaine levels. Therefore, I compared the endogenous betaine in blastocysts isolated from both BHMT wildtype and BHMT knockout mice.

Unexpectedly, my results showed that the endogenous betaine levels of *Bhmt*$^{+/+}$ and *Bhmt*$^{-/-}$ blastocysts were nearly the same. Indeed, there was slightly less betaine in the knockout group, although this difference was not significant. This does not support the hypothesis that BHMT activity is the cause of the decrease in betaine since knockout blastocysts should then have higher betaine levels than wildtype. These results are also contrary to previous work, where deleting *Bhmt* resulted in a significant increase of betaine in several tissues (Teng *et al*., 2011). Endogenous choline was also measured and revealed that the knockout blastocysts had less choline than wildtype blastocysts. However, this agrees with previous data, where it was found that choline was lower in all tissues isolated from *Bhmt* knockouts (Teng *et al.,* 2011). The lower choline in blastocysts may be a result of this lower-level circulating choline in the knockouts.

The low levels of betaine in the knockout blastocysts implies that although betaine is almost certainly metabolized by BHMT (Lee *et al*., 2012; Zhang *et al.,* 2015), the amount consumed must be small and the decrease in endogenous betaine is caused by an alternative mechanism. As VSOAC has been documented in the blastocyst stage (Van Winkle *et al*., 1994; Kolajova *et al*., 2001), it is possible that VSOAC induces the efflux of betaine at this time. Early preimplantation embryos also contain high levels of endogenous glycine at ~4-10 pmoles/embryo, but in blastocysts, glycine decreases to approximately 10% or less of the content measured in two-cell embryos (Schultz *et al*., 1981; Van Winkle & Dickinson, 1995; Tartia *et al*., 2009). Therefore, it appears that blastocysts may not have a requirement for a large reservoir of betaine, and that VSOAC may induce the release of organic osmolytes such as glycine and betaine during the blastocyst stage while preferentially retaining betaine in earlier stages. Further research to profile VSOAC activity and its substrate preferences during preimplantation embryo development through the blastocyst stage is ultimately required.

## 7. Conclusions

The results presented in this thesis have provided a deeper understanding of the mechanisms of intracellular betaine regulation utilized by growing oocytes and preimplantation embryos. My data suggests that betaine accumulation begins earlier than the earliest growing oocytes assessed (from P5 ovaries). By mid-growth (P17), with the appearance of larger follicles, saturable betaine transport is present and persists in fully grown (P21) antral follicles. However, despite the large reservoir of endogenous betaine and choline in follicles, especially by the time they are fully grown antral follicles, neither betaine nor choline appears to be significantly transferred to the enclosed growing oocyte. The elevated concentrations of betaine and choline may therefore be used for other functions within the follicle.

Betaine was conserved from the two-cell embryo to the morula, and then decreased in the blastocyst stage in both *in vitro* and *in vivo* groups. Moreover, one-cell embryos exhibited swelling-activated betaine efflux in hypotonic culture media, showing that betaine is permeable through the swelling-activated channel at least at that stage. The expression of *Lrrc8* isoforms across oocyte and preimplantation embryo stages suggests that *Lrrc8* family mRNAs are maternal, and that transcript numbers decrease as the maternal mRNA degrades. This resulting decrease in expression in later preimplantation embryo stages suggests that VSOAC is inactive, allowing betaine levels to be retained. Whether a swelling-induced increase in betaine permeability occurs in late preimplantation embryo stages should be investigated. Overall, these results suggest that the retention of betaine levels prior to the blastocyst stage may be due to the downregulation of LRRC8 proteins. However, it is possible that VSOAC can be activated at any stage of preimplantation embryo growth and mediate the swelling-induced loss of betaine.

Finally, contrary to our hypothesis, endogenous betaine levels still decreased in blastocysts collected from *Bhmt*$^{-/-}$ mice. This suggests that there is an alternate mechanism driving the decrease in endogenous betaine at the blastocyst stage, such as VSOAC that potentially upregulates at that time, and mediates the efflux of organic osmolytes like betaine and glycine. However, further research on the mechanisms of betaine regulation during the blastocyst stage is needed.

## 8. Significance

My research has provided knowledge for the field of cell volume regulation in oocytes and preimplantation embryos and oocyte and embryo physiology in general. The results presented here show that endogenous betaine is present in the oocyte during oogenesis and in preimplantation embryos to the blastocyst stage and is regulated via a variety of mechanisms at various stages of development. Certain specifics of betaine regulation remain to be elucidated, such as how exactly betaine enters growing oocytes, the molecular profile of VSOAC in preimplantation embryos, and what causes the decrease of endogenous betaine in the blastocyst.

In addition to increasing the information concerning the mechanisms of intracellular betaine regulation, my findings align with the suggestion that adding betaine to culture media for IVM in ART would be beneficial. Betaine may be influential in oocyte, embryo, and even offspring health and has several functions aside from cell volume regulation and supplying the methyl pool such as ICM development (Lee *et al*., 2012; Zhang *et al*., 2015). These functions are critical for fertility and embryo development, and oocytes and preimplantation embryos have therefore evolved analogous pathways to ensure these requirements are met. Importing the amino acid derivative betaine is just one of the crucial mechanisms involved in reproductive physiology, and adding betaine to culture media may therefore be a considerable improvement to embryo health.

## 9. Literature Cited


Ackert, C.L., Gittens, J.E., O'Brien, M.J., Eppig, J.J., & Kidder, G. M. (2001). Intercellular communication via connexin34 gap junctions is required for ovarian folliculogenesis in the mouse. *Dev Biol*. 15(2), 258-270.

Adams, C.E. (1956). Egg transfer and fertility in the rabbit. Third Int. Congr. Anim. Repro'd., Cambridge, Section 3, pp. 5-8.

Adhikari, D., Zheng, W., Shen, Y., Gorre, N., Ning, Y., Halet, G., Kaldis, P., & Liu, K. (2012). Cdk1, but not Cdk2, is the sole Cdk that is essential and sufficient to drive resumption of meiosis in mouse oocytes. *Hum Mol Genet*. 21(11), 2476-2484.

Argyropoulos, C., Rondon-Berrios, H., Raj, D.S., Malhotra, D., Agaba, E.I., Rohrscheib, M., Khitan, Z., Murata, G.H., Shapiro, J.I., & Tzamaloukas, A. H. (2016). Hypertonicity: Pathophysiologic Concept and Experimental Studies. *Cureus*. 8(5), e596. DOI 10.7759/cureus.596.

Alexandre, H. (2001). A history of mammalian embryological research. *Int. J. Dev. Bio*. 45, 457-467.

Alirezaei, M., Niknam, P., & Jelodar, G. (2012). Betaine Elevates Ovarian Antioxidant Enzyme Activities and Demonstrates Methyl Donor Effect in Non-Pregnant Rats. *Int. J. Pept. Res. Ther.* 18, 281-290.

Anas, M.K.I., Hammer, M.A., Lever, M., Stanton, J.A., & Baltz, J.M. (2007). The organic osmolytes betaine and proline are transported by a shared system in early preimplantation mouse embryos. *J. Cell. Physiol*. 210, 266-277.

Anas, M.K.I., Lee, M.B., Zhou, C., Hammer, M.A., Slow, S., Karmouch, J., Liu, X.J., Broer, S., Lever, M., & Baltz, J.M. (2008). SIT1 is a betaine/proline transporter that is activated in mouse eggs after fertilization and functions until the 2-cell stage. Development. 135, 4123-4130.

Anbari, K., & Schultz, R.M. (1993). Effect of sodium and betaine in culture media on development and relative rates of protein synthesis in preimplantation mouse embryos in vitro. *Mol. Reprod. Dev.* 35, 24-28.

Baltz, J.M., Biggers, J.D., & Lechene, C. (1991). Two-cell Stage Mouse Embryos Appear to Lack Mechanisms for Alleviating Intracellular Acid Loads. *J. Bio. Chem.* 266(10), 17212-17217.

Baltz, J.M. (2001). Osmoregulation and cell volume regulation in the preimplantation embryo. *Curr. Top. Dev. Bio.* 52, 55-106.

Baltz, J.M., & Tartia, A.P. (2010). Cell volume regulation in oocytes and early embryos: connecting physiology to successful culture media. *Hum. Rep. Update*. 16(2), 166-176.

Baltz, J.M. (2013). Connections between preimplantation embryo physiology and culture. *J Assist. Reprod. Genet.* 30(8), 1001-1007.

Bell, C.E., Lariviere, N.M., Watson, P.H., & Watson, A.J. (2009). Mitogen-activated protein kinase (MAPK) pathways mediate embryonic responses to culture medium osmolarity by regulating Aquaporin 3 and 9 expression and localization, as well as embryonic apoptosis. *Hum. Reprod.* 24, 1373-1386.

Benkhalifa, M., Monjean, D., Cohen-Bacrie, P., & Menezo, Y. (2010). Imprinting: RNA expression for homocysteine recycling in the human oocyte. *Fertil. Steril*. 93, 1585-1590.

Biggers, J.D., Whittingham, D.G., & Donahue, R.P. (1967). The pattern of energy metabolism in the mouse oocyte and zygote. *Proceedings of the National Academy of Sciences of the United States of America*, 58(2), 560-567.

Biggers, J.D., Lawitts, J.A., & Lechene, C.P. (1993). The protective action of betaine on the deleterious effects of NaCl on preimplantation mouse embryos in vitro. *Mol. Reprod. Dev*. 34, 380-390.

Biggers, J.D. (1998). Reflections on the culture of the preimplantation embryo. *Int. J. Dev. Biol.* 42,879-884.

Blanco, M.R., Demyda, S., Moreno Millan, M., & Genero, E. (2011). Developmental compeence of in vivo and in vitro oocytes: a review. *Biotech. Mol. Biol. Rev.* 6(7), 155-165.

Brachet, A. (1912). Development in vitro de blastodermes et de jeunes embryons de mammiferes. *CR Acad. Sci Paris*. 155, 1191-1193.

Brännström M, Zackrisson U, Hagström H, Josefsson B, Hellberg P, Granberg S, Collins D, Bourne T. (1998). Preovulatory changes of blood flow in different regions of the human follicle. *Fertil. Steril.* 69:435–442.

Brinster, R.L. (1963). A method for in vitro cultivation of mouse ova from two-cell to blastocyst. *Exp. Cell Res..,* 32 (1), 205-208.

Bruzzone, R., White, T. W., & Paul, D. L. (1996). Connections with Connexins: The Molecular Basis of Direct Intercellular Signaling. *Eur. J. Biochem.* 238(1), 1–27.

Chang, H-M., Wu, H-C., Sun, Z-G., Lian, F., & Leung, P.C.K. (2019). Neurotrophins and glial cell line-derived neurotrophic factor in the ovary: physiological and pathophysiological implications. *Hum. Reprod. Update.* 25(2), 224-242.

Chatot, C.L., Ziomek, C.A., Bavister, B.D., Lewis, J.L. and Torres, I. (1989). An improved culture medium supports development of random-bred 1-cell mouse embryos in vitro. *J Reprod Fertil*. 86(2), 679-688.

Chen N.H. et al. (2004). Synaptic uptake and beyond: the sodium- and chloride-dependent neurotransmitter transporter family SLC6. *Pflugers Arch*. 447(5):519-31.

Collins, J.L., & Baltz, J.M. (1999). Estimates of mouse oviductal fluid tonicity based on osmotic responses of embryos. *Biol. Reprod*. 60, 1188-1193.

Collinsova, M., Strakova, J., Jiracek, J., & Garrow, T.A. (2006). Inhibition of Betaine-Homocysteine S-Methyltransferase Causes Hyperhomocysteinemia in Mice. *J. Nutr*. 136(6), 1493-1498.

Corbett, H.E., Dubé, C.D., Slow, S., Lever, M., Trasler, J.M., & Baltz, J.M. (2014). Uptake of Betaine into Mouse Cumulus-Oocyte Complexes via the SLC7A6 Isoform of y+L Transporter. *Biol. Reprod*. 90, 1-9.

Coticchio, G., Dal Canto, M., Renzini, M.M., Guglielmo, M.C., Brambbillasca, F., Turchi, D., Novara, P.V., & Fadini, R. (2015). Oocyte maturation: gamete-somatic cells interactions, meiotic resumption, cytoskeletal dynamics and cytoplasmic reorganization. *Hum. Rep. Update.* 21, 427-454.

Craig, S.A. (2004). Betaine in human nutrition. *Am. J. Clin. Nutr.* 80(3), 539. doi:10.1093/ajcn/80.3.539.

Dawson, K.M., & Baltz., J.M. (1997). Organic osmolytes and embryos: substrates of the Gly and β transport systems protect mouse zygotes against the effects of raised osmolarity. *Biol. Reprod*. 56, 1550-1558.

Dawson, K.M., Collins, J.L., & Baltz, J.M. (1998). Osmolarity-dependent glycine accumulation indicates a role for glycine as an organic osmolyte in early preimplantation mouse embryos. *Biol. Reprod.* 59, 225-232.

Day, C.R., & Kempson, S.A. (2016). Betaine chemistry, roles, and potential use in liver disease. *Biochim. Biophys. Acta.* 1860(6):1098-1106.

Decher, N., Lang, H.J., Nilius, B., Bruggemann, A., Busch, A.E., & Steinmeyer, K. Br. J. (2001). *Br. J. Pharmacol*. 134, 1467-1479.

Dekel, N. (2005). Cellular, biochemical and molecular mechanisms regulating oocyte maturation. *Mol Cell Endorinol*. 234(1-2):19-25

De La Fuente, R., & Eppig, J. (2001). Transcriptional Activity of the Mouse Oocyte Genome: Companion Granulosa Cells Modulate Transcription and Chromatin Remodeling. *Dev. Bio*. 229, 224-236.

Demeestere, I., Steiff, A.K., Suzuki, J., Al-Khabouri, S., Mahrous, E., Tan, S.L. and Clarke, H.J. (2012). Follicle-stimulating hormone accelerates mouse oocyte development in vivo. *Biol Reprod*. 87(1):1-11.

Duckworth, B.C, Weaver, J.S., & Ruderman, J.V. (2002). G2 arrest in Xenopus oocytes depends on phosphorylation of cdc25 by protein kinase A. *PNAS*. 99, 16794-16799.

Ebisch, I.M.W., Thomas, C.M.G., Peters, W.H.M., Braat, D.D.M., Steegers-Theunissen, R.P.M. (2007). The importance of folate, zinc and antioxidants in the pathogenesis and prevention of subfertility. *Hum. Reprod. Update.* 13, 163-174.

Egbert, J.R., Yee, S-P., & Jaffe, L.A. (2018). Luteinizing hormone signaling phosphorylates and activates the cyclic GMP phosphodiesterase PDE5 in mouse ovarian follicles, contributing an additional component to the hormonally induced decrease in cyclic GMP that reinitiates meiosis. *Dev Bio*. 435(1), 6-14.

Ellenbogan, A., Shavit, T., & Shalom-Paz, E. (2014). IVM results are comparable and may have advantages over standard IVF. *Facts Views Vis Obgyn.* 6(2), 77-80.

Elvin, J.A., Clark, A.T., Wang, P., Wolfman, N.M., & Matzuk, M.M. (1999). Paracrine actions of growth differentiation factor-9 in the mammalian ovary. *Mol Endocrinol.* 13(6), 1035-1048.

Eppig, J.J. (2001). Oocyte control of ovarian follicular development and function in mammals. *Reprod*. 122, 829-838.

Eppig, J.J., Viveiros, M.M., Marin Bivens, C., De La Fuente, R. (2004). Regulation of Mammalian Oocyte Maturation. In The Ovary (Eds. Leung, P.C.K. and Adashi, E.Y.), Ch 17, pp. 113-129.

Eppig, J.J. (1982). The relationship between cumulus cell-oocyte coupling, oocyte meiotic maturation, and cumulus expansion. *Dev Biol*. 89:268–272.

Erdogan, S., FitzHarris, G., Tartia, A. P., & Baltz, J.M. (2005). Mechanisms regulating intracellular pH are activated during growth of the mouse oocyte coincident with acquisition of meiotic competence. *Dev. Bio.* 286(1), 352-360.

Fagone, P., & Jackowski, S. (2013). Phosphatidylcholine and the CDP-Choline Cycle. *Biochim Biophys Acta*. 1831(3), 523-532

Fauser, B.C.J.M., and Van Heusden, A.M (1997). Manipulation of Human Ovarian Function: Physiological Concepts and Clinical Consequences. *Endocrine Reviews.*18, 71-106.

Freitas de Medeiros, S., Barbosa, B.B., Souto de Medeiros, M.A., & Winck Yamamoto, M.M. (2021). Morphology and Biochemistry of Ovulation. *Rev Bras Ginecol Obstet*. 43(6), 480-486.

Garcia-Perez, A., & Burg, M.B. (1991). Role of organic osmolytes in adaptation of renal cells to high osmolality. *J. Membr. Biol*. 119, 1-13.

Garnovskaya, M.N, Mukhin, Y.V., Vlasova, T.M., & Raymond, J.R. (2003). Hypertonicity activates Na+/H+ exchange through Janus Kinase 2 Activation by Angiotensin II: Involvement of PYK2. *Mol. Endocrinol.* 16, 367-377.

Garrow, T.A. (1996). Purification, Kinetic Properties, and cDNA Cloning of Betaine-Homocysteine Methyltransferase. *J. Biol. Chem.* 271, 22831-22838.

Gasperowicz, M., & Natale, D.R.C. (2011). Establishing Three Blastocyst Lineages-Then What? *Biol. Reprod*. 84, 621-630.

Gershon E., Plaks V., & Dekel, N. (2008). Gap junctions in the ovary: expression, localization and function. *Mol Cell Endocrinol.* 282:18–25

Gershon, E., & Dekel, N. (2020). Newly Identified Regulators of Ovarian Folliculogenesis and Ovulation. *Int. J. Mol. Sci.* 21(12), 4565. doi:10.3390/ijms21124565

Gilbert SF. Developmental Biology. 6th edition. Sunderland (MA): Sinauer Associates; 2000. An Introduction to Early Developmental Processes. Available from: https://www.ncbi.nlm.nih.gov/books/NBK9992/

Gilchrist, R.B, Lane, M., & Thompson, J.G. (2008). Oocyte-secreted factors: regulators of cumulus cell function and oocyte quality. *Hum Reprod Update.* 14, 159–77.

Ginsburg, M., Snow, M.H., & McLaren, A. (1990). Primordial germ cells in the mouse embryo during gastrulation. *Dev.* 110(2), 521-528.

Goddard, M.J., & Pratt, H.P.M. (1983). Control of events during early cleavage of the mouse embryo: an analysis of the '2-cell block'. *Development*. 73, 111-133.

Grossman, E.B. and Hebert, S.C. (1989). Renal inner medullary choline dehydrogenase activity: characterization and modulation. *Am J Physiol*. 256:F107–F112.

Guerin, P., El Mouatassim, S., & Menezo, Y. (2001). Oxidative stress and protection against reactive oxygen species in the pre-implantation embryo and its surroundings. *Hum. Reprod. Update.* 7(2), 175-189.

Hadi, T., Hammer, M.A., Algire, C., Richards, T. and Baltz, J.M. (2005). Similar effects of osmolarity, glucose, and phosphate on cleavage past the 2-cell stage in mouse embryos from outbred and F1 hybrid females. *Biol Reprod*. 72(1):179-87.

Hammer, M.A., & Baltz, J.M. (2002). Betaine is a highly effective organic osmolyte but does not appear to be transported by established organic osmolyte transporters in mouse embryos. *Mol. Reprod. Dev*. 62, 195-202.

Hammer, M.A., & Baltz, J.M. (2003). Beta-alanine but not taurine can function as an organic osmolyte in preimplantation mouse embryos cultured from fertilized eggs. *Mol. Reprod. Dev.* 66, 153-161.

He, M., Zhang, T., Yang, Y., and Wang, C. (2021). Mechanisms of Oocyte Maturation and Related Epigenetic Regulation. *Front. Cell. Dev. Biol*. 9, doi.org/10.3389/fcell.2021.654028.

Heape, W. (1891). Preliminary Note on the Transplantation and Growth of Mammalian Ova within A Uterine Foster Mother. Proc. Royal Soc. 48, 457-459.

Hizaki, H., Segi, E., Sugimoto, Y., Hirose, M., Saji, T., Ushikubi, F., Matsuoka, T., Noda, Y., Tanaka, T., Yoshida, N., Narumiya, S., & Ichikawa, A. (1999). Abortive expansion of the

cumulus and impaired fertility in mice lacking the prostaglandin E receptor subtype EP (2). *Proc. Natl. Acad. Sci. USA*., 96(18):10501–10506.

Hoffman, E.K., & Dunham, P.B. (1995). Membrane Mechanisms and Intracellular Signalling in Cell Volume Regulation. *Int. Rev. Cytol*. 161, 173-262.

Hoffman, E.K., Lambert, I.H., & Pedersen, S.F. (2009). Physiology of cell volume regulation in vertebrates. *Physiol. Rev.* 89, 193-277.

Hogan, B., Beddington, R., Constantini, F., & Lacy, E. (1994). Manipulating the mouse embryo, a laboratory manual. *Plainview: Cold Spring Harbor Press.*

Horio, M., Ito, A., Matsuoka, Y., Moriyama, T., Orita, Y., Takenaka, M., & Imai, E. (2001). Apoptosis induced by hypertonicity in Madin Darley canine kidney cells: protective effect of betaine. *Nephrol. Dial. Transplant.* 16, 483-490.

Humphreys, B.D., Jiang, L., Chernova, M.N., & Alper, S.L. (1995). Hypertonic activation of AE2 anion exchanger in Xenopus oocytes via NHE-mediated intracellular alkalinization. *Am. J. Physiol.* 268, C201-C209.

Hutt, K.J., & Albertini, D.F. (2007). An oocentric view of folliculogenesis and embryogenesis. *Reprod. Biomed. Online.* 14(6), 758-764.

Ikeda, S., Namekawa, T., Sugimoto, M., & Kume, S. (2010). Expression of methylation pathway enzymes in bovine oocytes and preimplantation embryos. *J. Exp. Zool. A. Ecol. Genet. Physiol.* 313(3), 129-136.

a) Ikeda, S., Koyama, H., Sugimoto, M., & Kume, S. (2012). Roles of One-carbon Metabolism in Preimplantation Period-Effects on Short-term Development and Long-term Programming. *J. Reprod. Dev*. 58, 38-43.

b) Ikeda, S., Sugimoto, M., & Kume, S. (2012). Importance of methionine metabolism in morula-to blastocyst transition in bovine preimplantation embryos. *J. Reprod. Dev.* 58, 91-96.

Innocenti, F., Fiorentino, G., Cimadomo, D., Soscia, D., Garagna, S., Rienzi, L., Ubaldi, F.M., & Zuccotti, M. (2022). Maternal effect factors that contribute to oocytes developmental competence: an update. *J Assist. Reprod. Genet.* 39(4), 861-871.

Jaffe, L.A., & Egbert, J.R. (2017). Regulation of Mammalian Oocyte Meiosis by Intercellular Communication Within the Ovarian Follicle. *Annu Rev Physiol.* 79, 237-260.

Jamshidi, M.B., & Kaye, P.L. (1995). Glutamine transport by mouse inner cell masses. *J. Reprod. Fertil*. 104, 91-97.

Jiang, L., Chernova, M.N., & Alper, S.L. (1997). Secondary regulatory volume increase conferred on Xenopus oocytes by expression of AE2 anion exchanger. *Am. J. Physiol*. 272, C191-C202.

Johnson, A.R., Craciunescu, C.N., Guo, Z., Teng, Y-W., Thresher, R.J., Blusztajn, & Zeisel, S.H. (2010). Deletion of murine choline dehydrogenase results in diminished sperm motility. *FASEB. J.* 24, 2752-2761.

Jones, K.T. (2005). Mammalian egg activation: from Ca2+ spiking to cell cycle progress. *Reproduction*. 130(6), 813-823.

Kanatsu-Shinohara, M., Schultz, R.M., & Kopf, G.S. (2000). Acquisition of Meiotic Competence in Mouse Oocytes: Absolute Amounts of $p34^{cdc2}$, Cyclin B1, cdc25C, and wee1 in Meiotically Incompetent and Competent Oocytes. *Bio. Reprod.* 63(6), 1610-1616.

Kawamura K, Cheng Y, Kawamura N, Takae S, Okada A, Kawagoe Y, Mulders S, Terada Y, & Hsueh AJW. (2011). Pre-ovulatory LH/hCG surge decreases C-type natriuretic peptide secretion by ovarian granulosa cells to promote meiotic resumption of pre-ovulatory oocytes. *Hum. Reprod.* 26, 3094–3101.

Kempson, S.A., Zhou, Y., & Danbolt, N.C. (2014). The betaine/GABA transporter and betaine: roles in brain, kidney, and liver. *Front Physiol.* 24(5), 159. doi: 10.3389/fphys.2014.00159

Kern, D.M., Oh, S., Hite, R.K., & Brohawn, S.G. (2019). Cryo-EM structures of the DCPIB-inhibited volume regulated anion channel LRRC8A in lipid nanodiscs. eLife. 8, e42636.

Kiyokawa, H., & Ray, D. (2008). In vivo roles of CDC25 phosphatases: Biological insight into the anti-cancer therapeutic targets. *Anticancer Agents Med Chem.* 8(8), 832-836.

Kolajova, M., & Baltz., J.M. (1999). Volume-regulated anion and organic osmolyte channels in mouse zygotes. *Biol. Reprod.* 60, 964-972.

Kolajova, M., & Baltz., J.M. (2001). Developmentally regulated cell cycle dependence of swelling-activated anion channel activity in the mouse embryo. *Development*. 128, 3427-3434.

Krokowski, D., guan, B-J., Wu, J., Zheng, Y., Pattabiraman, P.P., Jobava, R., gao, x-H., Di, X-J., Snider, M.D., Mu, T-W., Liu, S., Storrie, B., Pearlman, E., Blumental-Perry, A., & Hatzoglou, M. (2017). GADD34 function in protein trafficking promotes adaptation to hyperosmotic stress in human corneal cells. *Cell Rep.* 21(10), 2895-2910.

Kwon, H.M., & Handler, J.S. (1995). Cell volume regulated transporters of compatible osmolytes. *Curr. Opin. Cell. Biol.* 7, 465-471.

Lai, F-N., Liu, X-L., Li, N., Zhang, R-Q., Zhao, Y., Feng, Y-Z., Nyachoti, C.M., Shen, W., & Li., L. (2018). Phosphatidylcholine could protect the defect of zearalenone exposure on follicular development and oocyte maturation. Aging (Albany, NY). 10(11), 3486-3506.

Lawitts, J.A., & Biggers, J.D. (1991). Overcoming the 2-cell block by modifying standard components in a mouse embryo culture medium. *Biol Reprod.* 45, 245–251

Lawitts, J.A., & Biggers, J.D. (1992). Joint effects of sodium chloride, glutamine, and glucose in mouse preimplantation embryo culture media. *Mol Reprod Dev.* 31, 189– 194.

Lawitts, J.A., & Biggers., J.D. (1993). Culture of preimplantation embryos. *Methods Enzymol. In* 225, 153-164.

Lee, M. B., Kooistra, M., Zhang, B., Slow, S., Fortier, A.L., Lever, M., Trasler, J.M., & Baltz, J. M. (2012). Betaine Homocysteine Methyltransferase Is Active in the Mouse Blastocyst and Promotes Inner Cell Mass Development. *J. Biol. Chem.* 287(39), 33094-33103.

Liang, C-G., Su, Y-Q., Fan, H-Y., Schatten, H., & Sun, Q-Y. (2007). Mechanisms Regulating Oocyte Meiotic Resumption: Roles of Mitogen-Activated Protein Kinase. *Mol Endocrinol*. 21(9), 2037-2055.

Liu, L., Kong, N., Xia, G., & Zhang, M. (2013). Molecular control of oocyte meiotic arrest and resumption. *Reprod. Fertil. Dev.* 25(3), 463–471.

Liu, K., & Adhikari, D. (2014). The regulation of maturation promoting factor during prophase I arrest and meiotic entry in mammalian oocytes. *Mol. Cell Endo.* 382(1), 480-487.

Liu, J., & Maller, J.L. (2005). Calcium Elevation at Fertilization Coordinates Phopshorylation of XErp1/Emi2 by Plx1 and CaMK II to Release Metaphase Arrest by Cytostatic Factor. *Curr. Biol.*15(16), 1458-1468.

Lutter, D., Ullrich, F., Lueck, J.C., Kempa, S., & Jentsch, T.J. (2017). Selective transport of neurotransmitters and modulators by distinct volume-regulated LRRC8 anion channels. *J. Cell Sci*. 130(6), 1122-1133.

Macaulay, A.D., Gilbert, I., Caballero, J., Barreto, R., Fourner, E., Tossou, P., Sirard, M-A., Clarke, H.J., Khandjian, E.W., Richard, F.J., Hyttel, P., & Robert, C. (2014). The Gametic Synapase: RNA Transfer to the Bovine Oocyte. *Bio. Reprod.* 91(4), 1-12.

Madgwick, S., & Jones, K.T. (2007). How eggs arrest at metaphase II: MPF stabilization plus APC/C inhibition equals Cytostatic Factor. *Cell Dev*. 2, (4), doi: 10.1186/1747-1028-2-4

Maemura, M., Taketsuru, H., Nakajima, Y., Shao, R., Kakihara, A., Nogami, J., Ohkawa, Y., & Tsukada, Y-I. (2021). Totipotency of mouse zygotes extends to single blastomeres of embryos at the four-cell stage. *Sci Reports.* 11, doi.org/10.1038/s41598-021-90653-1

Marchais, M., Gilbert, I., Bastien, A., Macaulay, A., & Robert, C. (2022). Mammalian cumulus-oocyte complex communication: a dialog through long and short distance messaging. *J. Assist. Reprod.* 39, 1011-1025.

Martin-Coello, J., Gonzales, R., Crespo, C., & Gomendio, M. (2008). Superovulation and in vitro oocyte maturation in three species of mice (Mus musculus, Mus spretus and Mus spicilegus). *Theriogenology.* 70(6), 1004-1013.

Masciarelli, S., Horner, k., Liu, C., Park, S.H., Hinckley, M., Hockman, S., Nedachi, T., Jin, C., Conti, M., & Manganiello, V. (2004). Cyclic nucleotide phosphodiesterase 3A-deficient mice as a model of female infertility. *J Clin Invest*. 114, 196-205.

McClatchie, T., Meredith, M., Ouédraogo, M.O., Slow, S., Lever, M., Mann, M.R.W., & Baltz, J.M. (2017). Betaine is accumulated via transient choline dehydrogenase activation during mouse oocyte meiotic maturation. *J. Biol.Chem.* 292, 13784-13794.

McGee, E. A., Hsueh, A.J.W. (2000). Initial and Cyclic Recruitment of Ovarian Follicles. *Endocrine Reviews.* 21, 200-214.

Mehlmann, L.M. (2005). Stops and starts in mammalian oocytes: recent advances in understanding the regulation of meiotic arrest and oocyte maturation. *Reproduction.* 130(6), 791-799.

Menezo, Y., Khatchadourian, C.H., Gharib, A., Hamidi, J., Greenland, T., & Sarda, N. (1989). Regulation of S-adenosyl methionine synthesis in the mouse embryo. Life Sci. 44(21), 1601-1609.

Miao, Y-L., & Williams, C.J. (2012). Calcium signaling in mammalian egg activation and embryo development: Influence of subcellular localization. *Mol Reprod Dev.* 79(11), 742-756.

Mihalas, B.P., Redgrove, K.A., McLaughlin, E.A., & Nixon, B. (2017). Molecular Mechanisms Responsible for Increased Vulnerability of the Ageing Oocyte to Oxidative Damage. *Oxid Med Cell Longev.* doi: 10.1155/2017/4015874.

Mihaljlovic, A.I., & Bruce, A.W. (2017). The first cell-fate decision of mouse preimplantation embryo development: integrating cell position and polarity. *Open Biol.* 7(11), 170210.

Mitra, J., & Schultz, R.M. (1996). Regulation of the acquisition of meiotic competence in the mouse: changes in the subcellular localization of cdc25, cyclin B1, cdc25C and wee1, and in the concentration of these proteins and their transcripts. *J. Cell Sci.* 109(9), 2407-2415.

Miyakawa, H., Rim, J.S., Handler, J.S. & Kwon, H.M. (1999). Identification of the second tonicity-responsive enhancer for the betaine transporter (BGT1) gene. *Biochim Biophys Acta*. 1446(3):359-64.

Monk, M., Boubelik, M., & Lehnert, S. (1987). Temporal and regional changes in DNA methylation in he embryonic, extraembryonic and germ cell lineages during mouse embryo development. *Dev*. 99(3), 371-382.

Natale, D.R., Paliga, A.J., Beier, F., D'Souza, S.J., & Watson, A.J. (2004). p38 MAPK signaling during murine preimplantation development. *Dev Biol.* 268, 76 – 88

Nelson, N. (1998). The Family of Na+/Cl- Neurotransmitter Transporters. *J. Neurochem*. 71(5), 1785-1803.

Nishimura, T., Sai, Y., Fujii, J., Muta, M., Iizasa, H., Tomi, M., Deureh, M., Kose, N., & Nakashima, E. (2010). Roles of TauT and system A in cytoprotection of rat syncytiotrophoblast cell line exposed to hypertonic stress. *Placenta.* 31(11), 1003-1009.

Nishimura, T., Yagi, R., Usuda, M., Oda, K., Yamazaki, M., Suda, S., Takahashi, Y., Okazaki, F., Sai, Y., Higuchi, K., Maruyama, T., Tomi, M., & Nakashima, E. (2014). System A amino acid transporter SNAT2 shows subtype-specific affinity for betaine and hyperosmotic inducibility in placental trophoblasts. *Biochim. Biophys. Acta. Biomembr.* 1838(5), 1306-1312.

Nixon, V.L., Levasseur, M., McDougall, A., & Jones, K.T. (2002). Ca2+ Oscillations Promote APC/C-Dependent Cyclin B1 Degradation during Metaphase Arrest and Completion of Meiosis in Fertilizing Mouse Eggs. *Curr. Bio.* 12(9), 746-750.

Norris, R.P., Freudzon, M., Mehlmann, L.M., Cowan, A.E., Simon, A.M., Paul, D.L., Lampe, P.D., & Jaffe, L.A. (2008). Luteinizing hormone causes MAP kinase-dependent phosphorylation and closure of connexin 43 gap junctions in mouse ovarian follicles: one of two paths to meiotic resumption. *Development*. 135, 3229-3238.

Norris, R.P, Ratzan, W.J., Freudzon, M., Mehlmann, L.M., Krall, J., Movsesian, M.A., Wang, H., Ke, H., Nikolaev, V.O., & Jaffe, L.A. (2009). Cyclic GMP from the surrounding somatic cells regulates cyclic AMP and meiosis in the mouse oocyte. *Dev.* 136, 1869–1878.

Offenberg, H., Barcroft, L.C., Caveney, A., Viuff, D., Thomsen, P.D., & Watson, A. J. (2000). mRNAs encoding Aquaporins 1-9 are present during murine preimplantation development. *Mol. Reprod. Dev.* 57, 1-8.

Okada, Y. (1997). Volume expansion-sensing outward-rectifier Cl-channel: fresh start to the molecular identity and volume sensor. *Am. J. Physiol.* 273, C755-C789.

Okudaira, Y., Wakai, T., & Funahashi, H. (2017). Levels of cyclic-AMP and cyclic-GMP in porcine oocyte-cumulus complexes and cumulus-free oocytes derived from small and middle follicles during the first 24-hour period of *in vitro* maturation. *J. Reprod. Dev.* 63(2), 191-197

O'Neill, C. (1998). Endogenous folic acid is essential for normal development of preimplantation embryos. *Hum. Reprod.* 13, 1312-1316.

Orlowski, & J., Grinstein, S. (2004). Diversity of the mammalian sodium/proton exchanger SLC9 gene family. *Pflugers Arch.* 447, 549-565.

Pan, B., & Li., J. (2019). The art of oocyte meiotic arrest regulation. *Reprod. Biol. Endocrinol.* 17, doi.org/10.1186/s12958-018-0445-8.

Park, J.Y., Su, Y. Q., Ariga, M., Law, E., Jin, S.L. and Conti, M. (2004). EGF-like growth factors as mediators of LH action in the ovulatory follicle. *Science*. 303:682-684.

Park, S., Choi, S. G., Yoo, S.M., Son, J.H., and Jung, Y.K. (2014). Choline dehydrogenase interacts with sqstml/p62 to recruit Ic3 and stimulate mitophagy. *Autophagy.* 10, 1906-1920. doi: 10.4161/auto.32177.

Parrott, J.A., & Skinner, M.K. (1999). Kit-Ligand/Stem Cell Factor Induces Primordial Follicle Development and Initiates Folliculogenesis. *Endocrinology*. 140(9), 4262-4271.

Pastor-Anglada, M., Felipe, A., Casado, F.J., Ferrer-Martinez, A., & Gomez-Angelats, M. (1996). Long-term osmotic regulation of amino acid transport systems in mammalian cells. *Amino Acids.* 11, 135-151.

Peng, X.R., Hsueh, A. J., LaPlot, P. S., Bjersing, L. and Ny, T. (1991) Localization of luteinizing hormone receptor messenger ribonucleic acid expression in ovarian cell types during follicle development and ovulation. *Endocrinology.* 129:3200-3207.

Peters-Regehr, T., Bode, J.G., Kubitz, R., Haussinger, D. (1999). Organic Osmolyte Transport in Quiescent and Activated Rat Hepatic Stellate Cells (Ito Cells). *Hepatology*. 29, 173-180.

Phillips, K.P., Petrunewich, M.A.F., Collins, J.L., Booth, R.A., Liu, X.J., & Baltz, J.M. (2002). Inhibition of MEK or cdc2 Kinase Parthogenetically Activates Mouse Eggs and Yields the Same Phenotypes as *Mos*$^{-/-}$ Parthenogenotes. *Dev. Bio.* 247, 210-223.

Planells-Cases, R., Lutter, D., Guyader, C., Gerhards, N. M., Ullrich, F., Elger, D. A., Kucukosmanoglu, A., Xu, G., Voss, F. K., Reincke, S. M., Stauber, T., Blomen, V.A., Vis, D.J., Wessels, L.F., Brummelkamp, T.R., Borst, P., Rottenberg, S., & Jentsch, T.J. (2015). Subunit composition of VRAC channels determines substrate specificity and cellular resistance to Pt-based anti-cancer drugs. *EMBO J.* 34, 2993-3008.

Pratt, H.P.M., Ziomek, C.A., Reeve, W.J.D., & Johnson, M.H. (1982). Compaction of the mouse embryo: an analysis of its components. *Dev.* 70, 113-132.

Qiu, Z., Dubin, A.E., Mathur, J., Tu, B., Reddy, K., Miraglia, L.J., Reinhardt, J., Orth, A.P., & Patapoutian, A. (2014). SWELL1, a plasma membrane protein, is an essential component of volume-regulated anion channel. *Cell.* 157(2), 447-458.

Ratriyanto, A., Mosenthin, R., Bauer, E., Eklund, M. (2009). Metabolic, Osmoregulatory and Nutritional Functions of Betaine in Monogastric Animals. Asian-Aust. J. Anim. Sci. 22(10):1461-1476.

Richani, D., & Gilchrist, R.B. (2018). The epidermal growth factor network: role in oocyte growth, maturation and developmental competence. *Hum Reprod Update.* 24(1), 1-14.

Richard, S., & Baltz, J.M. (2017). Preovulatory suppression of mouse oocytes cell volume-regulatory mechanisms is via signalling that is distinct from meiotic arrest. *Sci. Rep.* 7, 702. DOI:10.1038/s41598-017-00771-y

Richards, J.S. (2005). Ovulation: New factors that prepare the oocyte for fertilization. *Mol. Cell Endocrinol.* 234 (1-2), 75-79.

Robinson, J. W., Zhang, M., Shuhaibar, L. C., Norris, R. P., Geerts, A., Wunder, F., Eppig, J. J., Potter, L. R., & Jaffe, L. A. (2012). Luteinizing Hormone Reduces the Activity of the NPR2 Guanylyl Cyclase in Mouse Ovarian Follicles, contributing to the Cyclic GMP Decrease that Promotes Resumption of Meiosis in Oocytes. *Dev. Biol*. 366(2), 308–316.

Rose, U.M., Hanssen, R.G.J.M., & Kloosterboer, H.J. (1999). Development and Characterization of an In Vitro Ovulation Model Using Mouse Ovarian Follicles. *Biol. Reprod*. 61(2), 503-511.

Ruiz-Montasell, B., Gomez-Angelats, M., Casado, F.J., & Pasto-Anglada, M. (1994). Evidence for a regulatory protein involved in the increased activity of system A for neutral amino acid transport in osmotically stressed mammalian cells. *PNAS.* 91(20), 9569-9573.

Russell, D.L., Gilchrist, R.B., Brown, H.M., & Thompson, J.G. (2016). Bidirectional communication between cumulus cells and the oocyte: old hands and new players? *Theriogenology.* 86, 62–8.

Salustri, A. and Siracusa, G. (1983). Metabolic coupling, cumulus expansion and meiotic resumption in mouse cumuli oophori cultured in vitro in the presence of FSH or dcAMP,or stimulated in vivo by hCG. *J Reprod Fertil*. 68:33-341.

Salvi, F. and Gadda, G. (2013) Human choline dehydrogenase: medical promises and biochemical challenges. *Arch Biochem Biophys*. 537: 243–252.

Santos, F., Hendrich, B., Reik, W., & Dean., W. (2002). Dynamic Reprogramming of DNA Methylation in the Early Mouse Embryo. *Dev. Bio.* 241(1):172-182.

Saunders, C.M., Larman, M.G., Parrington, J., Cox, L.J., Royse, J., Blayney, L.M., Swann, K., & Lai, F.A. (2002). PLCζ: a sperm-specific trigger of Ca2+ oscillations in eggs and embryo development. *Dev.* 129(15), 3533-3544.

Scheffler, K., Uraji, J., Jentoft, I., Cavazza, T., Mönnich, E., Mogessie, B., & Schuh, M. (2021). Two mechanisms drive pronuclear migration in mouse zygotes. *Nat Commun*. 5;12(1):841. doi: 10.1038/s41467-021-21020-x.

Schultz, G.A., Kaye, P. L., McKay, D.J., & Johnson, M.H. (1981). Endogenous amino acid pool sizes in mouse eggs and preimplantation embryos. *J. Reprod. Fert*. 61, 387-393.

Schultz, R.M. (1993). Regulation of zygotic gene activation in the mouse. *Bioessays.* 15(8), 531-538.

Seguin, D.G., & Baltz, J.M. (1997). Cell volume regulation by the mouse zygote: mechanism of recovery from a volume increase. *Am. J. Physiol.* 272, F1102-F1110.

Sha, Q.Q., Zhu, Y.Z., Li, S., Jiang, Y., Chen, L., Sun, X.H., Shen, L., Ou, X.H., & Fan, H.Y. (2020). Characterization of zygotic genome activation-dependent maternal mRNA clearance in mouse. *Nucleic Acids Res.* 48, 879–894.

Sheikh-Hamad, D. and Gustin, M.C. (2004). MAP kinases and the adaptive response to hypertonicity: functional preservation from yeast to mammals. Am J Physiol Renal Physiol. 287(6): F1102-10.

Shiels, A., & Griffin, C.S. (1993). Aberrant expression of the gene for lens major intrinsic protein in the CAT mouse. *Curr. Eye. Res.* 12, 913-921.

Shuhaibar, L.C., Egbert, J.R., Norris, R.P., Lampe, P.D., Nikolaev, V.O., Thunemann, M., Wen, L., Feil, R., & Jaffe, L.A. (2015). Intercellular signaling via cyclic GMP diffusion through gap junctions restarts meiosis in mouse ovarian follicles. *Proceedings of the National Academy of Sciences of the United States of America,* 112(17), 5527-5532.

Simon, A.M., Goodenough, D.A., Li E. and Paul, DL. (1997). Female infertility in mice lacking connexin37. *Nature*. 385:525-529.

Siyanov, V., & Baltz, J.M. (2013). NHE1 is the Sodium-Hydrogen Exchanger Active in Acute Intracellular pH Regulation in Preimplantation Mouse Embryos. *Bio. Reprod.* 88(6), 157, 1-11.

Slow, S., Lever, M., Chambers, S. T., and George, P. M. (2009) Plasma dependent and independent accumulation of betaine in male and female rat tissues. *Physiol. Res.* 58, 403–410

Solc, P., Schultz, R.M., & Motlik, J. (2010). Prophase I arrest and progression to metaphase I in mouse oocytes: comparison of resumption of meiosis and recovery from G2-arrest in somatic cells. *Mol. Hum. Reprod.*16(9), 654-664.

Sonoda, M., Okamoto, F., Kajiya, H., Inoue, Y., Honjo, K., Sumii, Y., Kawarabayashi, T., & Okabe, K. (2003). Amino acid-permeable anion channels in early mouse embryos and their possible effects on cleavage. *Biol. Reprod.* 68, 947-953.

Sorensen, R.A., & Wasarman, P.M. (1976). Relationship between Growth and Meiotic Maturation of the Mouse Oocyte. *Dev. Bio.* 50, 531-536.

Steptoe, P.C., & Edwards, R. G. (1978). Birth after the reimplantation of a human embryo. *Lancet (London, England),* 2(8085), 366.

Strange, K., Emma, F., & Jacksson, P.S. (1996). Cellular and molecular physiology of volume-sensitive anion channels. *Am. J. Physiol.* 270, C711-C730.

Strange, K. (2004). Cellular volume homeostasis. *Adv. Physiol. Educ.* 28(4), 155-159.

Steeves, C.L., Hammer, M-A., Walker, G.B., Rae, D., Stewart, N.A., & Baltz, J.M. (2003). The glycine neurotransmitter transporter GLYT1 is an organic osmolyte transporter regulating cell volume in cleavage-stage embryos. *PNAS.* 100(24), 13982-13987

Streiter, S., Fisch, B., Sabbah, B., Ao, A., & Abir, R. (2016). The importance of neuronal growth factors in the ovary. *Mol Hum Rep*. 22(1), 3-17.

Syeda, R., Qiu, Z., Dubin, A.E., Murthy, S.E., Florendo, M.N., Mason, D.E., Mathur, J., Cahalan, S.M., Peters, E.C., Montal, M., Patapoutian, A. (2016). LRRC8 Proteins Form Volume-Regulated Anion Channels that Sense Ionic Strength. *Cell*. 164(3), 499-511.

Takahashi, T., & Ohnishi, J. (1995). Molecular mechanisms of follicle rupture during ovulation. *Zool. Sci.* 12:359–365.

Tartia, A.P., Rudraraju, N., Richards, T., Hammer, M.A., Talbot, P., & Baltz, J.M. (2009). Cell volume regulation is initiated in mouse oocytes after ovulation. *Dev.* 136, 2247-2254.

Teng, Y.W. et al. (2011) Deletion of BHMT in mice perturbs choline and 1-carbon metabolism *J. Biol. Chem.* 286: 36258-67.

Thomas, F.H., & Vanderhyden, B.C. (2006). Oocyte-granulosa cell interactions during mouse follicular development: regulation of kit ligand expression and its role in oocyte growth. *Reprod Biol Endocrinol* 4, 19. https://doi.org/10.1186/1477-7827-4-19

Tora, L., & Vincent, S.D. (2021). What defines the maternal transcriptome? *Biochem. Soc. Trans.* 49(5), 2051-2062.

Trama, J., Go, W.Y., & Ho, S.N. (2002). The Osmoprotective Function of the NFAT5 Transcription factor in T Cell Development and Activation. *Immunol.* 169(10), 5477-5488.

Tsai-Turton, M., & Luderer, U. (2006). Opposing effects of glutathione depletion and follicle-stimulating hormone on reactive oxygen species and apoptosis in cultured preovulatory rat follicles. *Endocrinology.* 147(3), 1224-1236.

Tscherner, A. K., Macaulay, A.D., Ortman, C.S., & Baltz, J.M. (2021). Initiation of cell volume regulation and unique cell volume regulatory mechanisms in mammalian oocytes and embryos. *J. Cell. Physiol.* DOI:10.1002/jcp.30352.

Tscherner, A.K., McClatchie, T., Macaulay, A.D., & Baltz, J.M. (2023). Relationship of quantitative RT-PCR to RNAseq transcriptome identifies mouse preimplantation embryo reference genes. Biol. Reprod. ioad107, https://doi.org/10.1093/biolre/ioad107

Turathum, B., Gao, E-M., & Chian, R-C. (2021). The function of cumulus cells in oocyte growth and maturation and in subsequent ovulation and fertilization. *Cells.*10:2292. doi: 10.3390/cells10092292.

Vanderhyden, B.C., Caron, P.J., Buccione, R., & Eppig, J.J. (1990). Developmental pattern of the secretion of cumulus expansion-enabling factor by mouse oocytes and the role of oocytes in promoting granulosa cell differentiation. *Dev. Bio*. 140(2), 307-317.

Van Winkle, L.J., Haghighat, N., & Campione, A.L. (1990). Glycine protects preimplantation mouse conceptuses from a detrimental effect on development of the inorganic ions in oviductal fluid. *J. Exp. Zool.* 253, 215-219.

Van Winkle, L.J., Patel, M., Wasserlauf, H.G., Dickinson, H.R., & Campione, A.L. (1994). Osmotic regulation of taurine transport via system beta and novel processes in mouse preimplantation conceptuses. *Biochim. Biophys. Acta.* 1191, 244-255.

Van Winkle, L.J., & Dickinson, H.R. (1995). Differences in Amino Acid Content of Preimplantation Mouse Embryos That Develop In Vitro Versus in Vivo: In Vitro Effects of Five Amino Acids That Are Abundant in Oviductal Secretions. *Bio. Reprod.* 52, 96-104.

Van Winkle L.J., Haghighat, N., Campione, A.L. and Gorman, J.M. (1988). Glycine transport in mouse eggs and preimplantation conceptuses. Biochim Biophys Acta. 941(2):241-56.

Voss, F.K., Ullrich, F., Munch, J., Lazarow, K., Lutter, D., Mah, N., Andrade-Navarro, M.A., von Kries, J.P., Stauber, T., & Jentsch, T.J. (2014). Identification of LRRC8 Heteromers as an Essential Component of the Volume-Regulated Anion Channel VRAC. *Science.* 344(6184):634-638.

Vuong, L.N., Ho, V.N.A., Ho, T.M., Dang, V.Q., Phung, T.H., Giang, N.H., Le, A. H., Pham, T.D., Wang, R., Norman, R.J., Smitz, J., Gilchrist, R.B., & Mol, B.W. (2018). Effectiveness and safety of in vitro maturation of oocytes versus in vitro fertilization in women with high antral follicle count: study protocol for a randomized controlled trial. *BMJ Open*. 8(12), e023413. doi: 10.1136/bmjopen-2018-023413

Wigglesworth, K., Lee, K.-B., O'Brien, M. J., Peng, J., Matzuk, M. M., & Eppig, J. J. (2013). Bidirectional communication between oocytes and ovarian follicular somatic cells is required for meiotic arrest of mammalian oocytes. *Proceedings of the National Academy of Sciences of the United States of America*, 110(39), E3723-3729.

Walser, C.B., Lipshitz, H.D. (2011) Transcript clearance during the maternal-to-zygotic transition. Curr. Opin. Genet. Dev. 21, 431–443.

Wang, F., Kooistra, M., Lee, M., Lin, L., & Baltz, J.M. (2011). Mouse Embryos Stressed by Physiological Levels of Osmolarity Become in the Late 2-Cell Stage Before Entry into M Phase. *Biol. Reprod.* 85, 702-713.

Wassarman, P.M., Schultz, R.M., Letourneau, G.E., LaMarca, M.J., Josefowicz, W.J. and Bleil, J.D. (1979). Meiotic maturation of the mouse oocytes in vitro. *Adv. Exp. Med. Biol.* 112:251-268.

Wen, B., Wei, Y-T., & Zhao, K. (2021). The role of high mobility group protein B3 (HMGB3) in tumor proliferation and drug resistance. *Mol. Cell. Biochem.* 4, 1729-1739.

Wulff, H. (2008). New Light on the "Old" Chloride Channel Blocker DIDS. *ACS. Chem. Biol.*3(7), 399-401.

Whitten, W. K. (1956). Culture of Tubal Mouse Ova. *Nature,* 177, article 4498.

Whitten, W. K. (1957). Culture of tubal ova. *Nature*, 179(4569), 1081-1082.

Whittingham, D. G. (1971). Culture of mouse ova. *Journal of Reproduction and Fertility Supplement.* 14, 7-21.

Woo, S.K., Lee, S.D., & Kwon, H.M. (2002). TonEBP transcriptional activator in the cellular response to increased osmolality. *Pflugers Arch*. 444(5):579-85.

Xie, Y., Zhong, W., Wang, Y., Trostinskaia, A., Wang, F., Puscheck, E.E., & Rappolee, D.A. (2007). Using hyperosmolar stress to measure biologic and stress-activated protein kinase responses in preimplantation embryos. *Mol. Hum. Reprod.* 13, 473-481.

Xu, Z., Kopf, G.S., & Schultz., R.M. (1994). Involvement of inositol 1,4,5-triphosphate-mediated Ca2+ release in early and late events of mouse egg activation. *Dev.* 120, 1851-1859.

Yancey, P.H., Clark, M.E., Hand, S.C., Bowlus, R.D., & Somero, G.N. (1982). Living with water stress: evolution of osmolyte systems. *Science.* 217, 1214-1222.

Yeo, S.K., Wang, C., & Guan, J-L. (2020). Role of FIP200 in inflammatory processes beyond its canonical autophagy function. Biochem. Soc. Trans. 48, 1599-1607.

Yoshida, H., Takakura, N., Kataoka, H., Kunisada, T., Okamura, H., & Nishikawa, S.I. (1997). Stepwise requirement of c-kit tyrosine kinase in mouse ovarian follicle development. *Dev Biol*. 184: 122-137.

Zeisel, S.H. (2006). Choline: critical role during fetal development and dietary requirements in adults. *Annu Rev Nutr.* 26, 229-250.

Zhang, Y., Zhang, Z., Xu, X-Y., Li, X-S., Yu, M., Yu, A-M., Zong, Z-H., Yu, B-Z. (2008). Protein kinase a modulates Cdc25B activity during meiotic resumption of mouse oocytes. *Dev Dyn.* 237(12), 3777-3786.

Zhang, B., Denomme, M.M., White, C.R., Leung, K-Y., Lee, M.B., & Baltz, J.M. (2015). *FASEB J*. 29, 069-1079.

Zhao, G., He, F., Wu, C., Li, P., Li, N., Deng, J., Zhu, G., Ren, W., & Peng, Y. (2018). Betaine in Inflammation: Mechanistic Aspects and Applications. *Front. Immunol.* 9, doi.org/10.3389/fimmu.2018.01070.

Zhou, C., & Baltz, J.M. (2013). JAK2 Mediates the Acute Response to Decreased Cell Volume in Mouse Preimplantation Embryos by Activating NHE1. *J. Cell. Physiol*. 228, 428-438.

Zhuo, L., & Kimata, K. (2001). Cumulus oophorus extracellular matrix: its construction and regulation. *Cell Struct Funct.* 26(4), 189-196.

## 10. Appendix A: PCR troubleshooting

Multiple primers for conventional RT-PCR were tested for each isoform and a temperature gradient was performed for each primer. Primers that appeared to work were gel extracted and sent for sequencing prior to starting qRT-PCR.

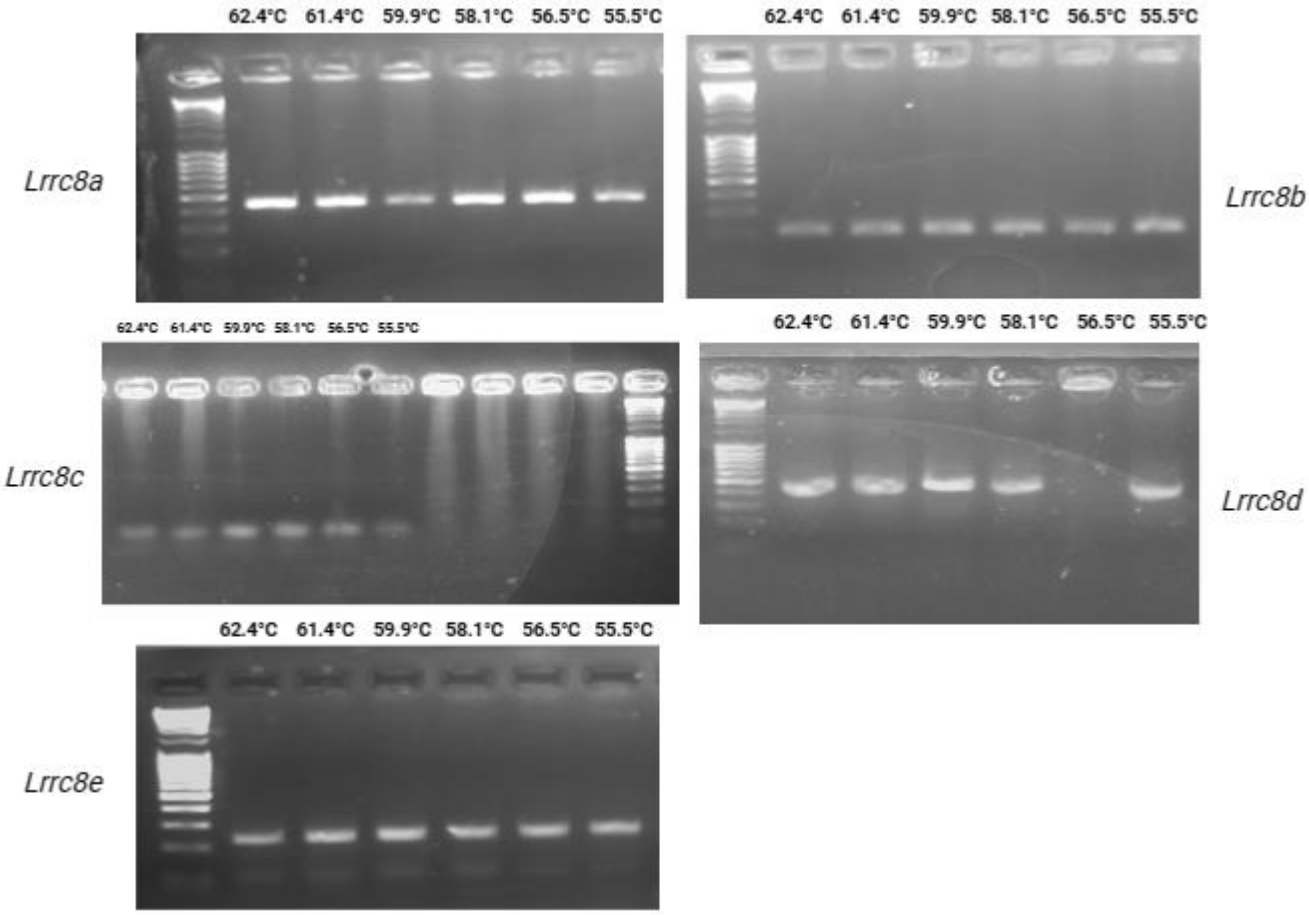


**Figure A1. Identifying the annealing temperature of *Lrrc8* primers using conventional RT-PCR.** RT-PCR was performed using *Lrrc8a-e* primers and cDNA extracted from liver (*Lrrc8a* and *Lrrc8d*), kidney (*Lrrc8b* and *Lrrc8e*), and spleen (*Lrrc8c*). *Lrrc8a-e* bands are at 436 bp, 210 bp, 184 bp, 441 bp, and 290 bp, respectively. The samples were run in a 1.75% agarose gel with ethidium bromide for 1 hour at 110 V.

Melt curves were generated for each primer and qPCR reaction. Figure A2 shows the melt curves for *Hmgb3, Rb1cc1,* and *Lrrc8a,* each displaying one peak and therefore a single product. The melt curves generated for *Lrrc8d* and *Lrrc8e* showed amplification of a secondary product and were therefore not usable (Figure A3).

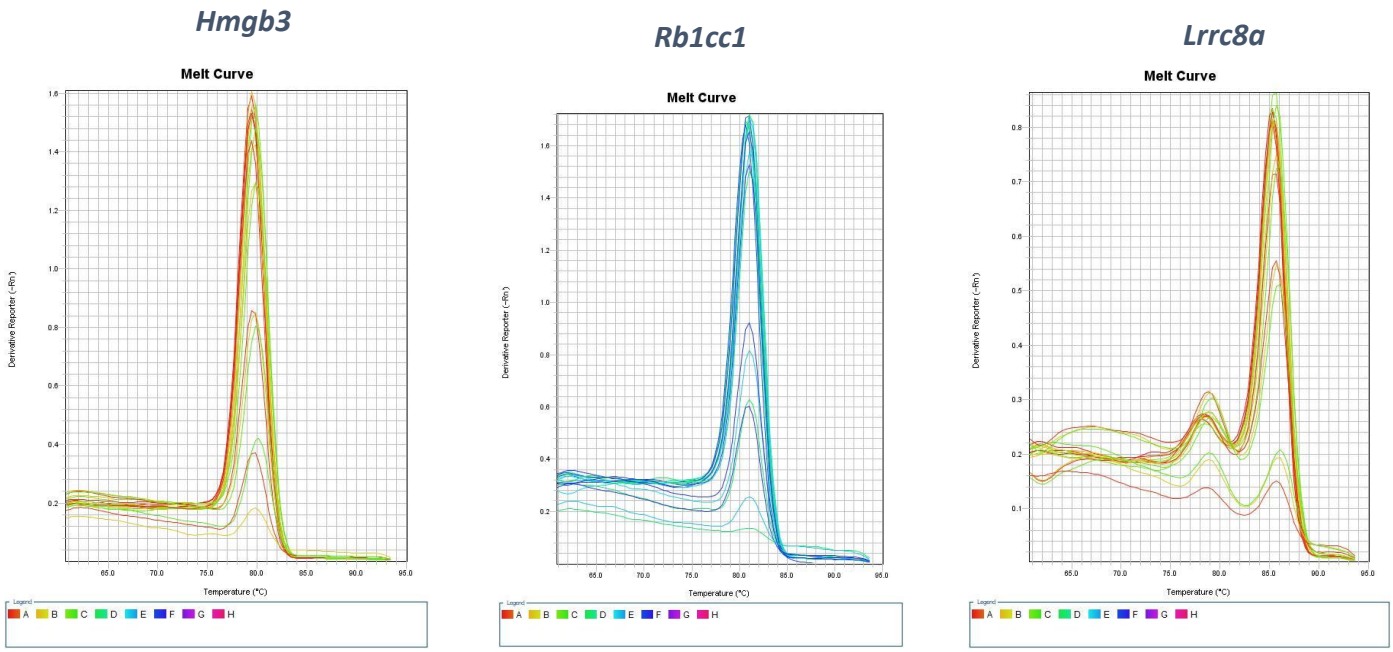


**Figure A2. Melt curves of *Hmgb3, Rb1cc1,* and *Lrrc8a* primers used for qRT-PCR.** Melt curves for *Hmgb3*, *Rb1cc1*, and *Lrrc8a* primers, indicating amplification of a single product. Each sample was loaded in triplicate wells and was averaged for one independent repeat. The qPCR program was 50°C (3 min), 95°C (10 min), followed by 35 cycles of 95°C (15 sec), 60°C (15 sec), and 72 (1min). A melt curve protocol was60-95-60°C (15 sec each).

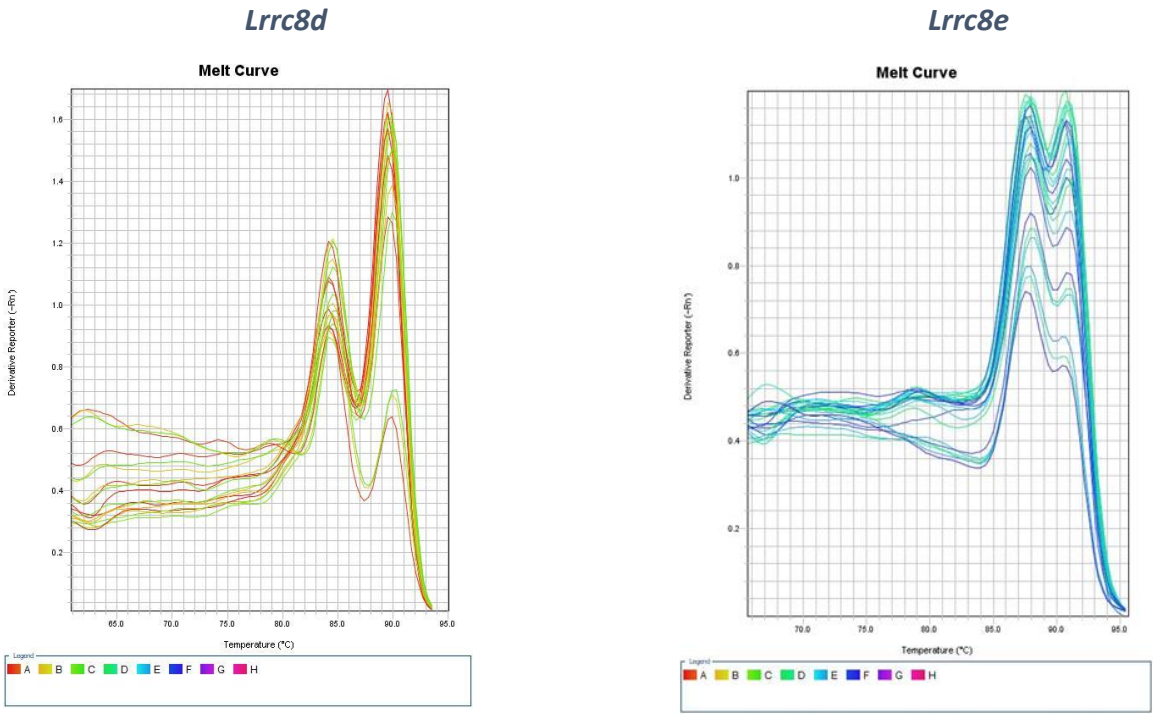


**Figure A3. Melt curves of *Lrrc8d* and *Lrrc8e* primers.**

Melt curves for *Lrrc8d* and *Lrrc8e* primers, indicating amplification of a secondary product. Each sample was loaded in triplicate wells and was averaged for one independent repeat. The qPCR program was 50°C (3 min), 95°C (10 min), followed by 35 cycles of 95°C (15 sec), 60°C (15 sec), and 72 (1min). A melt curve protocol was60-95-60°C (15 sec each).

## 11. Appendix B: [$^3$H]-betaine troubleshooting

### Identifying the betaine transporter in growing follicles

As an attempt to identify the betaine transporter in growing follicles, groups of ~ 10 P21 follicles were isolated and incubated in 2 μM [$^3$H]-betaine for 10 minutes to measure the total amount of betaine uptake. Parallel experiments were performed in which ~10 P21 follicles were incubated with 2 μM [$^3$H]-betaine and 5 mM unlabeled betaine, alanine, lysine, and arginine. These competitive inhibitors have been used previously to identify $y^+$LAT2 in COCs (Corbett *et al*., 2014).

As shown in Figure B1, unlabeled betaine, lysine and arginine did not inhibit [$^3$H]-betaine uptake, which was contradictory to the results previously seen in COCs. To determine whether the radiolabeled betaine had degraded, uptakes were performed with one-cell embryos incubated in [$^3$H]-betaine and unlabeled betaine, proline or glycine as described in the Methods section. Unlabeled betaine and proline failed to significantly inhibit betaine uptake, and there was no overall significant difference between groups (Figure B2).

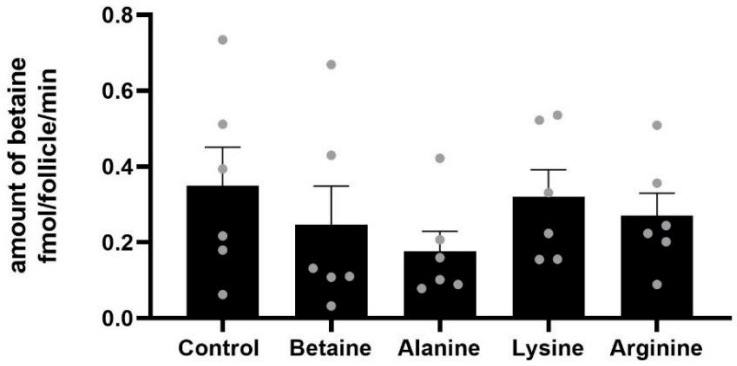


**Figure B1. Inhibition of betaine uptake by competitive amino acids in P21 follicles.**
P21 follicles were obtained from neonates during the initial wave of oogenesis. Follicles were isolated mechanically and incubated in groups of ~10 for 10 minutes in mKSOM medium containing 2 μM [$^3$H]-betaine with 5 mM unlabeled betaine, alanine, lysine, or arginine. Control indicates [3H]-betaine uptake with no addition of unlabeled amino acid. There was no statistical difference between groups ($p>0.05$ by one-way ANOVA with Tukey test).

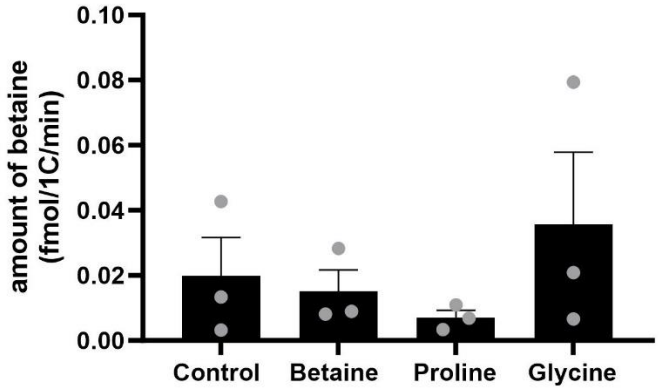


**Figure B2. Competitive inhibition of betaine uptake in one-cell embryos.**
One-cell embryos in groups of 5-10 were incubated in 2 μM [$^3$H]-betaine and 5 mM unlabeled betaine, proline, or glycine for 10 minutes. Control indicates no addition of unlabeled amino acid. There was no significant difference between groups ($p>0.05$ by one-way ANOVA with Tukey test).

[$^3$H]-betaine uptake was also measured in COCs with unlabeled betaine, sarcosine, and glycine to rule out a potential other transporter. None of the amino acids used displayed any competitive inhibition, which was observed as no statistical difference between any of the groups (Figure B3).

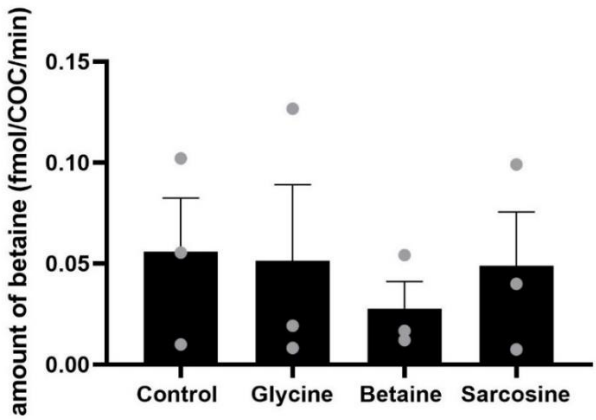


**Figure B3. Competitive amino acid inhibition of betaine uptake in cumulus-oocyte complexes (COCs).**

Groups of 5-10 COCs were incubated in 2 μM [$^3$H]-betaine with 5 mM unlabeled glycine, betaine, and sarcosine for 10 minutes. Control indicates [$^3$H]-betaine uptake with no addition of unlabeled amino acid. There was no significant difference between groups ($p>0.05$ by ANOVA with Tukey test).

**Inhibiting betaine efflux out of one-cells with DCPIB**

DCPIB is a VSOAC-specific inhibitor that inhibits LRRC8A via a cork-in-bottle mechanism (Kern *et al*., 2019). DCPIB has previously shown to block the swelling-induced chloride current ($I_{Cl,\ swell}$) in Xenopus oocytes, bovine pulmonary artery endothelial cells, and guinea-pig atrial myocytes (Decher *et al*., 2001). It was hypothesized that VSOAC is permeable to betaine, so my objective was to load one cells with [$^3$H]-betaine and transfer the embryos to a hypotonic dish with DCPIB to inhibit the efflux of betaine in response to cell-swelling. One-cell embryos were incubated in 250 mOsM mKSOM with 2 µM [3H]-betaine, a subset of embryos was removed for t=0 and the remainder transferred to a drop of 180 mOsM mKSOM with 0-20 µM DCPIB. There was no significant difference between the concentrations of DCPIB (Figure B4). This experiment was performed before we confirmed the [$^3$H]-betaine had degraded, so it is very likely that these results were due to the [$^3$H]-betaine.

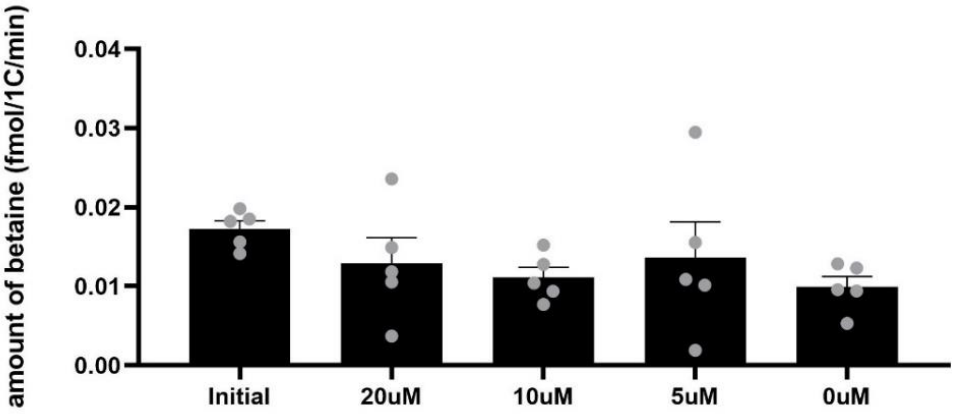


**Figure B4. Inhibition of betaine efflux with VSOAC-specific inhibitor, DCPIB.**

One-cell embryos in groups of 5-10 were incubated in 2 µM [$^3$H]-betaine in 250 mOsM mKSOM for 30 minutes, followed by a 30-minute incubation in 0-20 µM DCPIB in 150 mOsM mKSOM. The group labelled initial was a subset of one-cells removed after the first 30-minute

uptake period. There was no statistical difference between groups ($p>0.05$ by ANOVA with Tukey test).

## 12. Appendix C: Culture experiments with DCPIB and DIDS

To measure the endogenous betaine content across preimplantation embryo stages, the experimental plan was to culture one-cell embryos to the morula stage, collect embryos in groups of 30, and measure the betaine content with LC-MS/MS. Embryos were collected and cultured in pre-equilibrated 4-well plates with 750 µL mKSOM and a Cl- channel inhibitor. We first attempted to culture one-cell embryos to the morula stage in DCPIB, however, embryos only reached the morula stage when cultured at concentrations lower than 1 µM (Figure B6). We next tried the nonspecific Cl- channel inhibitor, DIDS, that has been previously used in our lab to inhibit the swelling-activated anion current (Kolajova and Baltz 1999; Kolajova *et al*., 2001). DIDS hydrolyzes in aqueous solutions and forms tetra- and pentameric polythioureas that obstruct Cl- channels (Wulff, 2008). Two-cell embryos were isolated and cultured in 100 µM DIDS, however, nearly all embryos in DIDS died before reaching the morula stage (Figure B7). Both DIDS and DCPIB were dissolved in DMSO. As a control, embryos were cultured in 1 µL DMSO, and nearly all embryos survived to the morula stage.

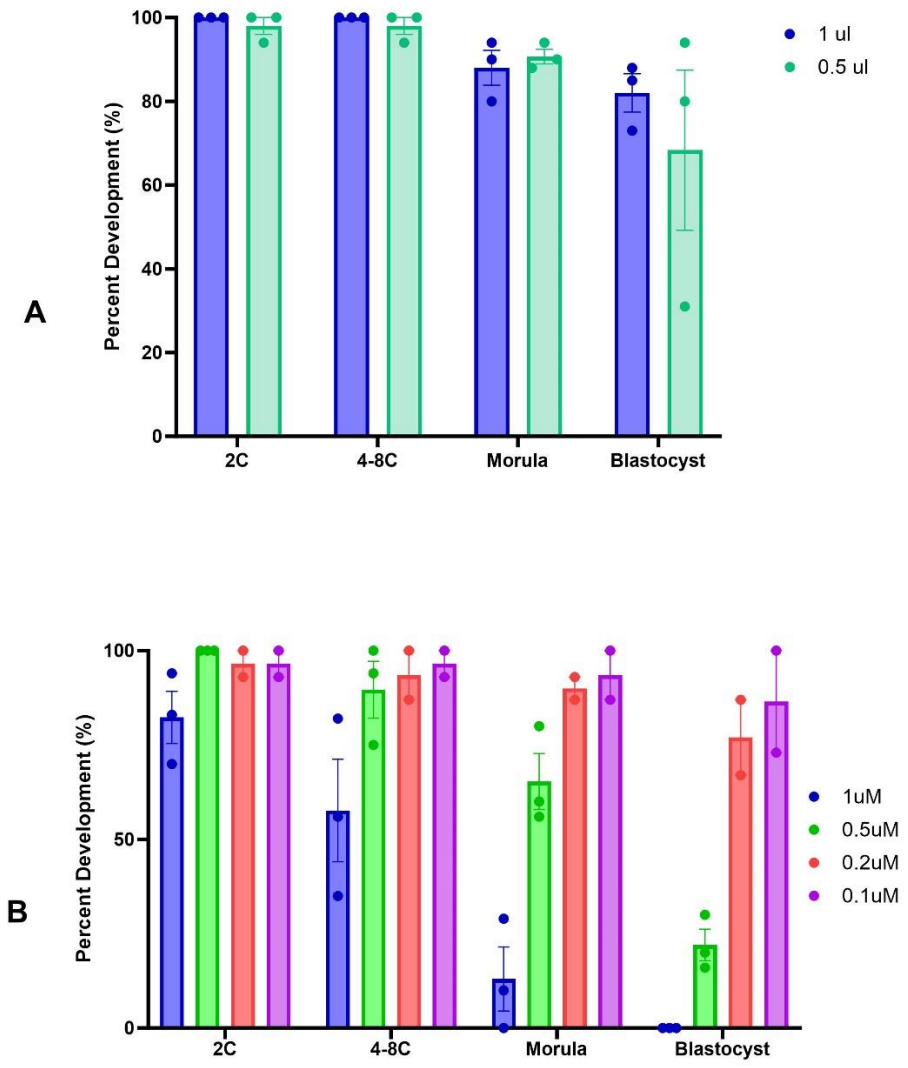


**Figure C1. Percent development of one-cell embryos cultured in DCPIB.**

One-cell embryos were collected in groups of ~20 and cultured in DMSO for the positive control (A) or in DCPIB (B) in mKSOM until the blastocyst stage at various concentrations. DPCIB was dissolved in DMSO for a stock concentration of 10 mM and further diluted to 1, 0.5, 0.2 or 0.1 µM. The highest amount of DMSO in mKSOM was 0.01%.

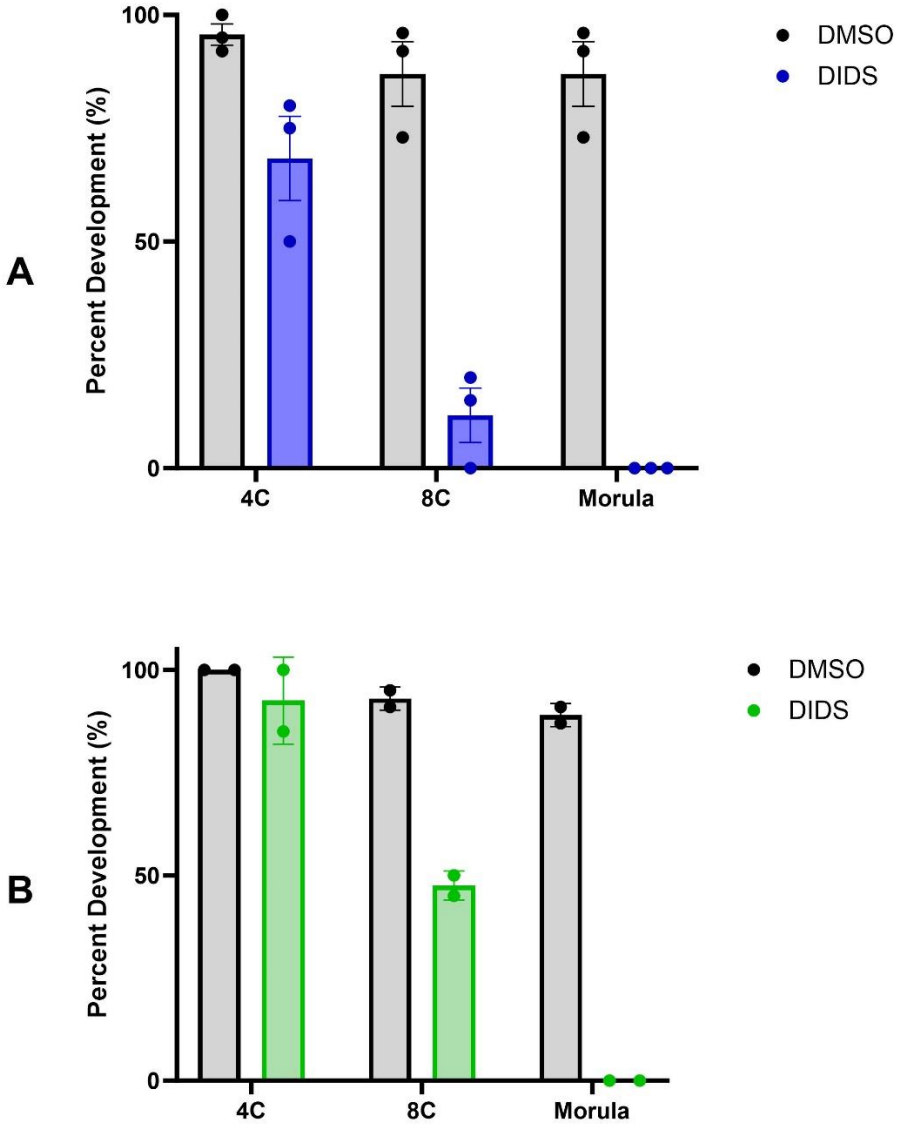


**Figure C2. Percent development of two-cell embryos cultured in DIDS.**

Two-cell embryos were collected in groups of ~20 and cultured until the morula stage in 100 µM DIDS or DMSO for the positive control. DIDS was dissolved in DMSO for a stock concentration of 100 mM and further diluted to 100 µM. The highest amount of DMSO in mKSOM was 0.1%. A: Two-cells isolated at the normal time of collection (9-11 am). B: Two-cells isolated later than the normal time of collection (3-5 pm).